AWARD NUMBER: W81XWH-13-1-0090

TITLE: Targeting Androgen Receptor in Breast Cancer: Enzalutamide as a Novel Breast Cancer Therapeutic

PRINCIPAL INVESTIGATOR: Jennifer Richer, Ph.D.

CONTRACTING ORGANIZATION: University of Colorado, Anschutz Medical Campus
Aurora, CO 80045-0508

REPORT DATE: September 2016

TYPE OF REPORT: Annual

PREPARED FOR: U.S. Army Medical Research and Materiel Command
Fort Detrick, Maryland 21702-5012

REPORT DOCUMENTATION PAGE

Form Approved
OMB No. 0704-0188

1. REPORT DATE	2. REPORT TYPE	3. DATES COVERED
September 2016	Annual	8/15/2015/-8/14/2016

4. TITLE AND SUBTITLE
Targeting Androgen Receptor in Breast Cancer: Enzalutamide as a Novel Breast Cancer Therapeutic

5a. CONTRACT NUMBER

5b. GRANT NUMBER
W81XWH-13-1-0090

5c. PROGRAM ELEMENT NUMBER

6. AUTHOR(S)

Jennifer K. Richer, Ph.D.

E-Mail: Jennifer.richer@ucdenver.edu

5d. PROJECT NUMBER

5e. TASK NUMBER

5f. WORK UNIT NUMBER

7. PERFORMING ORGANIZATION NAME(S) AND ADDRESS(ES)

University of Colorado
Anschutz Medical Campus
12800 E. 19th Ave
Aurora, CO 90010

8. PERFORMING ORGANIZATION REPORT NUMBER

9. SPONSORING / MONITORING AGENCY NAME(S) AND ADDRESS(ES)

U.S. Army Medical Research and Materiel Command
Fort Detrick, Maryland 21702-5012

10. SPONSOR/MONITOR'S ACRONYM(S)

11. SPONSOR/MONITOR'S REPORT NUMBER(S)

12. DISTRIBUTION / AVAILABILITY STATEMENT

Approved for Public Release; Distribution Unlimited

13. SUPPLEMENTARY NOTES

14. ABSTRACT

In breast cancers, the androgen receptor (AR) is more widely expressed than estrogen receptor alpha (ER) or the progesterone receptor (PR) (1), which are used as therapeutic targets and biomarkers, suggesting a potential role for AR in BC. To explore the function of AR in models of the three main subtypes of breast cancer (ER positive, ER negative and Her2+), we are using a new-generation AR inhibitor, enzalutamide, which impairs nuclear localization of AR. This is a very different mode of action than previous generation anti-androgens such as bicalutamide (Casodex), which is a competitive inhibitor of endogenous androgens that allows ligand-mediated nuclear localization of AR. Enzalutamide has shown success in the clinic in patients with late stage prostate cancer. The research in this proposal generates preclinical data testing whether inhibition of AR with enzalutamide will be effective in breast cancer and utilize preclinical models of the three main subtypes of breast cancer. Our goal is to determine if and how enzalutamide should be combined with currently used standard of care treatments in the three main types of breast cancer, with the primary objectives of the research being to guide the design of future clinical trials with enzalutamide.

15. SUBJECT TERMS
Breast cancer, androgen receptor, estrogen receptor, growth factors, enzalutamide, endocrine resistance, targeted therapy

16. SECURITY CLASSIFICATION OF:			17. LIMITATION OF ABSTRACT	18. NUMBER OF PAGES	19a. NAME OF RESPONSIBLE PERSON
U			U	130	USAMRMC
a. REPORT	b. ABSTRACT	c. THIS PAGE	Unclassified		19b. TELEPHONE NUMBER *(include area code)*
U Unclassified	U Unclassified	U Unclassified			

Table of Contents

Page

INTRODUCTION:

In breast cancers, the androgen receptor (AR) is more widely expressed than estrogen receptor alpha (ER) or the progesterone receptor (PR), which are used as therapeutic targets and biomarkers, suggesting a potential role for AR in BC. We examined the primary tumors of women treated with tamoxifen or aromatase inhibitor therapy and found that a higher AR to ER protein ratio correlates with worse response to traditional the anti-estrogen tamoxifen (see figure 1 in our published manuscript Cochrane et al in the appendix). To explore the function of AR in models of the three main subtypes of breast cancer (ER positive, ER negative and Her2+), we are using a new-generation AR inhibitor, enzalutamide, which impairs nuclear localization of AR. This is a very different mode of action than previous generation anti-androgens such as bicalutamide (Casodex), which is a competitive inhibitor of endogenous androgens that allows ligand-mediated nuclear localization of AR. Enzalutamide has shown success in the clinic in patients with late stage prostate cancer refractory to bicalutamide and is now FDA approved as a prostate cancer therapy. The research in this proposal seeks to determine whether inhibition of AR with enzalutamide will be effective in breast cancer and utilize preclinical models to determine if and how it should be combined with currently used standard of care treatments in the three main types of breast cancer, with the primary objectives of guiding the design of future clinical trials with enzalutamide.

KEYWORDS: Breast cancer, androgen receptor, estrogen receptor, growth factors, enzalutamide, endocrine resistance, targeted therapy.

ACCOMPLISHMENTS: Below we describe for each task in the official statement of work the major activities; specific objectives; significant results or key outcomes, including major findings, developments, or conclusions (both positive and negative); and/or other achievements. We include a discussion of stated goals not met or tasks not fully completed. We include pertinent data and graphs in sufficient detail to explain significant results achieved. Detailed description of the methodology used is provided in the methods section of two manuscripts in the appendix. The first manuscript was published in January of 2014 and was submitted with the first annual progress report. The second manuscript arising from this work investigated AR in the non-LAR subtype of TNBC was published in Jan 2015. We also wrote two reviews of AR in TNBC. A third primary manuscript on AR in ER+ breast cancer has just been accepted Aug 2016. A fourth manuscript, under preparation, is included as a draft in the appendix of this report, and demonstrates that AR is anti-apoptotic, supports anchorage independent growth and androgens and AR expand a cancer stem cell-like population in TNBC. This study evaluated enzalutamide given either simultaneous with or sequential to chemotherapy and found that simultaneous treatment was more effective at preventing recurrence after cessation of chemotherapy. A fifth manuscript, in preparation, focuses on combining enzalutamide with an mTOR inhibitor, everolimus in HER2+ and TNBC breast cancer. Everolimus was found in clinical trials to be very effective in ER+ breast cancer, but less so in HER2+ and TNBC. Our studies show that everolimus increases the amount of AR and AR activity and therefore combining the anti-androgen enzalutamide with everolimus gives a synergistic effect over either drug alone.

Manuscripts in red are new since last annual report

Dawn R. Cochrane, Sebastian Bernales, Britta M. Jacobsen, Diana M. Cittelly, Erin N. Howe, Nicholas C. D'Amato, Nicole S. Spoelstra, Annie Jean, Paul Jedlicka, Kathleen C. Torkko, Andy Protter, Anthony D. Elias and **J. K. Richer**. Role of the Androgen Receptor in Breast Cancer and Preclinical Analysis of Enzalutamide. BREAST CANCER RESEARCH 2014 Jan 22;16(1). PMID: 24451109 Designated as Highly Cited by the journal Breast Cancer Research.

Barton VN, D'Amato NC, Gordon MA, Lind HT, Spoelstra NS, Babbs B, Heinz RE, Elias A, Jedlicka P, Jacobsen BM, **Richer JK**. Multiple molecular subtypes of triple negative breast cancer critically rely on androgen receptor and respond to Enzalutamide in vivo. Mol Cancer Ther.015 Mar;14(3):769-78. Epub 2015 Feb 23. PMID: 25713333

Barton VN, Gordon MA, Christenson J, D'Amato N, **Richer JK**. Androgen receptor biology in triple negative breast cancer: A case for AR+ and quadruple negative disease subtypes. Hormones and Cancer, 2015 July 23. PMID: 26201402

Barton VN, Gordon MA, **Richer JK**, Elias A. Anti-androgen therapy in triple-negative breast cancer. Ther Adv Med Oncol. 2016 Jul;8(4):305-8. 2016 May 31. PMID: 27482289

D'Amato NC, MA Gordon, BL Babbs, NS Spoelstra, KT Butterfield, KC Torkko, VT Phan ,VN Barton, TJ Rogers, CA Sartorius, AD Elias, J Gertz, BM Jacobsen, and **JK Riche**r. Cooperative Dynamics of AR and ER Activity in Breast Cancer. *Molecular Cancer Research*, accepted Aug 2016.

Gordon MA, D'Amato NC, Gu H, Babbs B, Butterfield K, Liu B, Elias, Richer JK. Dual inhibition of androgen receptor and mTOR in breast cancer. *In Preparation.*

Barton VN, Christenson JL, Rogers TJ, Butterfield K, Babbs B, Spoelstra NS, D'Amato NC, Richer JK (2016) Androgen receptor supports a cancer stem cell-like population in triple-negative breast cancer. *In preparation.*

The objective of Stage I of this proposal is to rapidly generate preclinical data testing Enza alone or in combination with standard of care therapeutics in different subtypes of BC to help guide the clinical trials described in **Stage II** (PI clinical partner Dr.Anthony Elias) and steer the rational design and focus on patients most likely to benefit from enzalutamide alone or in combination with currently used therapeutics.

Preclinical Aim 1. **To test enzalutamide (enza) in combination with currently approved therapies for breast cancer (BC) in the various subtypes of BC.**

Task 1 – Evaluate enzalutamide in combination with anti-estrogen therapy in ER+/AR+ BC lines (MCF7, BCK4) and a ER+/AR+ patient derived xenograft.
Task 2. Test enza in three different tamoxifen resistance models *in vitro.*
Task 3. Test enzalutamide in combination with Her2 directed therapy in ER+ and ER- Her2+ models
Task 4. Examine enzalutamide in combination with an mTOR inhibitor (Afinitor/everolimus)
Task 5. In true TNBC cell lines and explants that retain AR, enzalutamide will be evaluated alone and in combination with chemotherapy and everolimus, *in vitro* and *in vivo*.).

What was accomplished under these goals?

TASK1- Evaluate enzalutamide in combination with anti-estrogen therapy in ER+/AR+ BC lines (MCF7, BCK4) and a ER+/AR+ patient derived xenograft. Months 1-4. 100% completed.

We have a manuscript that was just accepted to Mol Cancer Res (D'Amato et al. 2016) see above. On this Task 1 topic. The full manuscript is also included in the appendix.

Abstract from ER+/AR+ paper: Cooperative Dynamics of AR and ER Activity in Breast Cancer. *Molecular Cancer Research,* accepted Aug 2016:

Androgen receptor (AR) is expressed in 90% of estrogen receptor alpha positive (ER+) breast tumors, but its role in tumor growth and progression remains controversial. Use of two anti-androgens that inhibit AR nuclear localization, enzalutamide and MJC13, revealed that AR is required for maximum ER genomic binding. Here, a novel global examination of AR chromatin binding found that estradiol induced AR binding at unique sites compared to dihydrotestosterone (DHT). Estradiol-induced AR binding sites were enriched for estrogen response elements and had significant overlap with ER binding sites. Furthermore, AR inhibition reduced baseline and estradiol-mediated proliferation in multiple ER+/AR+ breast cancer cell lines, and synergized with tamoxifen and fulvestrant. *In vivo*, enzalutamide significantly reduced viability of tamoxifen-resistant MCF7

xenograft tumors and an ER+/AR+ patient derived model. Enzalutamide also reduced metastatic burden following cardiac injection. Lastly, in a comparison of ER+/AR+ primary tumors versus patient-matched local recurrences or distant metastases, AR expression was often maintained even when ER was reduced or absent. These data provide preclinical evidence that anti-androgens that inhibit AR nuclear localization affect both AR and ER, and are effective in combination with current breast cancer therapies. In addition, single agent efficacy may be possible in tumors resistant to traditional endocrine therapy, since clinical specimens of recurrent disease demonstrate AR expression in tumors with absent or refractory ER.

The first therapy of choice to treat an ER+ tumor will always likely be an anti-estrogen, even though this may change because we have shown that the relative expression of AR to ER protein (percent cells positive) can predict a poor response to tamoxifen and poor overall survival (Cochrane DR et al 2014). We have also shown that the enzalutamide is efficacious in tamoxifen resistant MCF 7 cells *in vivo* (Figure 5 E of manuscript in preparation in appendix). However, ER+ tumors will likely be treated first with tamoxifen (if the woman is premenopausal) or aromatase inhibitor (AI) if post-menopausal or having recurred while on tamoxifen, then if there is a recurrence of disease, with the ER degrader Fulvestrant. Therefore, we tested for synergy between these two drugs. Since Fulvestrant must be given IM in oil, being able to reduce the effective dose necessary would definitely be helpful. The dose reduction index in Fig 1 demonstrates that combining Fulvestrant with Enzalutamide may allow a reduction in the amount of both drugs used to get the same efficacy. Importantly (and why we show this here in the progress report), this is promising for the proposed investigator initiated trial that we will do with neoadjuvant Fulvestrant vs Fulvestrant plus Enza (see Dr. Elias's progress report.

Enzalutamide

Enza (uM)	% Inhibition
5	3.74%
10	9.29%
20	14.28%

Fulvestrant

ICI (nM)	% Inhibition
100	0.98%
250	15.77%
500	24.58%
750	21.99%
1000	26.23%

Combination Index

Enza \ Fulvestrant	100nM	250nM	500nM	750nM	1000nM
5uM	0.831	0.652	0.838	1.027	1.238
10uM	0.882	0.745	0.768	1.015	1.171
20uM	0.835	0.8	0.876	0.938	1.119

CI < 1 indicates synergy

BCK4 Enza + ICI E2-induced Growth

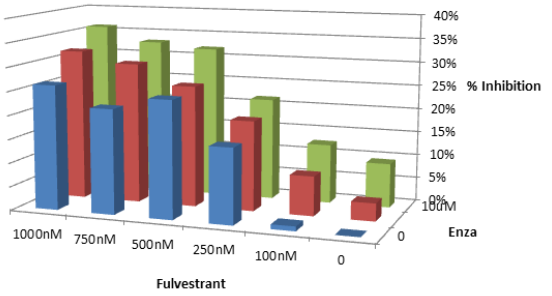

Dose Reduction Index (Fulvestrant)

Enza \ Fulvestrant	100nM	250nM	500nM	750nM	1000nM
5uM	2.873	2.194	1.424	1.093	.880
10uM	3.916	2.445	1.765	1.216	.998
20uM	6.121	3.116	1.927	1.522	1.178

Figure 1. Enza and Fulvestrant synergize to inhibit proliferation of ER+AR+ BCK4 breast cancer cells. *Enzalutamide synergizes with Fulvestrant (ICI) to oppose estrogen-induced proliferation of ER+/AR+ BCK4 cells. 20,000 BCK4 cells were plated into 96 well plates in phenol red free media with stripped serum. Cells were treated with increasing doses of Enzalutamide (Enza) and Fulvestrant (ICI) in different combinations for 6 days. Proliferation was measured using the IncuCyte live cell imaging system. The combination index and dose reduction index were calculated using CalcuSyn.*

In the the appendix, we show synergy with enza and tamoxifen or Fulvestrant in additional cell lines.

In ongoing studies, we are modeling the use of Enza *in vivo* with an AR+ER+ PDX HCI013 from Alana Welm that has an ESR1 mutation resulting in the ER Y537S amino acid change in the ligand binding domain and its E2 independent variant PDX HCI013.

Task 3. Test enzalutamide in combination with HER2-directed therapy in ER+ and ER- HER2+ models. (90% completed)

In HER2 amplified breast cancer cell lines we have continued the *in vitro* analysis of combining enza with the anti-HER2 agent trastuzumab. We have performed synergy experiments in two related cell lines: the

parental BT474 cells, which are ER+/HER2+, and a trastuzumab-resistant derivative of these cells, BT474-HR20 (Figure 4). These HR20 cells have been chronically treated with 20ug/mL trastuzumab, and have developed resistance through a mechanism of HER3/IGF1R activation, such that HER2 is still expressed, and the downstream activation of HER2/HER3 target genes is also maintained. Figure 4 shows results of a test of combining enza with trastuzumab. Our collaborator Dr. Bolin Liu has determined that the trastuzumab resistant BT474 cells grow better in vivo than the parental cell line. All HER2+ cell lines in general are all known for not growing well *in vivo*. These cells have a higher take rate in NOD/SCID mice. We performed an *in vivo* study using the trastuzumab resistant BT474-HR20 cells. We set up the experiment with 4 treatment groups: Veh, Enza, Trastuzumab, Enza+Trastuzumab. Mice were randomized to treatment groups after tumors grew to a size of approximately $50mm^3$. At day 47 post-treatment, mice in the vehicle group and the enza group were sacrificed. There was a statistically significant difference in tumor weight between these two groups, with the enza-treated tumors having lower tumor weight (Figure 5).

Figure 2. Enzalutamide shows synergy with trastuzumab in both trastuzumab responsive and resistant HER2+/ER+ BT474 breast cancer cells. *BT474 cells (HER2+/ER+) and trastuzumab-resistant BT474-HR20 cells were treated alone or in combination with enzalutamide and trastuzumab. Cells were grown for 5 days and then proliferation was measured by crystal violet assay. 3D bar graphs depict percent inhibition at dose combinations indicated. Synergy was calculated with Calcusyn software. A Combination index <1 indicates synergy, 1 indicates an additive effect, and >1 indicates an antagonistic effect. The dose reduction index measures the factor by which a drug dose can be reduced when it is combined with another drug, in order to get the same effect as single agent.*

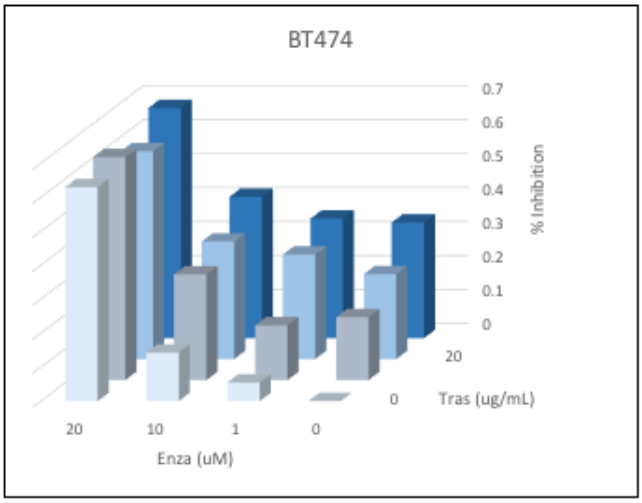

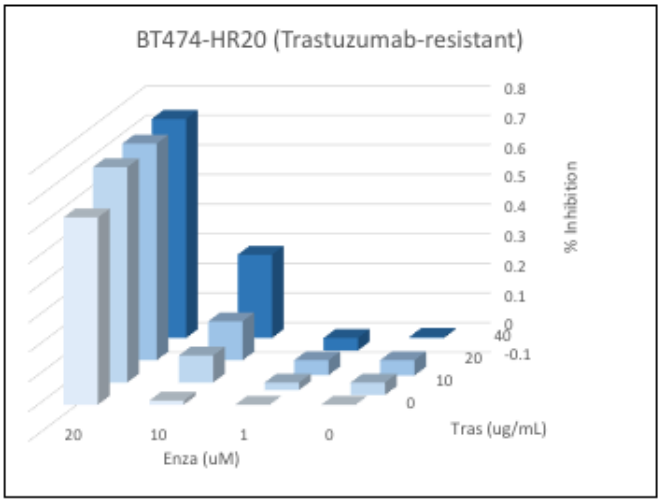

			Dose Reduction Index	
Enza (uM)	Tras (ug/mL)	Combination Index	Enza	Tras
1	10	1.537	4.384	0.764
1	20	0.73	12.911	1.108
1	40	0.98	10.477	1.577
10	10	1.245	1.067	3.248
10	20	1.267	1.257	2.121
10	40	1.155	1.712	1.753
20	10	0.446	2.387	37.237
20	20	0.586	1.954	13.443
20	40	0.471	2.637	10.944

			Dose Reduction Index	
Enza (uM)	Tras (ug/mL)	CI	Enza	Tras
1	10	1.242	1.223	2.355
1	20	1.232	1.689	1.562
1	40	1.267	2.589	1.136
10	10	1.026	1.041	15.371
10	20	0.903	1.26	9.088
10	40	0.66	1.96	6.69
20	10	0.435	2.39	58.434
20	20	0.448	2.416	29.495
20	40	0.472	2.465	15.007

At day 47, the mice that got vehicle (no drug treatment) and those that only had enzalutamide had to be sacrificed, but final tumor weight was significantly less in the Enza treated group than control. Mice in the trastuzumab only and enza+trastuzumab groups were not killed since they had a significantly lower tumor burden, but they were taken off drug, and weekly caliper measurements were performed to determine if there would be a difference in tumor re-growth. While not reaching significance, there is a trend towards the enza+trastuzumab treated mice having slower regrowth of tumors (Figure 3). This would indicate that even though the tumor volume was not different at day 47 between the trastuzumab only and the trastuzumab plus

Enza groups, the combination with Enza may be killing more cells and therefore will reduce the rate of recurrence, but this experiment is still ongoing. This work is very important because there is a trial for Enza plus trastuzumab in HER2+ disease that is just starting in breast cancer. This might tell us that even if there is not an obvious decrease in tumor size (if this is done in the neoadjuvant setting) or reduction in metastatic tumor burden, there may be some benefit still if it lowers the chance of recurrence or rate of progression in HER2+, particularly those that are not very sensitive to trastuzumab. Now there are other options for HER2 positive disease, but they all do target HER2 or HER3 and they may all benefit from the combination with an anti-androgen because we see that AR upregulates HER2 and HER3 (as shown in previous progress reports). Our in vivo work shown in will be added to a paper in preparation on targeting AR in HER2+ breast cancer.

Figure 3. HER2+ BT474-HR20 xenografts respond to trastuzumab and enzalutamide, but the combination achieves a sustained response after treatment is ceased. (A) *Mice were treated for 47 days, and tumor volume was measured 1x/week. Day 47 tumor volumes are shown. (B) All mice in the vehicle and Enza groups were sacrificed at day 47, and tumor weights were measured. There was a statistitcally significant difference in tumor weight between the vehicle group and the Enza group. (C) Mice in trastuzumab and trastuzumab+Enza groups were taken off treatment at Day 47, and tumors were allowed to regrow. Tumor volumes are being measured 1x/week, with day 85 shown (38 days after treatment cessation). The difference in tumor volume between the two groups is approaching statistical significance (p=0.519)*

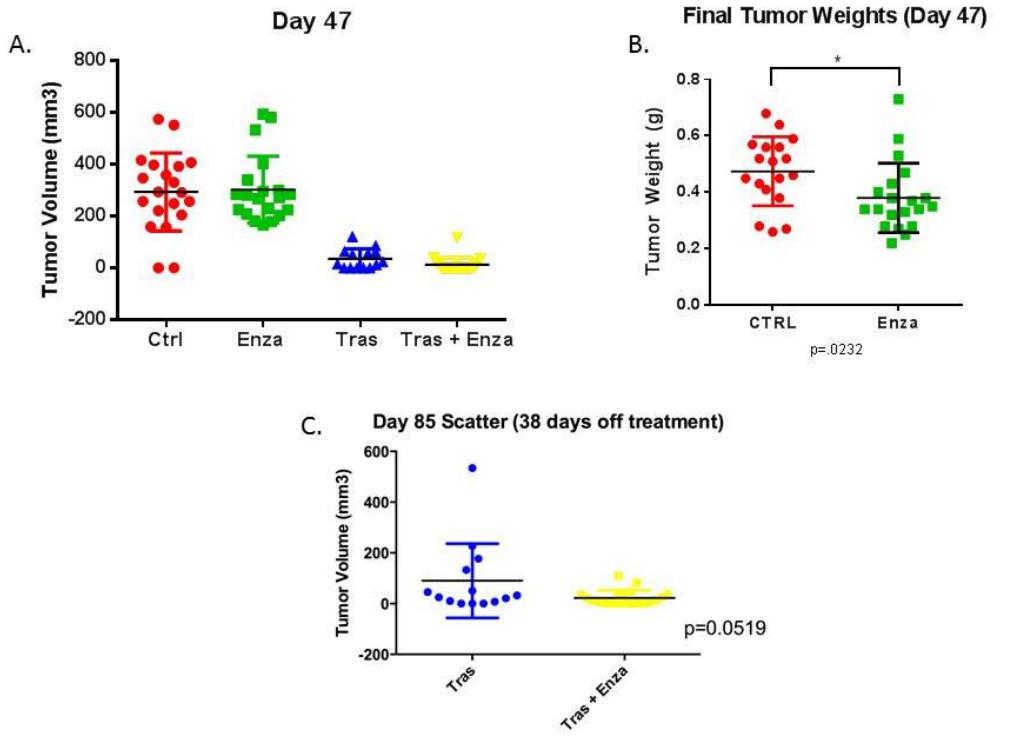

Task 4: Examine enzalutamide in combination with an mTOR inhibitor (Afinitor/everolimus) (90 % complete).

The HER2/PI3K/mTOR signaling axis is a critical pathway in the progression of breast cancer, and is frequently upregulated. HER2 has been an effective drug target in breast cancer over the last two decades, and agents such as trastuzumab have significantly improved survival rates for patients with HER2+ disease. However acquired or de novo resistance to HER2-targeted agents such as trastuzumab remains a critical problem, and multiple routes to resistance have been described, such as activation of alternative TKRs and activation of the PI3K pathway, and I'll propose today that AR activitation may also contribute to resistance.

More recently, therapeutic targeting of the mTOR signaling axis has demonstrated promise in pre-clinical models and clinical trials, leading to FDA approval of the anti-mTOR agent everolimus for advanced ER+ breast cancer. As demonstrated in the Phase III BOLERO-2 trial, patients with ER+/HER2- breast cancer who received everolimus in combination with the aromatase inhibitor exemestane had a significant progression-free survival benefit of 6.4 months when compared to patients who received exemestane plus placebo. However, in another Phase III trial examining everolimus in patients with HER2+ disease, there was a statistically

significant, but clinically insignificant survival benefit of only 1.2 months when everolimus was added to chemotherapy and trastuzumab. We propose that other confounding factors such as the androgen receptor may limit the efficacy of simultaneous inhibition of both mTOR and HER2.

Figure 4. Summary of hypothesis for Enza plus mTOR inhibitor.

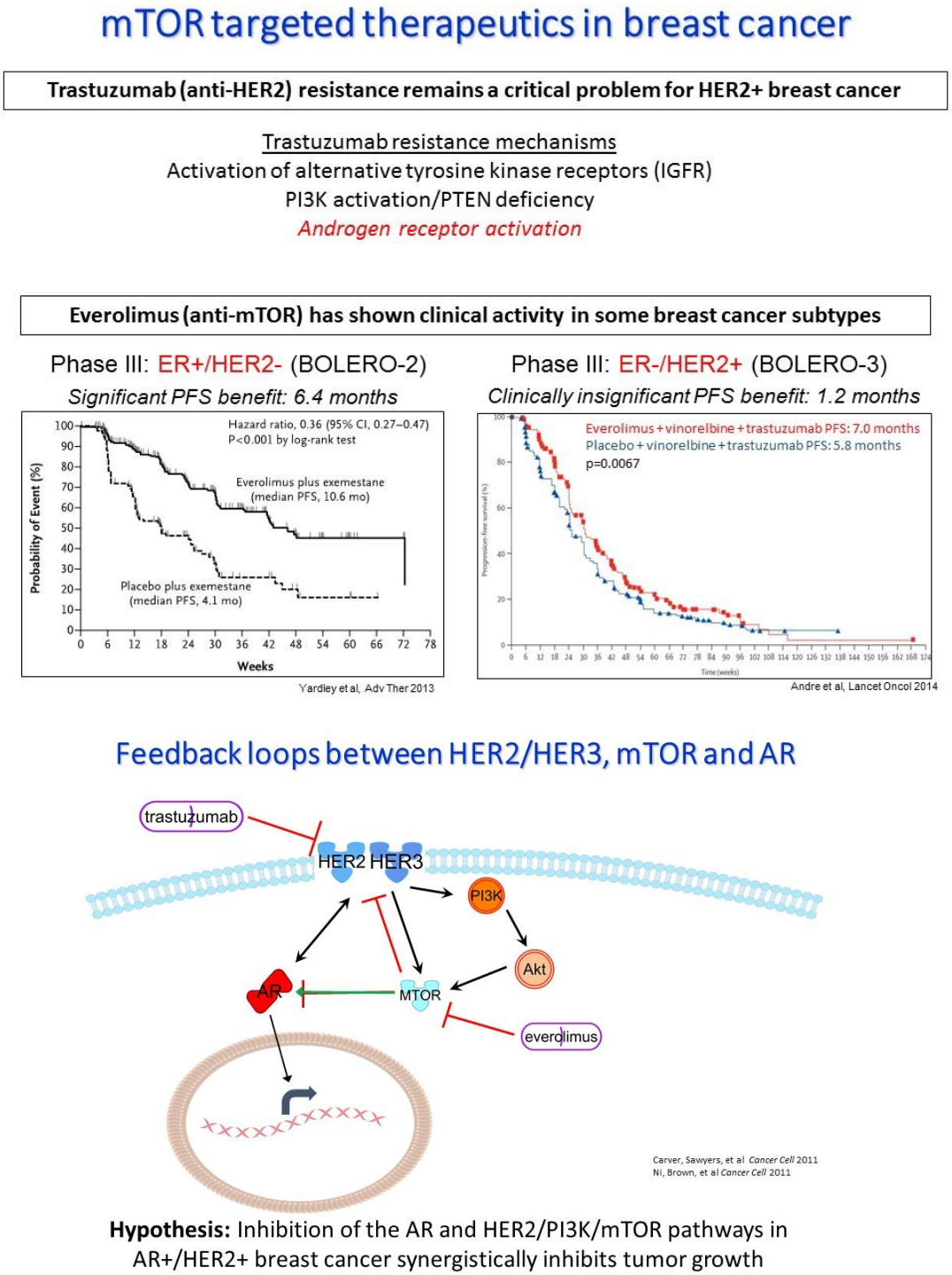

Hypothesis: Inhibition of the AR and HER2/PI3K/mTOR pathways in AR+/HER2+ breast cancer synergistically inhibits tumor growth

Our mechanistic studies in this Task have revealed that there is cross-regulation between AR and the HER2/PI3K/Akt/mTOR signaling axis. In previous progress reports we showed *in vitro* that enzalutamide synergizes with everolimus in HER2+ and TNBC cells. Everolimus causes an upregulation in AR protein expression, as well as phospho-HER2 and phospho-HER3 (through AR); addition of Enza plus everolimus abrogates these effects. We have demonstrated a synergistic interaction between the mTOR inhibitor everolimus

and Enza several HER2+ breast cancer cell lines. We now show in a paper in preparation that this combination works well *in vivo* as well. All of these in vitro and in vivo results are presented in a manuscript in preparation Gordon MA, D'Amato NC, Gu H, Babbs B, Butterfield K, Liu B, Elias, Richer JK. Dual inhibition of androgen receptor and mTOR in breast cancer. *In Preparation that is included in the appendix of this report.*

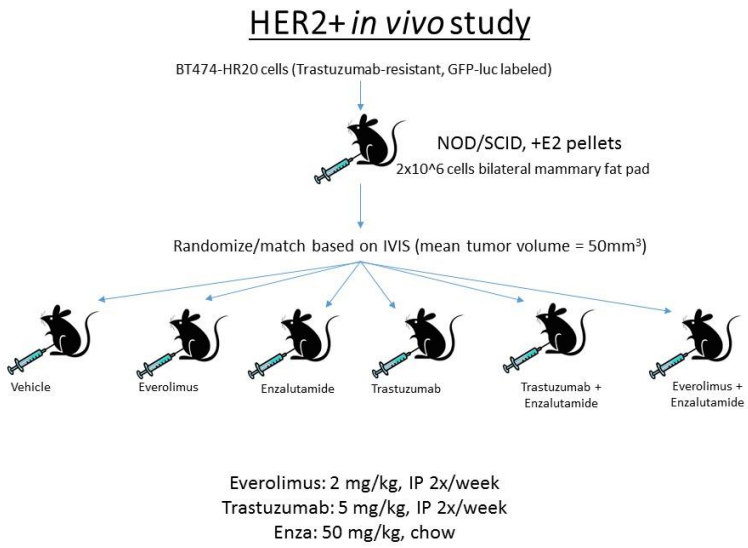

Figure 5. Experimental design of testing enzlutamide, everolimus, and trastuzumab in trastuzumab-resistant breast cancer cells in vivo.

Figure 6. Combination treatment with enzalutamide and everolimus inhibits tumor viability significantly more than single agent treatment. *Still working on this figure. (A) Total flux growth curve of trastuzumab-resistant BT474-HR20 xenografts. Mice were randomized to one of four treatment groups at day -3 and treatment was initiated at day 0. (B) IVIS signal on last day of study. (C) Change in total flux from day of randomization to end of study on day 26. (D) Western blots from 3 representative tumors per treatment group: vehicle, enzalutamide (Enza), everolimus (Everol), and combination (Enza/Everol). *p<0.05, **p<0.01, ***p<0.001,*

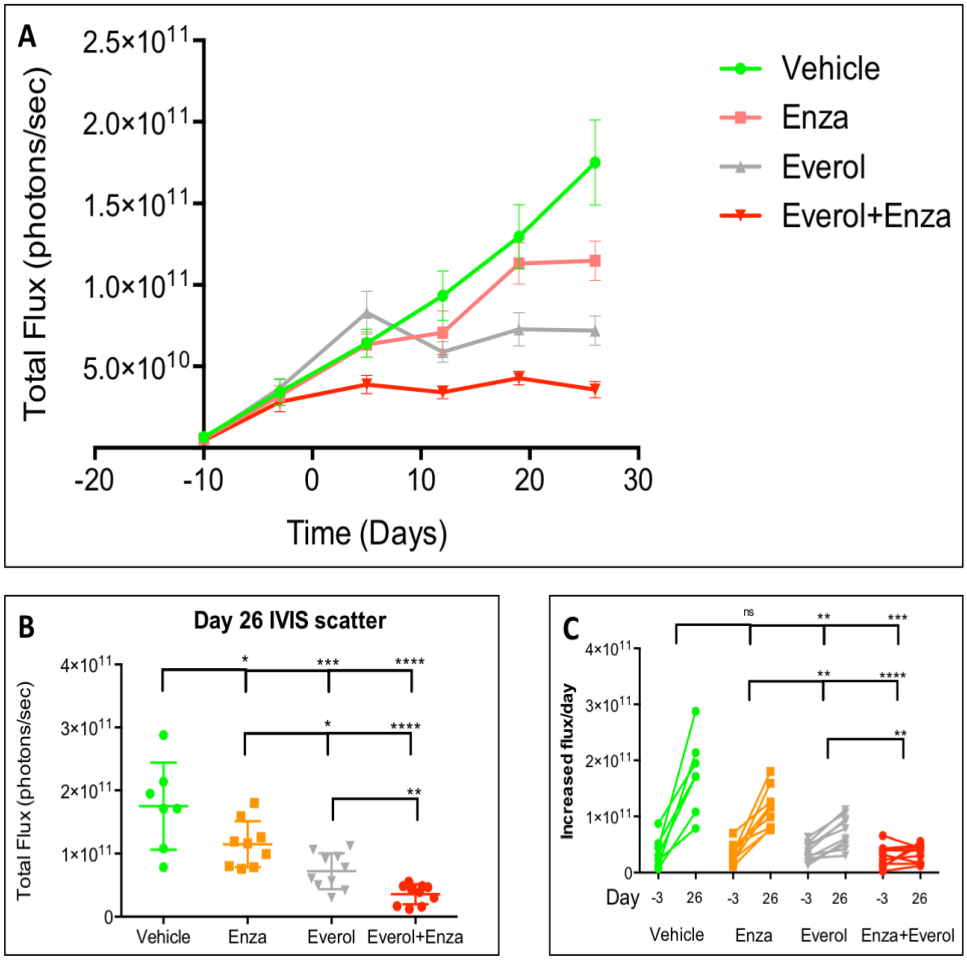

Task 5. In true TNBC cell lines and explants that retain AR, enzalutamide will be evaluated alone and in combination with chemotherapy and everolimus, *in vitro* and *in vivo*. (90% completed)

Dr. Valerie Barton (just defended), has a second manuscript almost ready to be sent Barton VN, Christenson JL, Rogers TJ, Butterfield K, Babbs B, Spoelstra NS, D'Amato NC, Richer JK (2016) Androgen receptor supports a cancer stem cell-like population in triple-negative breast cancer. *In preparation* (see appendix) on a unique role for AR in supporting a cancer stem-cell like population in TNBC.

Abstract: Triple-negative breast cancer (TNBC) is an aggressive breast cancer subtype lacking estrogen and progesterone receptors, and human epidermal growth factor receptor 2 (HER2). While to date there are no approved targeted therapies for TNBC, preclinical and early clinical trials indicate that up to 50% express some degree of positivity for androgen receptors (AR) and are sensitive to AR targeted therapy. However, the function of AR in TNBC and the mechanisms by which AR targeted therapy reduces tumor burden in preclinical and clinical settings are unknown. We hypothesized that AR maintains a cancer stem cell-like (CSC) tumor initiating population and that it serves as an anti-apoptotic factor that facilitates anchorage independence. **Methods** Anchorage independence/anoikis resistance was assessed on poly-Hema coated tissue culture plates used to achieve forced suspension culture and apoptosis was measured with cleaved caspase 3 antibody. AR was inhibited using the AR inhibitor Enzalutamide (Enza) or shRNAs targeting AR. CSC populations were assessed in vitro using ultra low attachment plates, CD44/CD24 staining, the ALDEFLUOR assay, and single cell mammosphere formation efficiency (MFE) assays in TNBC cell lines SUM159PT and MDA-MB-453.. In vivo, tumor-initiating capacity was assessed using a limiting dilution assay of SUM159PT cells pre-treated with or without Enza. Lastly, the efficacy of combination Enza and chemotherapy was assessed by caliper measurement and intravital imaging of TNBC xenografts in mice treated with Enza and paclitaxel. **Results** AR transcript ($P<0.05$), protein, and transcriptional activity ($P<0.01$) increased in tumor cells in suspension culture compared to attached conditions. Cells that expressed AR protein resisted detachment-induced apoptosis. The CSC population increased in suspension culture by ALEDFLUOR staining ($P<0.01$), CD44/CD24 staining ($P<0.001$), and MFE ($P<0.05$). AR inhibition decreased ADLH staining ($P<0.001$), increased CD24 staining ($P<0.05$), and decreased MFE($P<0.01$). In vivo, pre-treatment with Enza decreased the tumor-initiating capacity of TNBC cells in a limiting dilution assay ($P<0.05$). Enza significantly decreased tumor volume and viability when administered during or after chemotherapy in vivo ($P<0.05$) and simultaneous treatment significantly reduced tumor recurrence. **Conclusions** AR supports anchorage independence, maintenance of CSCs, tumor initiation and regrowth following chemotherapy in a TNBC preclinical model. Thus AR targeted therapies may enhance the efficacy of chemotherapy even in TNBC with very few cells positive for AR, perhaps by targeting a different cell population.

This paper draft is in the appendix with all the figures and they have been shown in previous reports, so the only one we will show here is the one most pertinent to clinical trials of Enza in TNBC, which is Figure 7 showing that Enza given *simultaneous with chemotherapy significantly reduces tumor burden and tumor recurrence.*

Figure 7 Enzalutamide and Paclitaxel combination therapy is more effective than Paclitaxel alone. A, total flux throughout study by treatment group. *B, comparison of total flux on study day 49. C, tumor burden throughout study by treatment group. D, comparison of tumor burden on study day 51. E, total flux (left, paired t-test) and tumor burden (right) per mouse between the final day of Paclitaxel and the end of study. Statistics represent two-tailed t-tests. #, P=0.06; *, P<0.05; **, P,0.01*

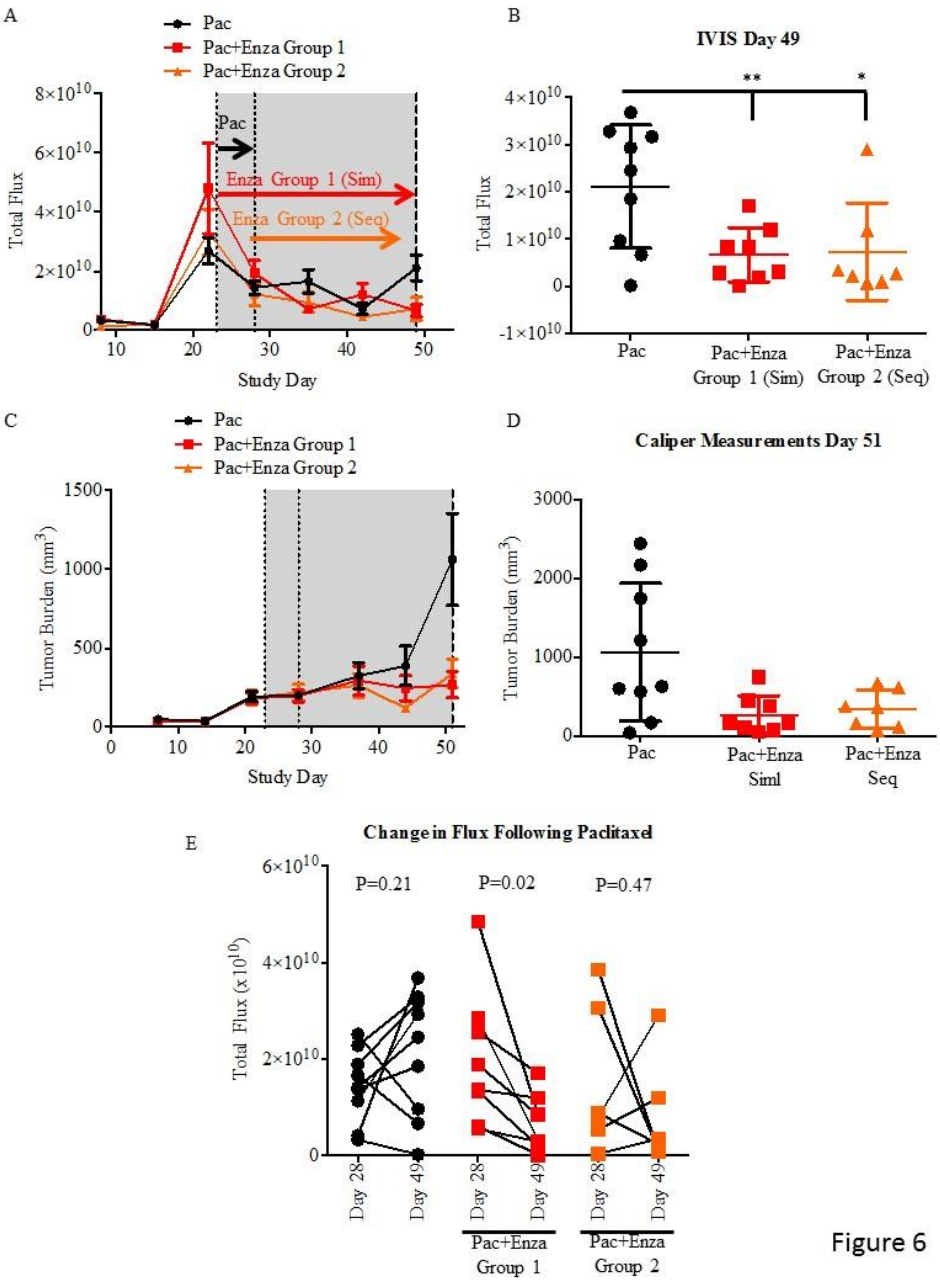

Figure 6

We have been testing Enza on various patient derived xenografts (PDX). Figure 8 shows an AR+ PDX HCI009 from Dr. Alana Welm that is highly AR+. We treated mice bearing these tumors with Enza and did not get much of an effect (Figure 8), so we are currently doing a similar experiment to the one shown above where we treat with paclitaxel with or without Enza. We will also perform an in vivo experiment with the HER2+ PK62 PDX to determine if enzalutamide and trastuzumab synergize to inhibit tumor growth in this model as we showed above in HER2+ cell lines.

Figure 8. Enzalutamide treatment of AR+ TNBC PDX. *5 NSG mice per group (plus or minus enzalutamide at 25 mg/kg in rodent chow or control chow) were treated to determine if this AR+ TNBC would respond to an anti-androgen. While the data were not significant by a repeated measures ANOVA, we will repeat with a larger group and try combining with chemotherapy given the results presented above with the SUM159 TNBC xenografts.*

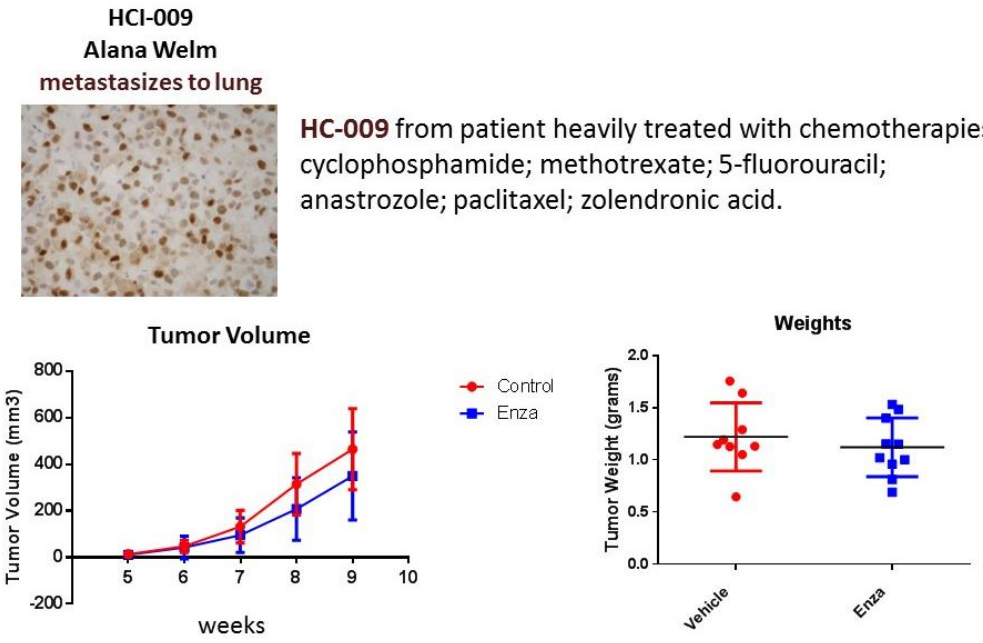

Preclinical Aim 2. **Using samples collected from the xenograft studies, examine if and how the mechanism of action by which enzalutamide works in the various subtypes of breast cancer.**

- **Task 1.** Perform IHC on xenograft tumors for AR, ER, Her3, BrdU, FOXA1, SDF1, Cyr61. Months 12-18.

We have performed IHC for all of these protein from the xenograft experiments on ER+, HER2+ and TNBC where relevant (see papers in appendix).

- **Task 2.** Make RNA from xenografts. Perform profiling. Analyze data. Months 15-18 (80% completed)

We continue to analyze RNA profiling from ER+ and TNBC cell line xenografts. We have performed RNA-seq on ER+PDX (the PT12 PDX grown with E2 plus or minus Enza and report this data in the D'Amato paper attached in the appendix. In short, inhibiting AR with Enza, inhibits many classic E2/ER regulated genes.

We have made RNA and protein from the BT474 HER+ xenografts treated with the different combinations of everolimus, trastuzumab or either with enzalutamide, shown above in Fig 6. We are also doing RPPA on the control, enza, everolimus versus the combination.

Preclinical Aim 3. Identify mechanisms of resistance to enzalutamide in triple negative breast cancers to elucidate pathways that impinge on the AR pathway to potentially target in combination with enzalutamide.

- **Task 1.** Sequence 3 AR+ triple negative cell lines resistant and 3 that are sensitive. Months 18-24

  Since the TNBC cell lines that we have studied so far are sensitive to enzalutamide and we have found it to particularly affect growth on soft agar (Barton V et al 2015), we have not performed sequencing of all of these yet because we are still trying to figure out the best conditions and timing. We are also exploring another approach, which is to chronically treat the cells with enza to generate resistant lines. We have taken this approach with the MDA-MB-453 TNBC line which we showed in Cochrane et al 2014 to be very responsive to enza in vitro and in vivo. We now have a resistant line and we will sequence it and compare to the parental line. We did do mutational analysis on the resistant line and it does not have the F876L mutation that has been reported to confer resistance to enzalutamide in prostate cancer cells and patient

tumors or the post-treatment biopsies that we obtained from the enzalutamide clinical trial described in Dr. Elias's report. It is likely that the cell line that we have rendered resistant is resistant via a different mechanism other than this AR mutation. It could also now be dependent on a completely different pathway other than AR and only RNA-seq would potentially tell us that, so we will proceed to do that compared to the wild-type line and continue to generate additional TNBC resistant lines.

Summary for this aim:

- No completely resistant TNBC lines. Enza IC50s does not correlate with AR protein.
- No clearly "sensitive" versus "resistant" cell lines. Still looking at PDX. Do have MDA-MB-231 with splice variant and they also express more GR.

Analysis of samples from biopsies of Phase 1 Enza trial. We got 6 breast cancers from this trial (see Fig 9 below**.** Because this was a Phase 1, the patient criteria was very loose and the tumors are therefore very different form each other.

Figure 9. Summary of archival (primary tumor) tumors from Phase 1 Enza trial. *We obtained 6 patient breast cancers from this trial. Characteristics of the primary disease and the clinical outcomes are summarized here.*

Clinical Characteristics

UPN	Age	Histology	ER arch	PR arch	Her2 arch	AR arch	Ki67 %	Adj CT	Adj HR	Prior CT	Prior HR	Regimen	Best Resp	TTP mos	OS mos	
001	78	IDC	3+ 96%	Pos	Neg	2-3+ 90%	20	No	Tam	4	7	E	PD	2	33+	
002	55	IDC	3+ 95%	3+ 63%	1+	2-3+ 80%	30	No	No	1	2	E	PD	2	14	
003	67	IDC	3+ 99%	?	Neg	2+ 80%	30	CAF	Tam	3	2	E	PD	2	5+	mut ESR1 Y537N
004	37	IMC/ IBC	Neg	Neg	Neg	1+ 30%	70	No	No	2	0	E	PD	2	3	
005	53	IDC	1+ 20%	Pos	Neg	2+ 90%	30	CMF	No	0	2	EF	SD	10	25+	mut ESR1 Y537S
006	57	ILC	3+ 95%	Neg	1+	3+ 60%	2	No	No	0	2	EF	SD	4	14	

Mutation analysis was performed for 3 most common ER mutations and the AR mutation resulting in the F876L variant. Two patient biopsies had the ER mutation resulting in Y537S, but none had the AR mutation.

For 3 of the 6 we had as part of the biopsy trial, obtained the pre-Enza and during Enza core biopsies. Figure 10 shows a summary of AR, ER and Ki67 for these three tumors and highlights some of the results.

Although the tumors are quite different from each other, we learned from this that AR is sometimes quite different between the primary tumor and the biopsied skin metastases. Although this is far to few to draw any conclusions, the patient's whose tumors had AR did have the best outcomes with stable disease and longer overall survival, but this could be because, as indicated by the Ki67, their disease was not as aggressive.

Figure 10. IHC from three patients from the Phase 1 Enza trial for whom we had the archival (primary FFPE sample, the pre-Enza biopsy and the on Enza biopsy. *IHC for AR, ER and Ki67 was performed and scored by breast cancer pathologist Sharon Sams.*

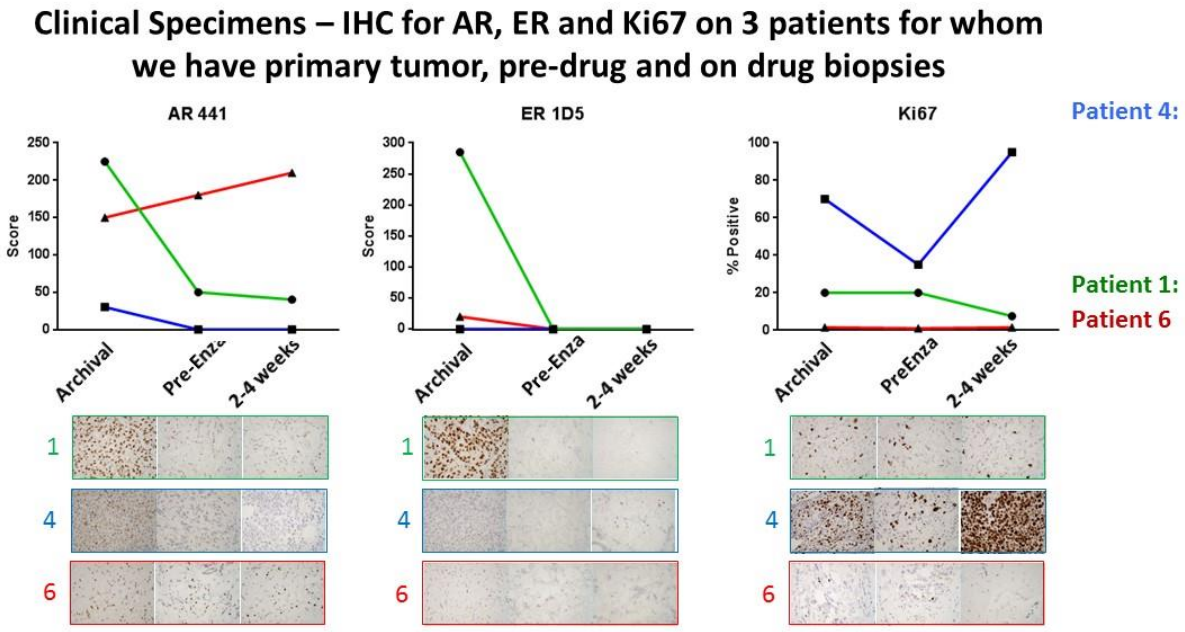

Primary tumor often quite different than metastatic disease.

Patient 1: Highly ER+/PR+ and AR+ primary tumor, but AR fell to 50% in pre-treatment biopsy. Had progressive disease, but overall survial of 33+ months

Patient 4: Had TN disease, and lost AR low status pre-treatment. Aggressive tumor (high Ki67)

Patient 6 Had highest pretreatment AR level and had **disease stabilization**. Also got fulvestrant before enza and also with.

Frozen sections were cut and analyzed for tumor by the Univ of CO Pathology Core and sent on dry ice to the laboratory of collaborator Dr. Chip Petricoin. RPPA for signaling proteins was performed according to methods in the appendix attached to this report.

Figure 11. RPPA results from 3 patient's tumors from biopsy trial comparing common phospho-proteins in pre-Enza versus during Enza of LCM dissected frozen sections from the core biopsies.

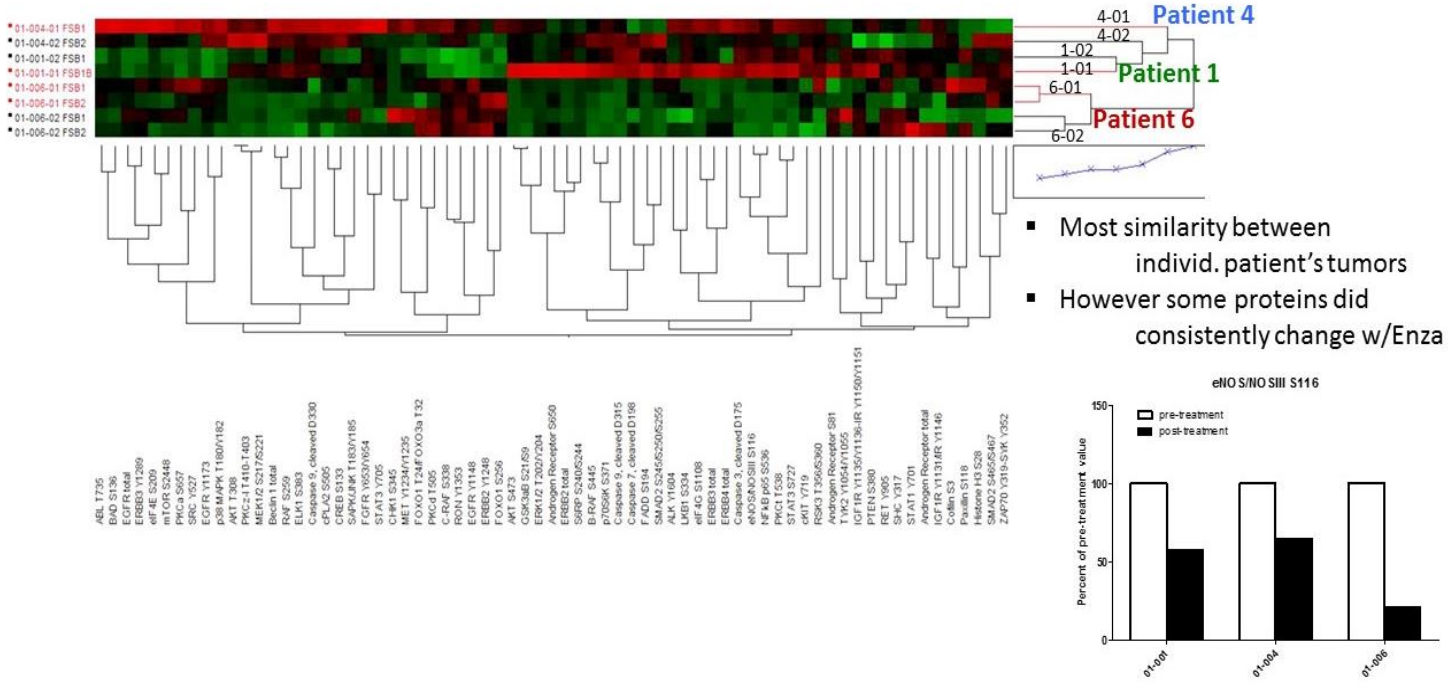

Figure 12. RPPA results showing individual phospho forms of proteins assayed from 3 patient's tumors that consistently changed in pre-Enza versus during Enza in LCM dissected frozen sections from the core biopsies.

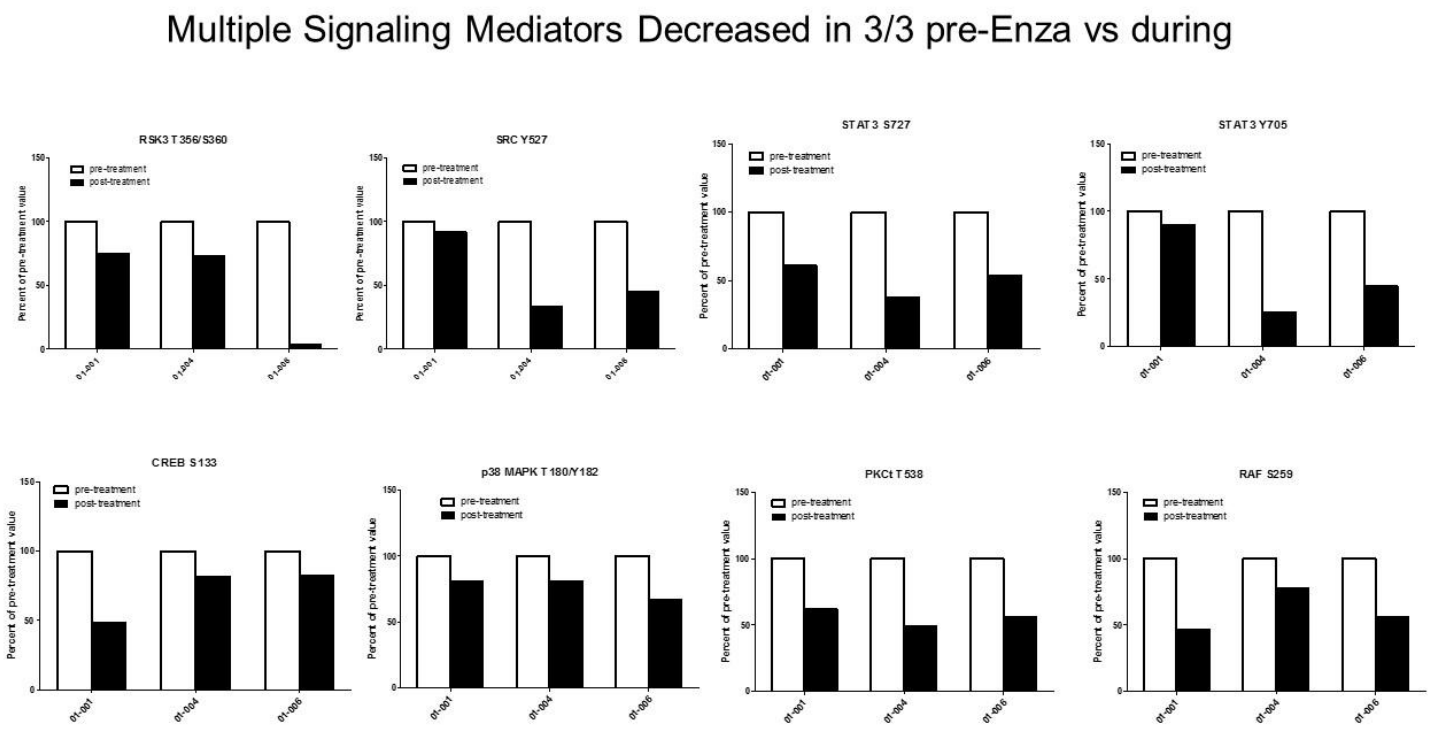

Since the samples were so different from each other, it is not surprising and actually rather conforting that they cluster based on which patient they came from rather than treatment (Figure 11). However, there were some proteins that changed consistently between pre-Enza and during Enza. A group of such proteins include many signaling intermediates (Figure 12). It is very interesting that Enza may change these growth factor signaling pathways, and it agrees with our published observation that AR regulates AREG and thereby stimulates EGFR and we also see that it upregulates components TGFbeta and Notch pathways (Figure 12 top).

What opportunities for training and professional development has the project provided?
Dr. Valerie Barton defended her dissertation in April 2016. She had obtained an NIH NRSA for work that stemed from this grant.

Cancer Biology Graduate Program doctoral candidate Valerie Barton and postdoctoral fellows Nicholas D'Amato and Michael Gordon have presented the following oral and poster presentations on this project at various national and local meetings:

Nicholas D'Amato Poster presentations:
D'Amato, NC, D Cochrane, N Spoelstra, A Chitrakar, B Babbs, A Protter, A Elias, and J Richer. (Mar 2014) Inhibiting Androgen Receptor Nuclear Localization Decreases ER Activity and Tumor Growth in ER+ Breast Cancer. University of Colorado Postdoctoral Research Day, Aurora, CO. * won best overall poster award.

D'Amato, NC, B Jacobsen, N Spoelstra, B Babbs, A Elias, J Gertz, and J Richer. (Oct 2014) Inhibiting Androgen Receptor Nuclear Localization Decreases Estrogen Receptor Activity and Tumor Growth in ER+ Breast Cancer. Cancer Biology Training Consortium Retreat, Estes Park, CO.

D'Amato, NC, B Jacobsen, N Spoelstra, B Babbs, A Elias, J Gertz, and J Richer. (Dec 2014) Inhibiting Androgen Receptor Nuclear Localization Decreases Estrogen Receptor Activity and Tumor Growth in ER+ Breast Cancer. San Antonio Breast Cancer Symposium, San Antonio, TX.

D'Amato, NC, B Jacobsen, N Spoelstra, B Babbs, A Elias, J Gertz, and J Richer. (Aug 2015) Inhibiting Androgen Receptor Nuclear Localization Decreases Estrogen Receptor Activity and Tumor Growth in ER+ Breast Cancer. Hormone-Driven Cancers Gordon Research Conference, Newry, ME.

Nicholas D'Amato Oral presentations:
Invited oral symposium presentation: Targeting Androgen Receptor in Her2-Driven Breast Cancer. Endocrine Society Annual Meeting, June 2013, San Francisco, CA.

Invited short talk: Targeting Androgen Receptor to Inhibit ER+ Breast Cancer Growth. Keystone Nuclear Receptors Meeting, January 2014, Taos, NM.

The Role of Androgen Receptor in Estrogen Receptor Activity in ER+ Breast Cancer. Functional Development of the Mammary Gland Program Project Grant Retreat, February 2014, Aurora, CO.

Targeting Androgen Receptor to Inhibit ER+ Breast Cancer Growth. UC Denver Anschutz Medical Campus Hormone Related Malignancies Retreat, March 2014, Aurora, CO.

Inhibiting Androgen Receptor Nuclear Localization Decreases ER Activity and Tumor Growth in ER+ Breast Cancer. UC Anschutz Medical Campus Postdoctoral Research Day, March 2015, Aurora, CO.

Inhibiting Androgen Receptor Nuclear Localization Decreases ER Activity and Tumor Growth in ER+ Breast Cancer. Division of Endocrinology Research Conference, March 2015, Aurora, CO.

Invited oral symposium presentation: Inhibiting Androgen Receptor Nuclear Localization Decreases Estrogen Receptor Activity and Tumor Growth in ER+ Breast Cancer. Hormone-Driven Cancers Gordon Research Conference, August 2015, Newry, ME.

Valerie Barton Oral presentations:

Barton VN, D'Amato N, Richer JK. Androgen receptor (AR) supports a cancer stem cell-like population in

AR+ triple negative breast cancer. Oral presentation at Gordon Research Conference, Hormone-Dependent Cancers, Newry ME, August 2015.

Barton VN, D'Amato N, Richer JK. Androgen receptor in triple negative breast cancer. Oral presentation at Obesity-Cancer Retreat, University of Colorado Anschutz Medical Campus, August 2015.

Barton VN, D'Amato N, Richer JK. Androgen receptor (AR) supports expansion of cancer stem-like cells in AR+ triple negative breast cancer. Oral presentation at Hormone Related Malignancies Symposium, University of Colorado Anschutz Medical Campus, May 2015.

Barton VN, D'Amato N, Richer JK. Endocrine therapy for triple negative breast cancer. Oral presentation at Pathology Grand Rounds, University of Colorado Anschutz Medical Campus, October 2014.

Graduate student Valerie Barton Poster presentations:
Barton VN, D'Amato NC, Gordon MA, Jacobsen BM, Richer JK. Multiple subtypes of triple negative breast cancer are dependent on androgen receptor. Presented at San Antonio Breast Cancer Sympoisum, December 2014.

Barton VN, D'Amato NC, Richer JK. Androgen receptor (AR) supports a tumor initiating population in AR+ triple negative breast cancer. Presented at Gordon Research Conference on Hormone Dependent Cancers, August 2015.

Postdoc Michael Gordon Poster presentations:
Gordon MA, D'Amato N, Gu H, Liu B, Elias A, Richer JK. Targeting multiple pathways in breast cancer: Androgen Receptor, HER2, and mTOR. Presented at San Antonio Breast Cancer Symposium, December 2014.

Gordon MA, D'Amato N, Gu H, Liu B, Elias A, Richer JK. The anti-androgen enzalutamide synergizes with trastuzumab and everolimus to inhibit breast cancer growth via distinct mechanisms. Selcted for oral poster preview presentation, Endocrine Society Annual Meeting, March 2015.

Oral presentation at Keystone meeting 2016, Nuclear Receptors Full Throttle – "Targeting multiple pathways in breast cancer: Androgen Receptor, HER2, and mTOR".

Postdoc Jessica Christenson presentations:
Oral presentation, University of Colorado Denver Hormone-Related Malignancies Seminar Series, 2016: **Christenson JL**, Butterfield K, Spoelstra N, Richer JK. *The potential role of AR in TNBC metastasis: Characterization of an AR+ immunocompetent model*

Abstract and oral presentation, Mammary Gland Biology – Gordon Research Seminar and Conference, 2016, Italy: **Christenson JL**, Butterfield K, Spoelstra N, Norris J, Josan J, Pollock J, Katzenellenbogen B, Katzenellenbogen J, Richer JK. *MMTV-PyMT and derived Met-1 mouse mammary tumor cells as models for studying the role of the androgen receptor in triple-negative breast cancer progression.*

- **How were the results disseminated to communities of interest?**

June 2013 Nicholas D'Amato gave a presentation to a group of donors for the **Colorado Springs, Colorado Chapter of the American Cancer Society** regarding the AR in breast cancer project.

July 2014 Nicholas D'Amato was invited to **Anchorage, AK** as the keynote speaker for an event for a new local chapter of the **American Cancer Society** - Making Strides kickoff event. I presented my work in lay terms to an audience of 150+ people, and also had separate meetings with physicians, caregivers, and local ACS staff to discuss

Dr Richer gave the following lectures locally, at various institutions, and national meetings

May 2014 **MD Anderson Breast Cancer Research Program Retreat** One of two Keynote Speakers with Thea Tilsty "Targeting Androgen Receptors in a Subset of Triple Negative Breast Cancers."

May 2015 **Bayer Scientific Advisory Board** Whippany, NJ "Landscape of Androgen Receptors in Breast Cancer Subtypes"

July 2015 **Virginia Commonwealth University** Department of Pathology Grand Rounds

Aut 2015 **Medivation Inc**. SF, CA Update on Androgen Receptors in Breast Cancer Preclinical Models

Sept 2015 **The US Oncology Network McKesson Annual Science Forum,** Dallas, TX "Role of Androgen Receptors in Breast Cancer"

July 2015 **Virginia Commonwealth University** Department of Pathology Grand Rounds

Aug 2015 **Medivation Inc**. SF, CA Update on Androgen Receptors in Breast Cancer Preclinical Models

Sept 2015 **Van Andel Institute/Michigan State University**, Department of Obstetrics, Gynecology and Reproductive Biology "Androgen Receptors in Breast Cancer: Estrogen Receptor alpha. Accomplice, Competitor, or Substitute?"

Feb 2016 **Huntsman Cancer Institute, Division of Oncological** Sciences "A Potential New Endocrine Therapy for Breast Cancer – Even Triple Negative"

Local:

2016 March 11 Hormone Related Malignancy Seminar University of Colorado Cancer Center Anschutz Medical Campus "Reflections on AR as a therapeutic target in breast cancer"

2016 March 7 Breast Cancer Research Program "University of Colorado Cancer Center A potential new endocrine therapy for breast cancer- even triple negative

National Meetings:

Jan 2016 "Subtype-Specific AR Action in Breast Cancer" **Keystone Symposium Nuclear Receptors**, Snowbird Utah.

April 2016 "Role of Androgen Receptors in Breast Cancers Resistant to Estrogen Receptor-Directed Endocrine Therapies" **Endocrine Society Annual Meeting 2016**, Boston, Massachusetts,

May 2016 **Richer, JK.** Invited short talk "Targeting the Androgen Receptor in Triple Negative Breast Cancer, **Gordon Research Conference on Mammary Gland Biology and Cancer**, Lucca, Italy,

- **What do you plan to do during the next reporting period to accomplish the goals?**

We will finish the drafts of the papers shown in appendix and submit them for publication. We will continue studies of Enza in PDX models and try to learn more about basic mechanisms from our RNA-seq and IHC analyses. We will continue to analyze patient samples when the new investigator initiated trials are activated.

IMPACT:

- **What was the impact on the development of the principal discipline(s) of the project?**

  These studies are helping to determine the role of androgen receptors in breast cancer and whether new anti-androgens might be utilized as therapy for breast cancers that fail to respond or reoccur while women are on current therapies such as anti-estrogens, trastuzumab or chemotherapy. These studies have provided preclinical evidence that the anti-androgen enzalutamide could serve as the first effective targeted therapy for a subset of triple negative breast cancers (TNBC). TNBC is the most aggressive type of breast cancer and there is currently no effective treatment for TNBCs with de novo or acquired resistance to chemotherapy. Our ongoing studies regarding timing (concurrent treatment with chemotherapy and enzalutamide versus sequential) will provide valuable information for upcoming clinical trials. Our studies on the effect of enzalutamide on the process of metastasis will also inform clinical trial design as will the studies of combined therapy with fulvestrant in breast cancer patients with ER+ disease.

- **What was the impact on other disciplines?** Our studies of how steroid hormone receptors affect each other is definitely pertinent to other cancers and development. Already other investigators and Ventana are looking closely at developing our idea of examining the AR to ER ratio not only in breast, but other cancers (lung and bladder and others) as we did in our published papers.

- **What was the impact on technology transfer?**
  - Transfer of results to entities in government or industry: The results of this project are also reported to our clinical industry partners Medivation Inc and Astellas Pharma who are running the clinical trials of enzalutamide in prostate and breast cancer. They are very interested in our preclinical results combining enzalutamide with other therapeutics currently being utilized in breast cancer since these results will guide the design of further industry or investigator initiated clinical trials. We filed a patent on the idea of looking at the AR to ER ratio in breast cancer and the company Ventana signed an agreement to pay the filing fees in Europe and to contract some additional sponsored research to design a clinical test to examine the ratio of these two receptors using their antibodies potentially simultaneously on the same section of tumor.

  - **What was the impact on society beyond science and technology?**
  - Since we have given reports of our research to several lay audiences in various community settings, we believe we are improving public knowledge regarding how hormones typically thought of as male hormones (such as androgens) are made by women and do affect women's health.

CHANGES/PROBLEMS: Nothing to Report

Changes in approach and reasons for change

- Describe any changes in approach during the reporting period and reasons for these changes. Remember that significant changes in objectives and scope require prior approval of the agency.
- **Actual or anticipated problems or delays and actions or plans to resolve them**. We found that AR protein expression in TNBC PDX models was decreasing even after two passages. However, we have now found that with androgen treatment, AR is re-expressed and we will now see if that confers an even better response to enzalutamide.
- **Changes that had a significant impact on expenditures**. Nothing to report.
- **Significant changes in use or care of human subjects, vertebrate animals, biohazards, and/or select agents** No significant changes, but we had to do a three year re-write of the protocol and that was approved by the local IACUC and the DOD.

  Significant changes in use or care of human subjects. None

- **Significant changes in use or care of vertebrate animals. None**
- **Significant changes in use of biohazards and/or select agents. None**

PRODUCTS:

Journal publications.

In addition to the Cochrane *et al* 2014 paper below, which was reported in the first Annual Progress report, we have published two manuscripts on AR in TNBC. One of these is a primary paper and one an invited review.

Dawn R. Cochrane, Sebastian Bernales, Britta M. Jacobsen, Diana M. Cittelly, Erin N. Howe, Nicholas C. D'Amato, Nicole S. Spoelstra, Annie Jean, Paul Jedlicka, Kathleen C. Torkko, Andy Protter, Anthony D. Elias and **J. K. Richer**. Role of the Androgen Receptor in Breast Cancer and Preclinical Analysis of Enzalutamide. BREAST CANCER RESEARCH 2014 Jan 22;16(1). PMID: 24451109 Designated as Highly Cited by the journal Breast Cancer Research.

Barton VN, Gordon MA, Christenson J, D'Amato N, Richer JK. Androgen receptor biology in triple negative breast cancer: A case for AR+ and quadruple negative disease subtypes. Hormones and Cancer, 2015 July 23. PMID: 26201402

BartonVN, D'Amato NC, Gordon MA, Lind HT, Spoelstra NS, Babbs B, Heinz RE, Elias A, Jedlicka P, Jacobsen BM, Richer JK. Multiple molecular subtypes of triple negative breast cancer critically rely on androgen receptor and respond to Enzalutamide in vivo. Mol Cancer Ther.015 Mar;14(3):769-78. Epub 2015 Feb 23. PMID: 25713333

We have another paper that is almost ready to submit and it is attached in the appendix.

- **Books or other non-periodical, one-time publications.** Nothing to report.
- **Other publications, conference papers, and presentations.**

Dr.Richer presented the following seminars/lectures/posters:

Dr Richer gave the following lectures:

May 2014 **MD Anderson Breast Cancer Research Program Retreat** One of two Keynote Speakers with Thea Tilsty "Targeting Androgen Receptors in a Subset of Triple Negative Breast Cancers."

May 2015 **Bayer Scientific Advisory Board** Whippany, NJ "Landscape of Androgen Receptors in Breast Cancer Subtypes"

Aug 2015 **Medivation Inc**. SF, CA Update on Androgen Receptors in Breast Cancer Preclinical Model

Sept 2015 **The US Oncology Network McKesson Annual Science Forum,** Dallas, TX "Role of Androgen Receptors in Breast Cancer"

- **Website(s) or other Internet site(s)**:

Expert Opinion piece in Oncology PracticeUpdate http://www.practiceupdate.com/journalscan/9370 or http://prac.co/j/5960d32c-988b-423e-ba24-14ca5c8cc39a?elsca1=soc_share-this acknowledgement of federal support –no

Highlight of Cochrane DR et al **Breast Cancer Research** 2014 in Feb issue of 2014 NATURE REVIEWS CLIICAL ONCOLOGY. acknowledgement of federal support –yes

- **Technologies or techniques**. None
- **Inventions, patent applications, and/or licenses**

  Richer *et. al*., PCT Patent Application WO 2014/031164 filed March 15, 2013, "Methods for Determining Breast Cancer Treatment."

  Protter and JK Richer, PCT Patent Application PCT/US2012/48471 Serial No. 14/236,036 filed on January 29, 2014 "Treatment of Breast Cancer."

- **Other Products**

  data or databases- we now have databases of genes expression data from the following experiments.

  ER+ MCF7 breast cancer cells treated in vitro with vehicle, enzalutamide alone, estradiol alone (E2), E2 plus enzalutamide for 48 hrs.

  ER+ MCF7 breast cancer cells grown as xenografts in nude mice treated with E2, E2 plus tamoxifen, or E2 plus enzalutamide**.**

  HCC1806 TNBC breast cancer line treated in vitro with either vehicle, DHT, enzalutamide alone, DHT plus enzalutamide.

  SUM159 treated in vivo.

  Are working on two TNBC PDX treated in vivo with or without DHT

- **biospecimen collections**;

  formalin fixed paraffin embedded xenograft tumors from the following experiments:

  MCF7 tumors grown in nude mice and treated with either E2, E2 plus tamoxifen, E2 plus enzalutamide or in a separate experment, the same treatments plus the combination of E2 plus enzalutamide and tamoxifen.

  Triple negative breast cancer (TNBC) cell line SUM159PT grown as xenograft tumors in mice treated with control rodent chow or enzalutamide containing chow.

  TNBC cell line HCC1806 grown as xenograft tumors in mice treated with control rodent chow or enzalutamide containing chow.

- research material (e.g., Germplasm; cell lines, DNA probes, animal models); We have generated luciferase labelled breast cancer cell lines to image by IVIS and put nuclear red and green expression vectors in these lines to utilize the Incucyte machine to count the number of red or green nuclei to do real time proliferation assays with enzalutamide alone or in combination with standard therapies for breast cancer.
- Biopsies (frozen and FFPE) cores obtained from Phase 1 trial are stored with our Pathology Core.

- **What individuals have worked on the project?**

nel since the last reporting period? Nothing to Report."

No changes in active support for the PD/PI(s) or senior/key personnel.

- **What other organizations were involved as partners?** Medivation Inc. and Astellas Pharma are the Industry partners.

SPECIAL REPORTING REQUIREMENTS

- **COLLABORATIVE AWARDS:** Partnering PI, Dr. Anthony Elias has sent a separate report on the clinical progress.
- **APPENDICES:** The Appendix contains the following documents

1. **Description of two tiers of CAP antibody validation:** validation to provide prognostic information requires 10 positive and negative cases, examination by a pathologist and sign off on documentation. Validation for predictive markers such as ER/PR and HER2 much more extensive.
2. **Documentation of AR staining in a CLIA certified lab, but all IHC funded by this grant is for research purposes only –** no clinical decisions are being made based on AR staining in the initial biopsy trial or in our future trials.
3. **Prostate diagnostic lab documentation of AR staining with Ventana/Cell Marque AR antibody**
4. **Explanation of AR and ER mutation analysis**
5. **Results of mutation analysis in 6 patients from Phase 1 trial of Enza.**
6. **CLIA certificate of two labs we are using for our AR IHC.**
7. **RPPA technology and methods**
8. **D'Amato NC, MA Gordon, BL Babbs, NS Spoelstra, KT Butterfield, KC Torkko, VT Phan ,VN Barton, TJ Rogers, CA Sartorius, AD Elias, J Gertz, BM Jacobsen, and JK Richer. Cooperative Dynamics of AR and ER Activity in Breast Cancer.** ***Molecular Cancer Research,*** **accepted Aug 2016.**
9. **Barton VN, Christenson JL, Rogers TJ, Butterfield K, Babbs B, Spoelstra NS, D'Amato NC, Richer JK (2016) Androgen receptor supports a cancer stem cell-like population in triple-negative breast cancer.** ***In preparation.***
10. **Gordon MA, D'Amato NC, Gu H, Babbs B, Butterfield K, Liu B, Elias, Richer JK. Dual inhibition of androgen receptor and mTOR in breast cancer.** ***In Preparation.***

CAP designates antibody validation under two "tiers". Normal validation to provide prognostic information only requires 10 positive and 10 negative cases. Examination by pathologist, and sign off on the documentation. Validation for predictive markers such as ER/PR and Her2 are MUCH more extensive and involve the following:

1. Pre-analytics. You must be able to document formalin fixation time of all specimens used for validation and the tissue processing procedures (times, solutions, etc). This is a requirement for Her2, but is applicable to all predictive markers. Formalin fixation time of 6 to 72 hours are required. Tissue must be placed in formalin within 1 hour of collection. All specimens must be submitted in 10% neutral buffered formalin. Any other fixative would require complete revalidation. Specimens accepted from outside institutions must be accompanied with documentation of formalin fixation time. Decalcification of tissues must be noted on the requisition form, and requires the use of a disclaimer on the surgical pathology report indicating that the predictive marker has not been validated on decalcified tissues and the results should be interpreted with caution due to the likelihood of false negatives.
2. Documentation of microscopic criteria to determine positive/negative results and appropriate scoring system to include but not limited to, percent + cells, staining pattern.
3. Annually, the lab must compare it's patient results to published benchmarks and no more than 10-15% of the cases evaluated may be negatives.
4. Annually, each pathologist that interprets results must be compared to each other for concordance, and competency levels must be established and documented.
5. Validation of the testing method requires 40 cases (20+ and 20-) for each FDA-cleared test. Laboratory developed tests (of which AR would be) must have a higher number of cases (left to the discretion of the medical director, so 25+ and 25- would be adequate). If changing methodology, as in the case of changing antibody or staining method, revalidation is necessary and concordance levels must be 90% for positive cases and 95% for negative cases compared to the established method.

These requirements represent about 1% of what it takes to operate a CAP/CLIA lab. Validating an antibody for CAP/CLIA includes many hours of documentation of procedures and policies not relating directly to staining or scoring slides. There are ~400 line items that must be documented. CAP amends these requirements to include more documentation eachyear.

E. Erin Smith, HTL(ASCP)^{CM}QIHC, Histopathology Supervisor
UC Denver Pathology
Histology Subspecialty Laboratory
12605 E. 16th Ave, AIP-1 Room 3.000
Aurora, CO 80045 Phone: 720-848-4281 Fax: 720-848-4233
Research Histology Shared Resource
12800 E. 19th Ave, P18-5404G
Aurora, CO 80045 Phone: 303-724-3775 Fax: 303-724-3781

PROSTATE DIAGNOSTIC LAB: RESEARCH REQUEST FORM

PI: Dr. Jennifer Richer Date Submitted: 10/21/15 MSL approval /date: _____

Study or Purpose: Stain cases with Cell Margen Androgen Receptor

Speedtype to charge for reagents: _____ ☐ Pilot Study

Material Submitted: Please Circle

Cultured cells Fresh Tissue Frozen Tissue Fixed Tissue Paraffin Block Slides

---

Work Requested: Immunohistochemistry

Technical Consultation (15 minute minimum): _____

Terms of Use for Submitting a Request to the Prostate Diagnostic Laboratory:

The provided specimens and isolated or derived products of these specimens will only be used for the studies that are proposed and disclosed to Dr. Lucia and that are sanctioned under a valid COMIRB protocol. Under no condition will materials be distributed or provided to other researchers outside the scope of the proposed project without written permission from Dr. Lucia. If materials need to be transferred to external sites for the purpose of this study, the investigator will provide Dr. Lucia with an approved and dated copy of the COMIRB protocol and/or Materials Transfer Agreement before the materials are transferred.

Acknowledgement:

I agree to acknowledge the contributions of the PIs and technical staff of the PDL in all publication, grant submissions, and presentations resulting from this request.

Suggested acknowledgement for manuscripts: The authors would like to acknowledge the contributions of the members of the Prostate Diagnostic Laboratory at the University of Colorado Denver for their technical assistance and professional expertise.

I will provide Dr. Lucia with a copy of the manuscript before submission to ensure proper acknowledgement and a copy of the article after publication.

The Prostate Diagnostic Laboratory reserves the right to deny work requests.

_____ _____

Name Date

PROSTATE DIAGNOSTIC LAB: IMMUNOHISTOCHEMISTRY REQUEST

Amount of Material Submitted: _____ Fixation: _____

Material Labeled As: PHT22A PHT148ML PHT33A PHT21B (LOW)
PHT19AM PHT118M (HIGH) PHT34B PHT27A (LOW)
PHT07AM PHT35A (LOW)

***Please Note: The IHC tech is not responsible for acquiring your control material. ***

☐ Antibody Specification Sheet is attached or
Literature Reference: _____

☐ Antibody provided by researcher: _____
Positive Control Tissue: Prostate Cancer
Antibody: Androgen Receptor Vendor: Cell Marque LOT: 1328403E
EXP: 09.2016 46.0 ug/mL

LAB USE:

Species: Rabbit Monoclonal Localization: nuclear
Dilution: 1:50 Diluent: PCRL
or Titration: in dispenser Diluent: _____
HEIR: 100 mM Citrate 10 mM Citrate/TBS BORG DIVA dI H_2O Trilogy
HEIR Time: CC1 Standard HEIR Method: Pressure Microwave Boil
EIER: Pronase Protease Trypsin Proteinase K EIER Time: _____
EIER Method: Room Temp 37°C Ventana 37°C Signet Plate
Peroxidase Block: kit
Serum or Protein Block: none Amplifier: _____
Primary Antibody Incubation: 32' 1°ab 37°C Overnight: _____
Detection Kit: Ventana UltraView
Secondary Incubation: NA Diluent: _____ Concentration: _____
Enzyme Incubation: kit Diluent: _____ Concentration: _____
Chromogen (DAB or Alk Phos Red): DAB
Counterstain: Harris Hematoxylin 2'

RESULTS: Date: 10.21.15

* Stain acceptable.
Transferred to Nicole.

Lab Use Only:

Date Received _____

Date Completed _____ By: _____

Comments: _____

PI acknowledgement of completed work:

_____ Date: _____ ☐ Additional Pages Attached

AR & ER mutations

AR develops more spontaneous mutations than almost any other protein (1). Point-mutations within the ligand binding domain often develop after chronic anti-androgen treatment leading to drug resistance (2). In prostate cancer cell lines, chronic enzalutamide treatment leads to a missense mutation (F876L) within AR that causes resistance and partial agonist activity (3-5). In prostate cancer patients treated with a second-generation anti-androgen (ARN-509) similar to enzalutamide, the F876L mutation arose in approximately 10.3% of patients (3/29). The mutation was first observed between 28-60 weeks post-treatment initiation and correlated with tumor recurrence as measured by serum PSA levels (4).

Mutations to ER are much less common than those observed in AR and are found primarily in the metastases of breast cancer patients previously treated with anti-estrogens. Similar to AR mutations, however, ER mutations are predominately located within the ligand binding domain and are responsible for resistance (6). The most commonly observed ER mutation is the D538G mutation that enables constitutive ligand-independent activity of the ER. It was observed in 38% of metastases from patients with endocrine resistance, but was not found in the matched primary tumors of these patients (7).

1. Gelmann EP. Molecular biology of the androgen receptor. J Clin Oncol 2002;20:3001-15.
2. Eisermann K, Wang D, Jing Y, Pascal LE, Wang Z. Androgen receptor gene mutation, rearrangement, polymorphism. Transl Androl Urol 2013;2:137-47.
3. Balbas MD, Evans MJ, Hosfield DJ, Wongvipat J, Arora VK, Watson PA, et al. Overcoming mutation-based resistance to antiandrogens with rational drug design. Elife 2013;2:e00499.
4. Joseph JD, Lu N, Qian J, Sensintaffar J, Shao G, Brigham D, et al. A clinically relevant androgen receptor mutation confers resistance to second-generation antiandrogens enzalutamide and ARN-509. Cancer Discov 2013;3:1020-9.
5. Korpal M, Korn JM, Gao X, Rakiec DP, Ruddy DA, Doshi S, et al. An F876L mutation in androgen receptor confers genetic and phenotypic resistance to MDV3100 (enzalutamide). Cancer Discov 2013;3:1030-43.
6. Toy W, Shen Y, Won H, Green B, Sakr RA, Will M, et al. ESR1 ligand-binding domain mutations in hormone-resistant breast cancer. Nat Genet 2013;45:1439-45.
7. Merenbakh-Lamin K, Ben-Baruch N, Yeheskel A, Dvir A, Soussan-Gutman L, Jeselsohn R, et al. D538G mutation in estrogen receptor-alpha: A novel mechanism for acquired endocrine resistance in breast cancer. Cancer Res 2013;73:6856-64.

SNaPshot methods

Mutational analysis of the samples is performed using the SNaPshot Multiplex Reagent Kit (Applied Biosystems, Foster City CA) and custom primer and probe sets. Target regions are PCR amplified and then probed with the SNaPshot multiplex reagent and custom probes that hybridize one base 5' to the base of interest. A labeled dideoxy NTP is incorporated, and the resultant labeled probe is visualized using a capillary sequencer. Sample DNA is extracted from FFPE source material using the QiaAmp DSP FFPE DNA Extraction Kit (Qiagen, Valencia CA). Target regions of the AR and ER genes are amplified using custom primer sets (IDT, Coralville Iowa): ARForward: TGCGAGAGAGCTGCATCA, ARReverse:

GAAAGGATCTTGGGCACTTG, and ERForward: CAGCATGAAGTGCAAGAACG, ERReverse: GATGAAGTAGAGCCCGCAGT. PCR amplification is performed with the Kapa 2G Robust Hot Start Polymerase system (Kapa Biosciences, Wilmington MA), using the following conditions: 5µl Buffer A, 5µl Enhancer 1, 0.5µl 10mM dNTPs, 0.5µl 10µM Forward Primer, 0.5µl 10µM Reverse Primer, 12.4µl Water, 0.1µl Kapa 2G Robust HotStart Enzyme, and 1µl DNA sample (5-50ng). The PCR reaction mix is amplified on a 9700 Thermocycler (ABI, Foster City CA) under the following cycling conditions: 96°C-3min, 20 cycles: [94°C-15sec, 65°C-15sec (-0.5°C per cycle), 72°C-15sec], 20 cycles: [94°C-15sec, 55°C-15sec, 72°C-15sec], 72°C-10min. The PCR products are treated with 5µl ExoSAPit (Affymetrix,) and incubated on the thermocycler (37°C-60min, 80°C-20min) to remove unincorporated primers and dNTPs. The resultant PCR products are probed using 5µl SNaPshot reagent, 3µl PCR template, and 2µl 10µM custom probes: AR2626_Rev: GATCGATCGATCGATCGATCGATCGATCTACTTGATTAGCAGGTCAAAAGTGA (base 2626, codon 876), AR2629_Rev: GATCGATCGATCGATCGATCGATCGATCTACTTGATTAGCAGGTCAAAAG (base 2629, codon 877), ER1609_Rev: GATCGATCGATCGATCGATCGATCGATCGATCGATCGCATCTCCAGCAGCAGGTCAT (base 1609, codon 537), ER1610_Rev: GATCGATCGATCGATCGATCGATCGATCAGCATCTCCAGCAGCAGGTCA (base 1610, codon 537), ER1613_Rev: GATCGATCGATCGATCTCCAGCATCTCCAGCAGCAGG (base 1613, codon 538). The SNaPshot reactions are run on the 9700 thermocycler under the following conditions: 96°C-30sec, 25 cycles [96°C-10sec, 55°C-15sec, 60°C-1min]. The SNaPShot reaction is treated with 1µl Antarctic Phosphatase (New England Biolabs) and incubated on the thermocycler (37°C-60min, 80°C-20min) to remove unincorporated dNTPs. The final SNaPshot products are diluted 1:50 and run on a 3730 capillary sequencer (Applied Biosystems) to resolve the labeled probes. Chromatograms are analyzed using Genemapper 5 software (Applied Biosystems) and single-base sequence at the site of interrogation is determined by the color of the probe label.

Sample ID	Panel	AR876_R	AR877_R	ER1609_R	ER1610_R	ER1613_R
CUD000006535	01-001-01	WT	WT	WT	WT	WT
CUD000006536	01-001-02	WT	WT	WT	WT	WT
CUD000006537	01-001-Archival	WT	WT	WT	WT	WT
CUD000006538	01-002-Archival	WT	WT	WT	WT	WT
CUD000007433	01-003-Archival	WT	WT	WT	WT	WT
CUD000006691	01-003-01	WT	WT	c.1609T>A, p.Y537N	WT	WT
CUD000006539	01-004-01	WT	WT	WT	WT	WT
CUD000006540	01-004-02	WT	WT	WT	WT	WT
CUD000006541	01-004-Archival	WT	WT	WT	WT	WT
CUD000006542	01-005-01	WT	WT	WT	1610A>C, Y537S	WT
CUD000007119	01-005-003	WT	WT	WT	1610A>C, Y537S	WT
CUD000006543	01-005-Archival	WT	WT	WT	1610A>C, Y537S	WT
CUD000006692	01-006-Archival	WT	WT	WT	WT	WT

CENTERS FOR MEDICARE & MEDICAID SERVICES

CLINICAL LABORATORY IMPROVEMENT AMENDMENTS

CERTIFICATE OF COMPLIANCE

LABORATORY NAME AND ADDRESS

UNIVERSITY OF COLORADO DENVER
DIVISION OF MEDICAL ONCOLOGY
12801 E 17TH AVE
RC1S-8402J
AURORA, CO 80045

CLIA ID NUMBER

06D2003207

EFFECTIVE DATE

12/03/2014

EXPIRATION DATE

12/02/2016

LABORATORY DIRECTOR

FRED R HIRSCH MD, PHD

Pursuant to Section 353 of the Public Health Services Act (42 U.S.C. 263a) as revised by the Clinical Laboratory Improvement Amendments (CLIA), the above named laboratory located at the address shown hereon (and other approved locations) may accept human specimens for the purposes of performing laboratory examinations or procedures.

This certificate shall be valid until the expiration date above, but is subject to revocation, suspension, limitation, or other sanctions for violation of the Act or the regulations promulgated thereunder.

CMS
CENTERS FOR MEDICARE & MEDICAID SERVICES

Judith A. Yost, Director
Division of Laboratory Services
Survey and Certification Group
Center for Clinical Standards and Quality

175 Certs2_110414

If you currently hold a Certificate of Compliance or Certificate of Accreditation, below is a list of the laboratory specialties/subspecialties you are certified to perform and their effective date:

LAB CERTIFICATION (CODE)	EFFECTIVE DATE	LAB CERTIFICATION (CODE)	EFFECTIVE DATE
HISTOPATHOLOGY (610)	12/03/2010		

FOR MORE INFORMATION ABOUT CLIA, VISIT OUR WEBSITE AT WWW.CMS.GOV/CLIA
OR CONTACT YOUR LOCAL STATE AGENCY. PLEASE SEE THE REVERSE FOR
YOUR STATE AGENCY'S ADDRESS AND PHONE NUMBER.
PLEASE CONTACT YOUR STATE AGENCY FOR ANY CHANGES TO YOUR CURRENT CERTIFICATE.

CENTERS FOR MEDICARE & MEDICAID SERVICES

CLINICAL LABORATORY IMPROVEMENT AMENDMENTS

CERTIFICATE OF ACCREDITATION

LABORATORY NAME AND ADDRESS

UNIV OF COLORADO ANSCHUTZ MEDICAL CAMP
DEPT OF PATHOLOGY
ANSCHUTZ INPATIENT PAVILION RM 3-128 ANATOMIC PATH
12605 E 16TH AVE MSF768
AURORA, CO 80045

CLIA ID NUMBER

06D1007855

EFFECTIVE DATE

02/23/2016

LABORATORY DIRECTOR

SCOTT LUCIA M.D.

EXPIRATION DATE

02/22/2018

Pursuant to Section 353 of the Public Health Services Act (42 U.S.C. 263a) as revised by the Clinical Laboratory Improvement Amendments (CLIA), the above named laboratory located at the address shown hereon (and other approved locations) may accept human specimens for the purposes of performing laboratory examinations or procedures.

This certificate shall be valid until the expiration date above, but is subject to revocation, suspension, limitation, or other sanctions for violation of the Act or the regulations promulgated thereunder.

CMS
CENTERS FOR MEDICARE & MEDICAID SERVICES

Karen W. Dyer, Acting Director
Division of Laboratory Services
Survey and Certification Group
Center for Clinical Standards and Quality

235 Certs2_012616

If you currently hold a Certificate of Compliance or Certificate of Accreditation, below is a list of the laboratory specialties/subspecialties you are certified to perform and their effective date:

LAB CERTIFICATION (CODE)	EFFECTIVE DATE
BACTERIOLOGY (110)	06/27/2012
VIROLOGY (140)	12/15/2008
ROUTINE CHEMISTRY (310)	06/16/2010
HISTOPATHOLOGY (610)	11/03/2004
CYTOLOGY (630)	02/23/2004
CYTOGENETICS (900)	11/03/2008

LAB CERTIFICATION (CODE)	EFFECTIVE DATE

FOR MORE INFORMATION ABOUT CLIA, VISIT OUR WEBSITE AT WWW.CMS.GOV/CLIA
OR CONTACT YOUR LOCAL STATE AGENCY. PLEASE SEE THE REVERSE FOR
YOUR STATE AGENCY'S ADDRESS AND PHONE NUMBER.
PLEASE CONTACT YOUR STATE AGENCY FOR ANY CHANGES TO YOUR CURRENT CERTIFICATE.

Reverse Phase Protein Microarray (RPPA)

The Reverse Phase Protein Microarray (RPPA) technology has been developed to address the analytical challenges of the sandwich and forward phase protein arrays (e.g. mismatch of sandwich antibody affinity, imprecision within and between analytes, and poor sensitivity). The platform has been designed to enable non-subjective, quantitative, multiplexed analysis of specific forms of cellular proteins (e.g. phosphorylated, unphosphorylated, and cleaved) from a limited amount of starting sample, such as with a fine needle aspirate or laser capture microdissected (LCM) cellular material to procure pure populations of the target cells of interest. Particularly suited for clinical tissue samples, RPPA uses a single antibody directed against the epitope of interest (Figure 1).

A key attribute of the RPPA is the ability to quantitatively measure hundreds of signaling proteins concomitantly from only a few thousand cells, thus providing a critical means of broad-scale cell signaling analysis directly from tissue samples, cell culture models, and animal tissues from pre-clinical studies. The RPPA technology, invented and in our (Petricoin/Liotta) laboratory and now optimized for routine clinical sample analysis (1-15), is currently being employed as a CLIA assay under development and evaluation within the CAP/CLIA accredited proteomics laboratory within the Center for Applied Proteomics and Molecular Medicine at George Mason University. No other technology can measure the activity of as many signaling proteins at once from such small amounts of input material.

Figure 1: Reverse Phase Protein Microarrays

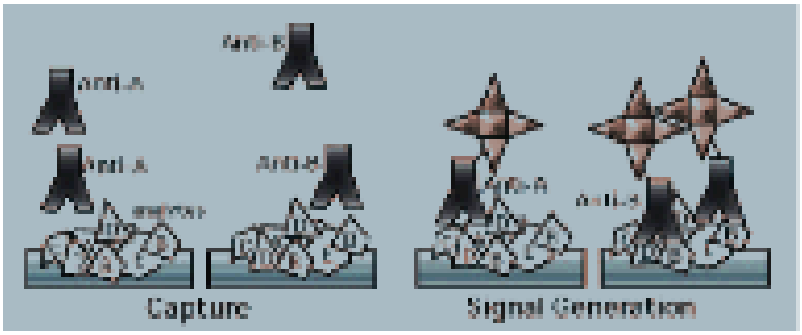

Figure 1. Reverse Phase Protein Microarrays (RPPA) immobilize the test sample analytes (eg. lysate from laser capture microdissected cells) on the solid phase. An analyte-specific ligand (e.g. antibody) is applied in the solution phase (Capture). Bound antibodies are detected by secondary tagging and signal amplification (Signal Generation). [1]

The RPPA consists of the following major steps. A graphic presentation of the testing process is presented in Figure 2.

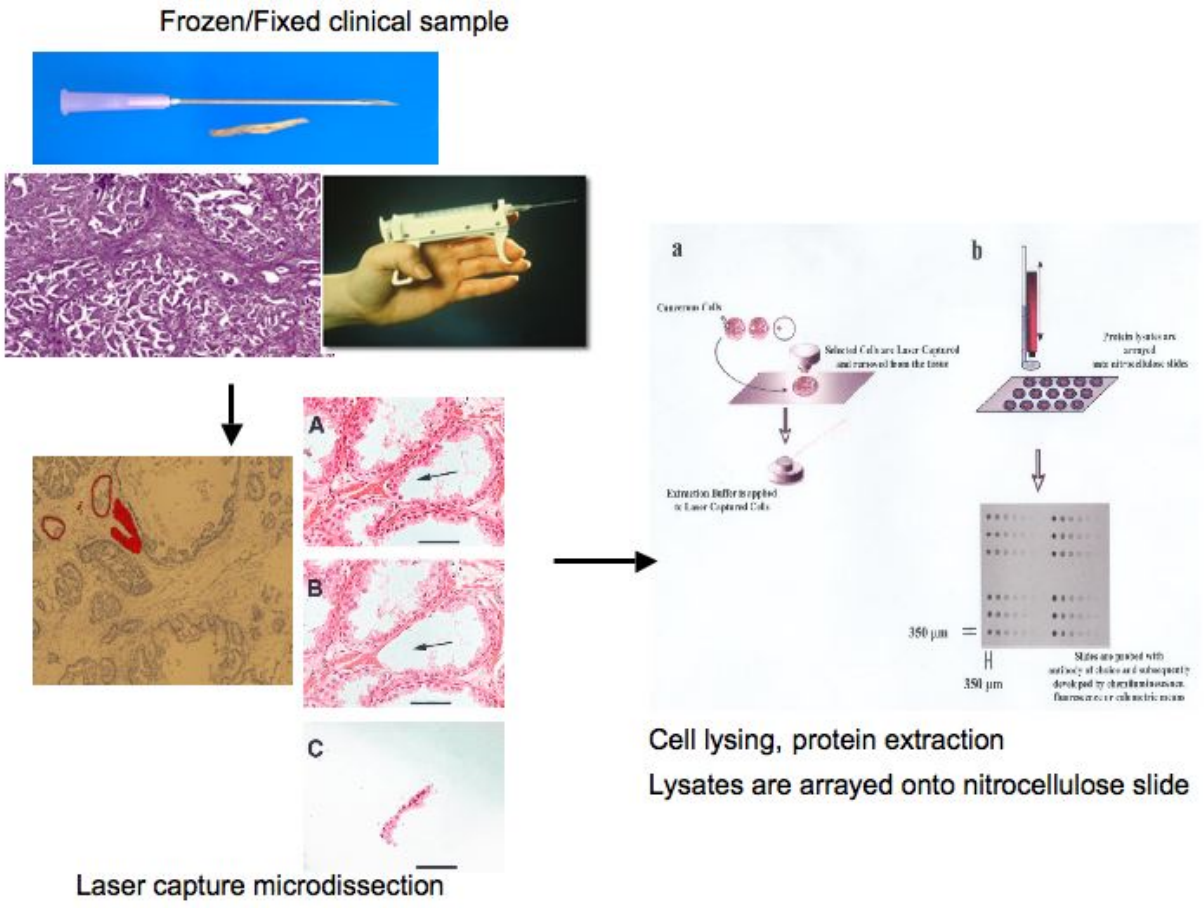

Figure 2: Overview of RPPA

A selection of peer-reviewed publications contains extensive detailed description of the basic core components RPPA methodology (1-15). The RPPA format immobilizes an individual test sample in each array spot. An array can be comprised of up to hundreds of patient samples or cellular lysates. Each array is incubated with a single primary antibody and a single analyte end point is measured. Since RPPAs maintain the concentration of the input sample, the sensitivity is greater as compared with a forward phase, (e.g. antibody array) probed with the same small number of input cells.

With the RPPA technology, serial dilutions are printed of each sample, control or standard, to maintain sample concentration. Each spot contains a bait zone measuring only a few hundred microns in diameter. The detection probe can be tagged and signal amplified independently from the immobilized analyte protein. Coupling the detection antibody with highly sensitive amplification systems can yield detection sensitivities to fewer than 1,000 to 5,000 molecules per spot with good linearity (correlation coefficient or R^2 = 0.990-0.999) and inter-experiment

precision (R^2= 0.973). Between run and within run analytical precision is between a 3-13% CV (coefficient of variation) (7).

The RPPA technology has been developed and optimized for performance as a fluorescent-based calibrated assay, generally identical in design and analysis to standard ELISA or standard clinical immunoassays. As a calibrated assay, each assay consists of:

a. Experimental patient samples printed in triplicate two-spot dilutions (neat and 1:4)
b. High, medium, and low controls printed in triplicate two-spot dilutions (neat and 1:4)
c. A calibrator, consisting of a 6-10-point curve whereby the analyte of interest is decreasing in concentration in the background of a constant protein concentration.

The analyte concentration is thereby determined by extrapolation to a non-parametrically determined curve fit of the calibration curve and reported in relative fluorescent units (Figure 3, below)

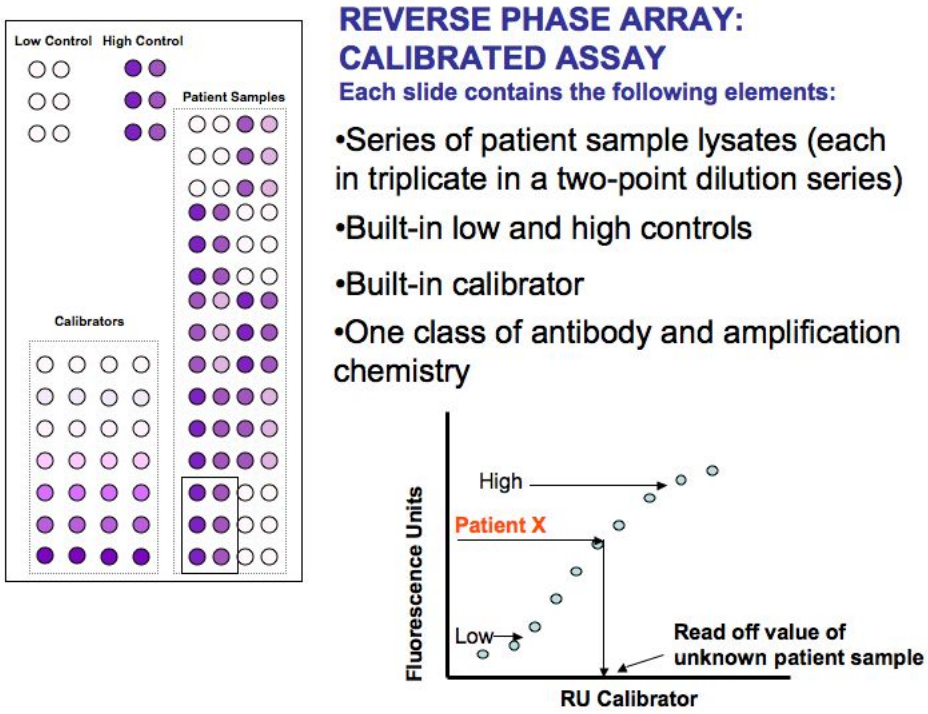

Figure 3. Illustrated schematic of a typical RPPA slide configuration

Sample Preparation for Microarray

In order to prepare the sample for arraying, proteins are extracted from the LCM polymer cap as a whole cell lysate using a heated sodium dodecyl sulfate-based lysing solution which produces a denatured lysate suspended in the sample/extraction buffer.

The optimal extraction buffer for extracting proteins from tissue cells that have been procured by LCM, with the purpose of performing reverse phase protein arrays, consists of a detergent, denaturing agent and buffer. This buffer is an efficient denaturing extraction buffer for the extraction and solubilization of cellular proteins from fixed and frozen tissue. An array layout grid is used to determine exact placement of sample and control cell lysates on the printed microarray. Cell lysate solutions for each sample, of a known volume and concentration are loaded into 384 well microtiter plates. Microtiter plates are specifically labeled and loaded into the well plate hotel in the correct order.

The RPPA uses slides coated with nitrocellulose. This type of slide is chosen for its high binding capacity, high surface area, minimum effect on protein structure, and intrinsically low background signal. For the printing run, up to 100 slides, (10 slides/platen and 10 platens within the Substrate Hotel), can be loaded into the Aushon 2470 Arrayer at a time.

Array Preparation

The Aushon 2470 Arrayer has a general software program to manage the printing process. The program enables customization of array printing, with parameters such as top and left offset of printing, depositions/feature, slide lot number, number of replicates, dwell time for pins, total number of immersions, maximum number of extractions and wash sequences.

Calibration of Values

As shown in Figure 3, each array contains a printed calibrator(s), a series of cell lystates derived from cells treated with a variety of mitogens such that broad pathway activation has been achieved. The calibrator(s) will consist of 6 – 10 dilutions of whole cell lysates from stimulated and unstimulated cells (eg. HeLa cells treated and untreated with pervandate for 30 minutes; jurkat cells treated and untreated with calyculin for 30 minutes; A431 cells treated and untreated with EGF for 30 minutes) pre-mixed in various ratios such that the total protein in any spot does not change, but the phospho-analyte changes in a predictable and defined concentration. Another type of calibrator can be prepared by spiking-in known amounts of recombinant protein or peptides that correspond to the target analyte and react specifically with antibodies directed to the target protein into a lystate that does not contain the target analyte. We print the EXACT SAME CALIBRATOR ON EVERY SINGLE SLIDE. The defining characteristic of this calibrator is that protein concentration does not vary but staining intensity does. Much like a clinical assay run in a diagnostic laboratory, each experimental value is extrapolated to a non-parametric curve fit of the calibrator within he region that span the dynamic range of the population such that results can be compared over time and across arrays. The calibrator is defined either in absolute amounts (if the analyte concentration is known), or in relative units (RUs) if the absolute amount of the analyte within the calibrator is not known. Most applications will use RU calibration units.

Data Normalization

Each protein analyte value is normalized to the total amount of protein printed on that spot by first incubated the slide with a florescent stain (Sypro Ruby Blot Stain, Molecular Probes, Eugene OR) that binds to proteins without bias and does not interfere with subsequent antibody binding. The protein loading value is also obtained by a calibrated assay technique. ON EVERY SLIDE WE PRINT A PROTIEN CALIBRATION CURVE OF THE EXACT SAME SAMPLE ON EVERY SINGLE SLIDE. This total protein calibrator consists of a protein lysate, which upon

dilution, spans the linear dynamic range of protein concentraion. Each sample value is then extrapolated to the calibrator. Consequently, while the total amount of protein may vary in any given sample compared to each other- thus affecting phopsho-protein measurements for each sample, this variance is greatly minimized by such a normalization procedure.

Blocking Procedure

Once arrays have been printed and stained for total protein, slides undergo a blocking procedure. Casein based solutions provide a uniform protein solution capable of binding to non antigenic sites on nylon, PVDF and nitrocellulose membranes. Casein blocks these sites, inhibiting binding of antibody. This results in reduced background staining for reverse phase protein arrays.

Staining and Image Acquisition

Arrays are probed using an antibody specific for the phospho-protein, or any protein analyte. Our current repertoire consists of over 350 phopshoproteins that have been extensively pre-validated for specificity using Western blotting and peptide competition. A Dako Cytomation Autostainer (FDA approved for the HercepTest) is used to perform the staining procedure. This includes the processes of incubation with primary antibody, specific for the analyte of interest as well as incubation with secondary antibody. A signal is generated using a near-IR fluorescent dye (LICOR Biosciences) that is coupled to the secondary antibody. The current iteration of the RPPA uses a fluorometric image capture processing system (e.g. NovaRay, Alpha Innotech) for image acquisition. The system measures the sample's fluorescence intensity value, subtracts the background, normalizes the result to the total protein, and extrapolates the value to the non-parametrically fit calibration curve to generate a final intensity value. The median of the triplicate values is reported.

Correlation of Calibrated Values with Clinical Outcomes

Calibrated values of patient samples are correlated with outcomes results (discontinuous variables (alive v dead, long v short survival), or continuous variables (overall survival, disease free survival, time to progression, etc). These values are usually reported in days, weeks or months. Statistical analysis is used for the correlative findings. Parametric (e.g, Student t-test) or non-parametric (e.g. Wilcoxon Rank Sum) of mean comparison is used, Kaplan Meir and ROC curves are used to uncover relationships between continuous clinical variables and continuous calibrated values. Optimally, any optimal cutpoint found by such analysis should be tested in independent study sets using ROC and or KM type analysis.

Selected References

1. Xia W, Liu Z, Zong R, Liu L, Zhao S, Bacus SS, Mao Y, He J, Wulfkuhle JD, Petricoin EF 3rd, Osada T, Yang XY, Hartman ZC, Clay TM, Blackwell KL, Lyerly HK, Spector NL. Truncated ErbB2 expressed in tumor cell nuclei contributes to acquired therapeutic resistance to ErbB2 kinase inhibitors. Mol Cancer Ther. 2011 Jun 14.

2. Popova TG, Narayanan A, Lance Liotta L Petricoin E F III, Bailey C, Kehn-Hall K, and Kashanchi F Reverse-phase phosphoproteome analysis (RPPA) of signaling pathways induced by HTLV-1 infection Retrovirology 2011, 8(Suppl 1)

3. Ibarra-Drendall C, Troch MM, Barry WT, Broadwater G, Petricoin EF 3rd, Wulfkuhle J, Liotta LA, Lem S, Baker JC Jr, Ford AC, Wilke LG, Zalles C, Kuderer NM, Hoffman AW, Shivraj M, Mehta P, Williams J, Tolbert N, Lee LW, Pilie PG, Yu D, Seewaldt VL. Pilot and feasibility study: prospective proteomic profiling of mammary epithelial cells from high-risk women provides evidence of activation of pro-survival pathways. Breast Cancer Res Treat. 2011 Jun 7.

4. Improta G, Zupa A, Fillmore H, Deng J, Aieta M, Musto P, Liotta LA, Broaddus W, Petricoin EF, Wulfkuhle J. Protein Pathway Activation Mapping of Brain Metastasis from Lung and Breast Cancers Reveals Organ Type Specific Drug Target Activation. J Proteome Res. 2011 May 16. [Epub ahead of print]

5. Anderson T, Wulfkuhle J, Petricoin E, Winslow RL. High resolution mapping of the cardiac transmural proteome using reverse phase protein microarrays. Mol Cell Proteomics. 2011 Apr 13. [Epub ahead of print]

6. Napoletani D, Signore M, Sauer T, Liotta L, Petricoin E. Homologous control of protein signaling networks. J Theor Biol. 2011 279(1):29-43.

7. Fodale V, Pierobon M, Liotta L, Petricoin E. Mechanism of cell adaptation: when and how do cancer cells develop chemoresistance? Cancer J. 2011 Mar-Apr;17(2):89-95.

8. Gallagher RI, Silvestri A, Petricoin EF 3rd, Liotta LA, Espina V. Reverse phase protein microarrays: fluorometric and colorimetric detection. Methods Mol Biol. 2011;723:275-301.

9. Silvestri A, Colombatti A, Calvert VS, Deng J, Mammano E, Belluco C, De Marchi F, Nitti D, Liotta LA, Petricoin EF, Pierobon M. Protein pathway biomarker analysis of human cancer reveals requirement for upfront cellular-enrichment processing. Lab Invest. 2010 May;90(5):787-96.

10. Anderson T, Wulfkuhle J, Liotta L, Winslow RL, Petricoin E 3rd. Improved reproducibility of reverse phase protein microarrays using array microenvironment normalization Proteomics. 2009 Dec;9(24):5562-6.

11. Pierobon M, Calvert V, Belluco C, Garaci E, Deng J, Lise M, Nitti D, Mammano E, Marchi FD, Liotta L, Petricoin E. Multiplexed Cell Signaling Analysis of Metastatic and

Nonmetastatic Colorectal Cancer Reveals COX2-EGFR Signaling Activation as a Potential Prognostic Pathway Biomarker. Clin Colorectal Cancer. 2009 Apr;8(2):110-7.

12. Wulfkuhle JD, Speer R, Pierobon M, Laird J, Espina V, Deng Jm Mammano E, Yang SX, Swain SM, Nitti D, Esserman LJ, Belluco C, Liotta LA and Petricoin EF. Multiplexed Cell Signaling Analysis of Human Breast Cancer: Applications for Personalized Therapy. J of Prot Res. 2008 Apr;7(4):1508-17.

13. Zhou, J, Wulfkuhle J, Zhang H, Gu P, Yang Y, Deng J, Margolick JB, Liotta LA, Petricoin EF, Zhang Y. Activation of the PTEN/mTOR/STAT3 pathway in breast cancer stem-like cells is required for viability and maintenance. PNAS 2007. Oct 9;104(41):16158-63.

14. VanMeter A, Signore M, Pierobon M, Espina V, Liotta LA, Petricoin EF Reverse-phase protein microarrays: application to biomarker discovery and translational medicine Expert Review of Molecular Diagnostics. 2007. 7(5): 625-633(9)

15. Rapkiewicz A, Espina V, Zujewski JA, Lebowitz PF, Filie A, Wulfkuhle J, Camphausen K, Petricoin EF 3rd, Liotta LA, Abati A. The needle in the haystack: Application of breast fine-needle aspirate samples to quantitative protein microarray technology. Cancer. 2007 Jun 25;111(3):173-84.

University of Colorado
Anschutz Medical Campus

Jennifer K. Richer, PhD
Professor of Pathology

Department of Pathology

Mail Stop 8104
Bldg P18-5122
12800 East 19th Avenue
Aurora, CO 80045
Office 303 724-3735
Fax 303-724-3712

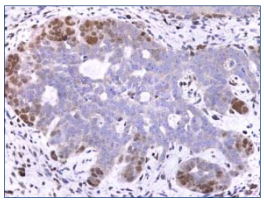

July 29th, 2016

Dear Dr. Knudsen,

Thank you for the review of our manuscript now titled **"Cooperative Dynamics of AR and ER Activity in Breast Cancer,"** as per the editor's recommendation. We appreciate the reviewers' comments and suggestions, and guided by the reviews, we have revised the manuscript as described point by point below.

Reviewer's Comments:

Reviewer #1:

1. ***In the Results section, page 9, the authors should rephrase the comment "to confirm that this is not due to off-target effects of Enza" as the experiments in Fig. 1 do not adequately address this issue.***

   We have eliminated this comment from the sentence since this doesn't directly disprove off-target effects. However, as mentioned in the next comment, we feel that when considered together, the similar effects of two different anti-androgens and the AR shRNAs demonstrate that the effects are AR-specific.

2. **It would be helpful to examine Enza effects in an ER+AR- control cell line and after knock down of AR**

   We agree that testing this in an ER+/AR- cell line would be interesting. However, all ER+ breast cancer cell lines that we have tested are AR+. Since we observe nearly identical effects between Enza and MJC13, two different anti-androgens that reduce nuclear translocation but bind to different regions of AR, and these results are also phenocopied by AR knockdown, we feel that these data are sufficient to show that the decreased proliferation in response to Enza is unlikely to be due to off-target effects.

3. **The sentences on page 9 (shown below) are confusing and require clarification. The authors conducted experiments in charcoal stripped serum with and without estradiol stimulation. Since charcoal stripped serum is also depleted of androgens, these conditions may not necessarily mimic those found in postmenopausal women treated with aromatase inhibitors who may experience higher levels of androgens. "Most studies of AR function in breast cancer focused on the effect of androgen stimulation in the presence of E2 in hormone depleted media. However, we believe it is more relevant to study the effects of antagonizing AR either in the absence of E2 to model postmenopausal women with breast cancer treated with aromatase inhibitors, or in full serum, which contains androgens as well as sufficient estrogens to induce ER activity and genomic binding (31)."**

   Based on this suggestion, we have now clarified this section to more clearly explain the experimental conditions and their rationale. Specifically, our reference to mimicking "postmenopausal women with breast cancer treated with aromatase inhibitors" who may experience higher levels of androgens, is referring to our data from experiments in charcoal stripped serum with and without DHT stimulation demonstrating that DHT is proliferative in breast cancer cells in the absence of E2. Additionally, in this manuscript we show new in vivo data using the PT12 xenograft model demonstrating that DHT is proliferative in an additional ER+/AR+ model in ovariectomized mice.

4. **Does knockdown of AR and/or treatment with Enza regulate ER protein levels in ER+AR+ breast cancer cell lines? This is an important control that is missing throughout the manuscript.**

This is an important question, and we have replaced the western in Figure 1c with a new western blot showing that AR knockdown does not significantly alter ER protein expression levels. We also include here a western blot demonstrating that two different AR siRNAs do not alter ER protein levels (Reviewer Figure 1a). In addition, we have previously published that in longer-term *in vivo* experiments, enza treatment did not significantly alter ER expression, although ER localization was more cytoplasmic and less nuclear (1). Importantly, as described in the current manuscript (page 11 and Figure 3a), ER is also more cytoplasmic with enza treatment in short-term *in vitro* assays (3 hrs) as determined by ICC and nuclear fractionation.

5. **Is E2 stimulation of AR chromatin binding blocked by tamoxifen (Fig. 4)?**

   This is an interesting an important question, but we believe it is beyond the scope of the current manuscript. We are currently working on further experiments to address this question and better understand the mechanistic details of AR activity in response to E2 stimulation.

6. **Please explain in Fig. 1c the difference in proliferation between cells expressing shAR17 compared to shAR15, since both constructs seem to be equally effective in knocking down AR (as demonstrated in the blot in Fig. 1c) and in their similar effects on E2 stimulated relative proliferation in Fig. 1f.**

   The new western blot for Figure 1c (as mentioned above in #4) more accurately shows that the cells with shAR17 have slightly more AR protein than those with shAR15, which may explain why shAR17 does not produce quite as strong a decrease in proliferation in normal serum-containing media. However, both shRNA constructs targeting AR result in a significant decrease compared to the non-targeting control. While not as strong as shAR15, the shAR17 construct decreased AR sufficiently to reduce E2-induced proliferation in CSS-containing media.

7. **Although the authors show that estradiol did not promote AR nuclear localization in MDA-435 cells (Fig. 3f), additional experiments confirming that estradiol does not act as a weak AR agonist should be included to definitely rule out this possibility.**

   The reviewer brings up an intriguing possibility. We have also performed these experiments in another ER-/AR+ breast cancer cell line, MDA-MB-231, and found similar results (now mentioned on page 11 and shown as Supplementary Figure S2a). Additionally, numerous publications have documented that E2 binds AR with approximately 100-fold lower affinity than DHT in breast cancer cells (2,3). However, there are reports that E2 can act as a weak agonist on AR in the presence of the cofactor ARA70 (4,5). This is a plausible mechanism by which AR could be translocated to the nucleus in response to E2, to a lesser extent than in response to DHT (as shown in Figure 3b). This would in no way contradict our data, and we now speculate on this possibility in the discussion on page 20. We are actively testing these hypotheses and plan to report the results in a future manuscript.

8. **It is perplexing how Enza (a competitive antagonist) blocks AR function in the absence of ligand (CSS media conditions). What is a probable mechanism?**

   We do not report any instance of enza blocking AR function in the absence of any hormone. All experiments in this manuscript were conducted either in CSS media + hormone (E2 or DHT) or in media containing full (not CSS) serum, which contains androgens.

9. **There are several examples in which the data are plotted in an unconventional manner or where there are inconsistencies in use of cell lines or controls. For example it would be better to show cell cycle distribution in the various conditions in Fig. 1e and not % increase in S/G2/M; it would be more helpful if the synergy experiments (Enza plus either tamoxifen or fulvestrant) in Fig. 5 were conducted in the same cell lines; pertaining to soft agar assays, colony size and colony number should both be reported; a combination treatment arm (anti-estrogen plus Enza) is missing in Fig. 6a.**

   We have changed Figure 1e to report the % of cells in S/G2/M, instead of the percent change. For the synergy experiments, these experiments are representative of many different cell lines and repetitions, and we believe showing that the synergy occurs in multiple cell lines, including those from PDXs, is important. In Figure 6a, the combination was not done in this experiment, as we were testing the ability of two different anti-androgens to

inhibit growth as single agents. We then pursued the combination in the soft agar experiment in Figure 6b. In Figure 6b we now show both colony number and colony size.

10. **It is unclear why the xenografts from the tamoxifen resistant cell line are inhibited by tamoxifen (Fig. 6d).**
    This is the first time this model of tam-resistant MCF7 cells (6) has been used *in vivo*. While the MCF7-TamR cell line is resistant to Tam *in vitro*, it is not completely refractory *in vivo*. That said, the growth inhibition by Tam is **not** significant compared to CTRL, and is minimal when compared to prior experiments using a non-resistant MCF7 cell line (1).

11. **There are several issues related to the statistical analysis of the data. The authors should only use parametric statistical analysis (such as T test and ANOVA) when appropriate. Parametric tests lose power when used inappropriately.**
    We consulted with our statistician and now use more appropriate tests for the data as recommended. If the data did not meet the assumptions for a parametric test, we tried transforming the data and dealing with potential outliers. If this did not work, we used a non-parametric equivalent. We have modified the methods to describe these changes.

In general: All the Figure Legends should include the statistical value (for example: in a Student's T test the T value obtained, in an ANOVA analysis the F value, as well as the p values.)

We removed the individual p-values from each figure legend in order to save space. However, we have now placed that information back into each legend as requested. We have made it more clear in the figure legends and methods exactly what type of test used, the type of error bars, and the sample sizes for each figure.

In particular:

For Fig 1f: The T test seems inappropriate for the data analyzed (please see note below). The standard errors of the different groups (veh vs E2) suggest lack of homogeneity of variances between groups. It is highly likely that with the appropriate statistical analysis the proliferation under E2 treatment in both AR knockdowns will be significantly higher than for the vehicle treated groups.

In Figure Fig 1F we tested if the variances were unequal between Veh and E2 and only shAR15 was different. When we did a t-test assuming unequal variances, the non-significance for shAR15 held. With only 6 samples in each group, it is not really meaningful to test if the data are normally distributed to meet the assumption of a t-test. Graphing the data showed some potential for skewed data. We therefore did a Wilcoxon rank sum on each pair of Veh-E2. The results did not change; Veh-E2 for shAR15 and shAR17 are still not significantly different. Appropriate changes were made to the Figure legend and text.

For Fig 4d: The ANOVA test performed seems inappropriate for the data analyzed (see note below). The standard error of the different groups suggests lack of homogeneity of variances

We apologize if it was unclear how the data were analyzed. ANOVA was performed separately for each gene (i.e. differences in binding events between the 4 conditions for ZBTB16 were examined using ANOVA and Dunnett's multiple comparison test, comparing each condition vs Veh, and this was repeated separately for each binding region.). Thus the samples with the higher standard error (ZBTB16) are only compared amongst themselves. Since these reactions were done in triplicate, it is not really meaningful to test if the data are normally distributed.

Fig 7e: The T test seems inappropriate for the data analyzed (please see note below)

Thank you for your comments regarding the statistical tests. Since the data at different time points represent repeated measures on the same tumors, we tried to do a repeated measures mixed models (the time points were unequal and the data were unbalance, which precluded a repeated measures ANOVA). The data, however, failed to meet the assumption of a normal distribution despite trying different types of data transformation. We therefore did a non-parametric Wilcoxon rank sum test on the two treatment groups at the last time point at week 12 for this metastasis experiment. We have updated the text and methods accordingly.

Reviewer #2:

1. **Are AR mRNA levels detected in the PT12 line. Such data would be nice to add as supplementary data to provide further support of positive AR status of the cell line.**

   AR transcript was detected in the PT12 xenograft RNAseq experiment. We did not show the data since no significant change in mRNA expression was observed between CTRL and Enza-treated tumors. We do show a western blot of AR in the PT12 cells as well as AR IHC in the PDX early passage (Supplementary Figure S6).

2. **Are the mice ovariectomized? Please add to Methods section to clarify.**

   Experiments with DHT were performed in ovariectomized NOD-SCID-IL2Rgc–/– mice, while PT12 experiments with E2 were performed in non-ovariectomized NOD-SCID-IL2Rgc–/– mice since the E2 pellet overrides the estrus cycle. This information is included in the Methods section under the "Tumor Studies" heading.

3. **Fig 1 - Do Enz and MJC13 affect ER levels?**

   We have added this data to Figure 1c showing that ER is not affected when AR is knocked down by shRNA, and show in Figure 3a that ER nuclear localization, rather than total expression, is altered by Enza and MJC13.

4. **Fig 2 - Authors show nicely how anti-androgens decrease ER binding. Is there also a shift in ER binding, ie are new binding sites generated? The answer would be informative (even if negative), and should be added.**

   In summary, there is no reproducible shift to new ER bound sites due to anti-androgens, and this is now mentioned on page 11 of the manuscript. Specifically, there are 50 new sites identified with enza treatment and 105 new sites identified with MJC13 treatment, representing less than 1% of the total ER binding sites. However, upon closer inspection, these new sites are simply the result of thresholding differences, but the ChIP-seq signal is similar between E2 alone and E2 with anti-androgens. Of the new sites identified with anti-androgens, none of them overlap between MJC13 and enza treatment.

5. **Would be great if authors can speculate a bit more on mechanism of E2-induced relocation of AR.**

   This is an interesting and important question, and it is an active area of research in our lab. One possibility is that the transcriptionally-active chromatin environment following E2 treatment may allow for DNA binding of AR that is activated independent of ligand via growth factor pathways such as MAPK. Alternatively, there is evidence from other groups that E2 can act as a weak AR agonist in the presence of the AR cofactor ARA70 (4,5). However, we only observe AR moving to the nucleus in response to E2 in the presence of ER, so we doubt the E2 binding to AR "promiscuity" theory. We are actively testing these hypotheses and plan to report the results in a future manuscript.

6. **Method for additive vs synergy should be defined in Methods.**

   For the determination of additive vs synergistic effects we used Calculsyn software, as described and cited in the Methods section and Figure 5 legend. A Combination Index value less than 1 is indicative of synergy. The citation provides details regarding the calculations.

7. **Is AR induced in TamR models?**

   There is data showing that AR overexpression can lead to Tam resistance *in vitro* and *in vivo* (7). In this particular model of acquired Tam resistance (6), we do not see elevated AR expression in the TamR cells compared to parental MCF7s. Interestingly, FOXA1 protein expression is higher in the TamR cells (now included as Supplementary Figure S5a), and we are currently testing whether this is important for their resistance to tamoxifen and utilization of AR.

8. **Authors state that "96% retained AR positivity" (page 15). Please define how "positivity" was defined.**

   AR positivity was defined as >1% positive nuclear staining for AR, which is the criteria currently being used for clinical trials testing enza in breast cancer. We have now added this detail to the sentence on page 15.

9. **Finally, it would be great if the authors could include a model showing bidirectional interaction between ER and AR, including the contribution of their studies to this model. While this is not absolutely necessary, it would be helpful for this study, and for overall field.**

We are working on a model that incorporates all of the hormonal situations relevant to the role of AR in ER+ breast cancer and how that might be affected by the hormonal milieu (in premenopausal vs. postmenopausal women, women with breast cancer that are being treated with tamoxifen (which we published to have partial agonist activity on AR (8)) or aromatase inhibitors (where there is extremely low E2, and an increase in androgens) versus fulvestrant (where ER is degraded). We would like to link these models to published data regarding AR and ER (including the data presented in this manuscript) because we believe that some of the data that appears on the surface to be contradictory, is in fact explained by the hormonal context in all of the above situations. This issue is so complex that in order to make it understandable and digestible and put it into the context of all of the literature, it requires the lengthier format of a review article.

In summary, we have made significant changes in response to the reviewers' comments, improved the statistical analyses (we added a statistics collaborator), and added additional experiments to the manuscript, particularly the inclusion of a highly significant *in vivo* experiment regarding how the anti-androgen enzalutamide affects late stage metastases of an ER+/AR+ model. We believe that these edits have further improved our manuscript and we hope that this novel manuscript will now be accepted for publication in *Molecular Cancer Research.*

Sincerely,

Jennifer Richer, Ph.D.
Associate Professor
Department of Pathology
University of Colorado Denver

1. Cochrane DR, Bernales S, Jacobsen BM, Cittelly DM, Howe EN, D'Amato NC, et al. Role of the androgen receptor in breast cancer and preclinical analysis of enzalutamide. Breast cancer research : BCR 2014;16(1):R7.
2. Asselin J, Melancon R, Moachon G, Belanger A. Characteristics of binding to estrogen, androgen, progestin, and glucocorticoid receptors in 7,12-dimethylbenz(a)anthracene-induced mammary tumors and their hormonal control. Cancer research 1980;40(5):1612-22.
3. Poulin R, Baker D, Labrie F. Androgens inhibit basal and estrogen-induced cell proliferation in the ZR-75-1 human breast cancer cell line. Breast cancer research and treatment 1988;12(2):213-25.
4. Thin TH, Kim E, Yeh S, Sampson ER, Chen YT, Collins LL, et al. Mutations in the helix 3 region of the androgen receptor abrogate ARA70 promotion of 17beta-estradiol-induced androgen receptor transactivation. The Journal of biological chemistry 2002;277(39):36499-508.
5. Yeh S, Miyamoto H, Shima H, Chang C. From estrogen to androgen receptor: a new pathway for sex hormones in prostate. Proc Natl Acad Sci U S A 1998;95(10):5527-32.
6. Fagan DH, Uselman RR, Sachdev D, Yee D. Acquired resistance to tamoxifen is associated with loss of the type I insulin-like growth factor receptor: implications for breast cancer treatment. Cancer research 2012;72(13):3372-80.
7. De Amicis F, Thirugnansampanthan J, Cui Y, Selever J, Beyer A, Parra I, et al. Androgen receptor overexpression induces tamoxifen resistance in human breast cancer cells. Breast cancer research and treatment 2010;121(1):1-11.
8. Harvell DM, Richer JK, Singh M, Spoelstra N, Finlayson C, Borges VF, et al. Estrogen regulated gene expression in response to neoadjuvant endocrine therapy of breast cancers: tamoxifen agonist effects dominate in the presence of an aromatase inhibitor. Breast cancer research and treatment 2008;112(3):489-501.

Cooperative Dynamics of AR and ER Activity in Breast Cancer

Nicholas C. D'Amato[1], Michael A. Gordon[1], Beatrice L. Babbs[1], Nicole S. Spoelstra[1], Kiel T. Carson Butterfield[1], Kathleen C. Torkko[1], Vernon T. Phan[2], Valerie N. Barton[1], Thomas J. Rogers[1], Carol A Sartorius[1], Anthony D. Elias[3], Jason Gertz[4], Britta M. Jacobsen[*1], and Jennifer K. Richer[*1]

[1]Department of Pathology and [3]Department of Medicine, Division of Oncology, University of Colorado Anschutz Medical Campus, Aurora, CO, USA
[2]Medivation, Inc., 525 Market Street, 36th Floor, San Francisco, CA 94105
[3] Department of Oncological Sciences, Huntsman Cancer Institute, University of Utah, Salt Lake City, UT, USA

Running title: AR is Required for ER Activity in Breast Cancer

* - Denotes co-senior authors

Keywords: Androgen Receptor, Estrogen Receptor, Enzalutamide, Breast Cancer

Funded by: BC120183 W81XWH-13-1-0090 DOD BCRP Clinical Translational Award to JKR and ADE; R01 CA187733-01A1 to JKR; American Cancer Society Award 124475-PF-13-314-01-CDD to NCD

Conflicts of Interest: Vernon T. Phan is a fulltime employee of Medivation, Inc.

Word count: 5,424

Figures: 7

Tables: 0

Supplementary figures: 6

Supplementary tables: 3

Corresponding author: Jennifer K. Richer
Email: Jennifer.Richer@ucdenver.edu
Phone: 303-724-3735
Fax: 303-724-3712
RC1 North P18-5127 Mail Stop 8104
12800 E. 19th Ave
Aurora, CO 80045
Ph. 303 724-3735

ABSTRACT (250/250)

Abstract: Androgen receptor (AR) is expressed in 90% of estrogen receptor alpha positive (ER+) breast tumors, but its role in tumor growth and progression remains controversial. Use of two anti-androgens that inhibit AR nuclear localization, enzalutamide and MJC13, revealed that AR is required for maximum ER genomic binding. Here, a novel global examination of AR chromatin binding found that estradiol induced AR binding at unique sites compared to dihydrotestosterone (DHT). Estradiol-induced AR binding sites were enriched for estrogen response elements and had significant overlap with ER binding sites. Furthermore, AR inhibition reduced baseline and estradiol-mediated proliferation in multiple ER+/AR+ breast cancer cell lines, and synergized with tamoxifen and fulvestrant. *In vivo*, enzalutamide significantly reduced viability of tamoxifen-resistant MCF7 xenograft tumors and an ER+/AR+ patient-derived model. Enzalutamide also reduced metastatic burden following cardiac injection. Lastly, in a comparison of ER+/AR+ primary tumors versus patient-matched local recurrences or distant metastases, AR expression was often maintained even when ER was reduced or absent. These data provide pre-clinical evidence that anti-androgens that inhibit AR nuclear localization affect both AR and ER, and are effective in combination with current breast cancer therapies. In addition, single agent efficacy may be possible in tumors resistant to traditional endocrine therapy, since clinical specimens of recurrent disease demonstrate AR expression in tumors with absent or refractory ER.

Implications: This study suggests that AR plays a previously-unrecognized role in supporting E2-mediated ER activity in ER+/AR+ breast cancer cells, and that enzalutamide may be an effective therapeutic in ER+/AR+ breast cancers.

INTRODUCTION

AR is more frequently expressed in breast cancer than estrogen receptor alpha (ER) or progesterone receptor (PR) (1); however the role of AR is complex, dependent on the hormonal milieu, and remains controversial. AR positivity is associated with better prognosis in ER+ breast cancer (2-4), possibly due to the fact that like ER, AR positivity is indicative of a more well-differentiated state. In the presence of estradiol (E2), the androgen dihydrotestosterone (DHT) decreased E2-induced proliferation (2) and ER transcriptional activity (5), leading to the conclusion that AR is protective in breast cancer. However, there is accumulating evidence that androgen signaling and AR are involved in resistance to ER-directed endocrine therapies. *De novo* or acquired resistance to anti-estrogen therapies is a frequent occurrence, and ultimately all metastatic ER+ breast cancers are resistant (6,7). In ER+ tumors responsive to neoadjuvant aromatase inhibitor (AI) therapy, AR mRNA and nuclear AR protein decreased, whereas in non-responsive tumors it remained elevated (8,9). AR over-expression in breast cancer cell lines resulted in resistance to tamoxifen (tam) and AIs *in vitro* and *in vivo* (10,11). One mechanism of resistance to anti-estrogen therapies may therefore be tumor adaptation from estrogen to androgen dependence.

AIs block the conversion of androgens to estrogens, and free testosterone and dehydroepiandrosterone sulfate (DHEA-S) increased in patients on AIs (12). Furthermore, high levels of the adrenal androgen DHEA-S are predictive of failure on AIs, and circulating DHEA-S increased during treatment in patients with tumors that progressed during AI treatment (13). Patients with tumors exhibiting a high ratio of percent cells positive for AR versus ER protein are more likely to have recurrent disease while on tamoxifen and also have a worse overall prognosis compared to those with a more equal ratio of these two receptors, as is found in normal breast epithelium (14). So although AR, like ER, is associated with a better prognosis, anti-androgen therapies may benefit patients with AR+ breast cancers if the tumors are dependent on activated AR.

We previously reported that the new generation AR antagonist enzalutamide (Enza), which inhibits AR nuclear localization, decreased estrogen-induced tumor growth, while the first-generation AR antagonist bicalutamide (bic) did not (14). However, the mechanism by which Enza affected ER activity was not known. Herein, we demonstrate for the first time that in response to E2, nuclear localization of AR supports maximum ER genomic binding, and that AR inhibition with the pure antagonist Enza significantly decreases E2-induced growth of ER+/AR+ cell lines and patient-derived xenografts, as well as tam-resistant tumors *in vivo*, and also decreases metastatic burden. Importantly, these data suggest that patients with ER+/AR+ breast cancer may benefit from combining anti-androgen therapy with anti-estrogen therapy, and that tumors resistant to traditional ER-directed therapies may be responsive to AR-directed drugs.

Materials and Methods

Cell Lines. All cell lines were authenticated by short tandem repeat analysis using AmpFLSTR Identifiler PCR Amplification Kit (Life Technologies) and tested negative for mycoplasma in January 2015. MCF7 cells were obtained from Dr. Kate Horwitz at the University of Colorado Anschutz Medical Campus. MCF7-TamR cells obtained from Dr. Doug Yee at the University of Minnesota were generated by chronic treatment of MCF7 cells with 100nM tamoxifen. All other cell lines were obtained from the ATCC. Additional cell culture details are included in supplementary material. The BCK4 cell line is an ER+/AR+ breast cancer line recently derived from a pleural effusion (15), and the PT12 breast cancer cell line is ER+/AR+ and created from a patient-derived xenograft (PDX) (16). Originally the PT12 PDX was described as AR-negative (16), but upon staining of the original passage with a more sensitive AR antibody (SP107 from Cell Marque), the PDX was found to be AR+ (Supplementary Figure S6a).

Cellular Assays and Reagents. Cells were treated with 10 nM estradiol (E2, Sigma Aldrich) and 10 nM dihydrotestosterone (DHT, Sigma Aldrich). Androgen concentrations have been previously examined in breast cancer (17) and intratumoral DHT concentrations (249 pg/g) were significantly higher than in blood. The DHT concentration of the present study is consistent with other *in vitro* studies of DHT in breast cancer (18,19), and approximates levels of circulating testosterone in obese, postmenopausal women (12) as well as DHT levels in FBS used during routine tissue culture. 10 μM Enza (Medivation, San Francisco, CA) approximates the IC_{50} of the three cell lines studied and is a clinically achievable, well-tolerated treatment concentration (NCT01889238).

Proliferation Assays. Proliferation assays were performed using the IncuCyte ZOOM live cell imaging system (Essen BioSciences) or crystal violet as previously described (20). For synergy experiments, percent inhibition was calculated compared to vehicle control, and the combination index was

calculated for each dose combination by Calcusyn (21) (BIOSOFT, Cambridge, UK). Soft agar assays were performed in 6-well plates using 0.5% bottom and 0.25% top layer agar (Difco Agar Noble, BD Biosciences). Wells were photographed and colony number and size was determined by ImageJ software (National Institutes of Health).

Tumor studies. Xenograft experiments were approved by the University of Colorado Institutional Animal Care and Use Committee (IACUC protocol 83614(01)1E) and were conducted in accordance with the NIH Guidelines of Care and Use of Laboratory Animals. $1x10^6$ MCF7-GFP-Luc cells were mixed with growth factor-reduced Matrigel (BD Biosciences) and injected bilaterally into the mammary fat pad of female ovariectomized athymic nu/nu mice (Taconic). E2 pellets (60-day release, 1.5 mg/pellet, Innovative Research of America) were implanted subcutaneously (SQ) at the back of the neck. Once tumors were established, mice were randomized into groups based on total tumor burden as measured by *in vivo* imaging. Mice received Enza in their chow (~50 mg/kg daily dose). Enza was mixed with ground mouse chow (Research Diets Inc.) at 0.43 mg/g chow. Control mice received the same chow without Enza. All mice were given free access to Enza-formulated chow or control chow during the study. Mice were euthanized by carbon dioxide asphyxiation followed by cervical dislocation, and tumors were harvested. The MCF7-TamR xenograft experiment was performed as described above without estrogen pellets. For the PT-12 xenograft study, $1x10^6$ cells were injected bilaterally into the mammary fat pad of NOD-SCID-IL2Rgc–/– female mice. Mice were implanted with a DHT (8mg) or E2 (2mg) pellet. For the metastasis experiment, 2.5x10^5 GFP-Luciferase labeled PT12 cells were injected intracardially in NOD-SCID-IL2Rgc-/- mice implanted with E2 pellets (2mg). PT12 experiments with DHT were performed in ovariectomized females, while PT12 experiments with E2 were performed in non-ovariectomized females since the E2 pellet overrides the estrus cycle.

Immunoblotting. Whole cell protein extracts (50 µg) were denatured, separated on SDS PAGE gels and transferred to PVDF membranes. After blocking in 3% BSA in TBS-T, membranes were probed overnight at 4°C. Primary antibodies used were: ERalpha (Neomarkers Ab-16, 1:500 dilution), AR (EMD Millipore PG-21, 1:500 dilution), Topo 1 (Santa Cruz C-21, 1:100 dilution) and alpha-tubulin (clone B-5-1-2 from Sigma, 1:30,000 dilution). After incubation with appropriate secondary antibody, results were detected using Western Lightning Chemiluminescence Reagent Plus (Perkin Elmer).

Nuclear-cytoplasmic fractionation. $1x10^6$ cells were seeded in 10cm dishes in medium supplemented with 5% charcoal stripped serum (CSS). After three days the cells were pre-treated with vehicle or 10 µM Enza for 3 hr and then co-treated with either DHT for 3 hr plus or minus Enza, or E2 for 1 hr plus or minus Enza. Cells were washed with phosphate buffered saline (PBS) and cellular fractionation was performed using the NE-PER Nuclear and Cytoplasmic Extraction Kit (Life Technologies) as per manufacturer's instructions.

Proximity ligation assay. PLA was performed using the Duolink kit according to manufacturer's instructions (Olink Bioscience, Uppsala, Sweden). Briefly, $1.5x10^4$ cells were plated in 8-well chamber slides and hormone starved in phenol red-free media with 5% CSS for 72hrs. Cells were then pre-treated with Veh or Enza for 3hrs, then treated with hormones +/- Enza as described for 1hr. After fixation with 4 % paraformaldehyde, cells were permeabilized then blocked. Samples were then incubated with primary antibodies AR D6F11 (Cell Signaling), and ERα clone 6F11 (Vector Laboratories) overnight at 4 degrees. Samples were then incubated with secondary antibodies linked to PLA probes and ligase was added. Detection reagent red was added and DAPI mounting media was added to visualize nuclei. Images were captured using a 20x objective. DAPI-labeled nuclei and red ERα/AR complexes were quantified using CellProfiler (22).

ChIP-seq . ChIP-seq was performed by Active Motif (Carlsbad, CA). Briefly, $1x10^6$ MCF7 cells were seeded in 15cm dishes in phenol red-free medium supplemented with 5% CSS for 72 hrs. Cells were pre-treated with vehicle, 10 μM Enza, or 30uM MJC13 for 3 hrs. E2 was then added for 1 hr in continued presence of vehicle, Enza, or MJC13. For AR ChIP-seq, an additional sample was treated with DHT for 4 hrs. The cells were washed with PBS then fixed as per manufacturer's instructions (Active Motif). AR antibody H-280 (Santa Cruz) or ER antibody HC-20 (Santa Cruz) were utilized. Peak calls were made by MACS2 (23) with default parameters using the sequence alignments obtained from Active Motif. Motif discovery was performed on 100 base pairs surrounding the peak summit using BioProspector (24). Patser (25) was used to determine significant matches to AREs and EREs.

RNA-seq. RNA Libraries were constructed using Illumina TruSEQ stranded mRNA Sample Prep Kit (Cat# RS-122-2101). Total RNA was combined with RNA purification beads to bind PolyA RNA to oligodT magnetic beads. mRNA was eluted and converted to double stranded DNA. A Tailing, adapter ligation, and PCR amplification using 15 cycles was used to complete the library construction. Libraries were quantitated via Qubit, analyzed on a Bioanalyzer Tape Station and diluted to appropriate concentration to run on an Illumina HiSEQ 2500 High Throughput Flow Cell. Reads were mapped to the human genome (hg19) by gSNAP, expression (FPKM) derived by Cufflinks, and differential expression analyzed with ANOVA in R (26,27).

Statistical analyses. For most analyses, statistical significance was evaluated using a 2-tailed Student t-test or ANOVA with Bonferroni or Dunnett's multiple comparisons test or non-parametric equivalents in GraphPad Prism (Ver 6, GraphPad Software, San Diego, CA) or SAS (ver 9.4, SAS Institute, Cary, NC). Test assumptions were check for all analyses. If data distributions were skewed, data transformations were

attempted to allow the use of parametric tests. If data transformations failed, than a non-parametric test was used. For the PT12 xenograft experiments, due to unequal time measurements, the repeated measures mixed model approach was used rather than a standard repeated measures ANOVA. The data met the assumption of normality (Shapiro-Wilk test $p>0.05$ and frequency distribution graphs were symmetrical without evidence of outliers). For the PT12 cardiac injection experiment, we were not able to use a repeated measures approach as the data did not meet the assumptions of a normal distribution despite different data transformations. Therefore a single Wilcoxon rank sum test was used to determine difference between E2 and E2 plus enzalutamide at week 12.$P \leq 0.05$ was considered statistically significant, with p-values indicated in figures as :* $p \leq .05$, **$p \leq 0.01$, *** $p \leq .001$, **** $p \leq .0001$. Error bars represent SEM unless otherwise noted.

RESULTS

AR inhibition impairs ER+/AR+ breast cancer cell proliferation

The role of AR in ER+/AR+ breast cancer remains controversial, with conflicting data suggesting either proliferative or protective effects on breast cancer cells *in vitro* (2,5,28-31). Most studies of AR function in breast cancer have focused on the effect of androgen stimulation in the presence of E2 in hormone-depleted media. However, we believe it is more relevant to study the effects of activating or inhibiting AR either 1) in the absence of E2, to model postmenopausal women with breast cancer treated with aromatase inhibitors, or 2) in full serum, which contains androgens as well as sufficient estrogens to induce ER activity and genomic binding (32).

Enza, which inhibits AR nuclear translocation and DNA binding (14,33), significantly decreased growth of MCF7 cells grown in full serum (Figure 1a) as well as two additional ER+/AR+ cell lines, T47D and ZR-75-1, (Supplementary Figure S1a) in a concentration-dependent manner. This shows that AR activity is necessary for ER+/AR+ cell growth under typical culture conditions. Enza also decreased colony size of MCF7 cells (Figure 1b) and T47D cells (Supplementary Figure S1b) grown in soft agar using complete culture media, similar in magnitude to the effect of the anti-estrogen tam. We next decreased AR expression in MCF7 cells using two different shRNA constructs, and AR protein was confirmed to be decreased by western blot (Figure 1c). AR knockdown led to a significant decrease in MCF7 cell growth over the course of 7 days (Figure 1c), further demonstrating that AR is required for baseline proliferation of ER+/AR+ breast cancer cells in hormone-replete conditions.

New-generation AR inhibitors decrease E2-induced proliferation

We previously showed that Enza, which does not bind to ER by ligand binding assay, inhibits E2-induced growth of ER+/AR+ breast cancer cells *in vitro* and *in vivo* (14). To demonstrate that this is AR-dependent

and not specific to Enza, we also utilized MJC13, which inhibits AR nuclear localization by targeting ligand-induced dissociation of AR from FKBP52 in the cytosol (34). Both Enza and MJC13 inhibited E2-induced proliferation in MCF7 cells (Figure 1d). Enza decreased E2-induced growth in a concentration-dependent manner in additional luminal cell lines T47D and ZR-75-1, as well as in ER+/AR+ PT12 cells recently created from a patient-derived xenograft (16) (Supplementary Figure S1c). EC50 values for Enza-mediated inhibition of E2-induced growth in MCF7 and T47D cells were determined to be 19.0 μM and 17.1 μM, respectively (Supplementary Figure S1d), which are concentrations readily achieved in patients.

To specifically determine whether Enza affected E2-induced proliferation, cell cycle analysis of E2-treated MCF7 and T47D cells was performed. Enza significantly decreased the percent cells in S and G2/M phases compared to E2 treatment alone (Figure 1e and Supplementary Figure S1e). Silencing AR using shRNA also significantly decreased E2-induced proliferation of MCF7 cells compared to cells transduced with non-targeting shRNA (Figure 1f). Together, these data confirm that pharmacological AR inhibition or AR knockdown similarly diminish E2-driven proliferation of ER+/AR+ breast cancer cells.

AR inhibitors diminish ER genome binding

AR is capable of interacting with ER and estrogen response elements (EREs) (2,5,35), thus, we postulated that inhibitors of AR nuclear localization might diminish baseline and E2-induced growth by altering ER genomic binding. To test this hypothesis, MCF7 cells were pretreated for 3 hrs with Veh, Enza, or MJC13 then treated with E2 1 hr and global ER ChIP-seq was performed. Surprisingly, the anti-androgens Enza or MJC13 dramatically decreased E2-induced ER genomic binding (Figure 2a). The majority of sites displayed an approximate 50% decrease in ER binding (Figure 2a-c), with no appreciable shift in the location of ER binding sites upon Enza or MJC13 treatment. The decrease in ER binding intensity by Enza or MJC13 was confirmed by qPCR after ChIP at previously-characterized ER binding sites including

GREB1, *GATA3*, and *PGR* (Figure 2d-e). Together, this suggests that the interaction of AR and ER is necessary for efficient ER genomic binding in response to E2, and that inhibition of nuclear AR localization decreases E2-induced ER activity by diminishing ER genome binding.

Enza decreases nuclear localization of both AR and ER

Since E2-induced ER genome binding was globally decreased by anti-androgens, we speculated that ER nuclear localization in response to E2 might be affected. Immunofluorescent staining of MCF7 cells grown in CSS revealed nuclear localization of both ER and AR following E2 treatment (Figure 3a). Notably, treatment with Enza decreased nuclear localization of both receptors (Figure 3a), while bic did not, suggesting that the mechanism by which Enza globally inhibits ER genomic binding may be by decreasing ER nuclear localization. We previously showed that Enza decreased E2-driven growth of MCF7 xenograft tumors equally as well as tamoxifen (14). IHC for ER performed on tumors from mice on Enza-containing chow had significantly decreased nuclear localization of ER compared to tumors from mice on control chow (14).

To further examine AR nuclear localization in response to E2, MCF7 cells were treated with E2 or DHT plus or minus Enza for 3 hrs, and nuclear and cytoplasmic protein fractions were isolated. DHT induced a strong increase in AR nuclear localization as expected, which was largely blocked by co-treatment with Enza, but not bicalutamide (bic) (Figure 3b). E2 treatment also increased AR nuclear localization, and this effect was blocked by Enza, but not bic (Figure 3c). E2-induced nuclear localization of AR was also observed in ZR-75-1 (Figure 3d). However, E2 did not induce AR nuclear localization in ER-/AR+ MDA-MB-453 cells (Figure 3e) or MDA-MB-231 cells (Supplemental Figure S2a), suggesting that the observed AR nuclear localization is not due to promiscuous binding of E2 to AR, but rather that AR becomes localized to the nucleus in an ER-dependent manner upon E2 stimulation in ER+/AR+ breast cancer cells.

Since both ER and AR were localized to the nucleus following E2 treatment, we next tested whether E2 induced AR and ER to co-localize using the proximity ligation assay (PLA). MCF7 cells treated with 10 nM E2 for 1hr demonstrated a strong increase in PLA signal when probed for ER and AR compared to vehicle control or Enza treatment alone. This E2-induced increase in PLA signal was dramatically inhibited by pre-treatment with Enza (Figure 3f-g). Similar results were observed in T47D cells (Supplementary Figure S2b-d), suggesting that AR co-localizes with ER in the nucleus in response to E2.

E2 induces AR DNA binding distinct from DHT

To examine whether the observed nuclear localization of AR in response to E2 was associated with AR genome binding, hormone-deprived MCF7 cells were treated with DHT or E2 followed by global AR ChIP-seq analysis**.** As expected, DHT treatment induced a significant increase in AR genome binding compared to vehicle treatment (Figure 4a-b). Among the 1,813 DHT-induced AR binding sites identified in MCF7 cells, 49% were previously identified as bound by AR in LNCaP, a prostate cancer cell line, while 73.6% were bound by AR in MDA-MB-453, an ER-/AR+ breast cancer cell line (36) (Supplementary Figure S3a). This indicated that DHT-induced AR binding may be more similar between luminal breast cancer cell lines than between breast and prostate cancer cell lines, and is similar to previously reported findings in ZR-75-1 cells (35).

Surprisingly, E2 also induced AR genome binding, with 1,380 AR binding events identified in E2-treated MCF7 cells (Figure 4a-b). Enza abolished E2-induced AR genomic binding, consistent with inhibition of AR nuclear localization and previously published reports in prostate cancer (33). Only 25% of all AR bound sites overlapped between the two hormone treatments, indicating a large shift in AR genomic binding between DHT and E2 (Figure 4c). For example, qPCR after ChIP demonstrated that DHT, but not E2, induced a robust increase in AR binding at previously-characterized AR targets *FKBP5* and *ZBTB16* (Figure 4d). Both E2 and DHT treatments resulted in AR binding to previously-characterized ER targets

GREB1 and *GATA3*, but only E2 treatment resulted in AR binding at a different ER target, *PGR* (Figure 4d-e).

The most highly-enriched motif among AR binding sites in response to DHT was a FOXA1 motif (Figure 4a), consistent with previous studies demonstrating strong overlap between AR and FOXA1 binding sites in breast cancer cells (36). However, the most highly-enriched motif among AR binding sites unique to E2 treatment was a slightly degenerate estrogen response element (ERE) (Figure 4a), suggesting that AR was bound within 200bp of ER binding sites in the presence of E2. Indeed, full palindromic EREs were highly enriched among these sites, compared to sites bound by AR in response to DHT (Supplementary Figure S3b-c). Validated nuclear ERα network was the most highly-enriched pathway among genes near AR binding sites unique to E2 treatment, whereas this network was not enriched among genes near AR binding sites in response to DHT (Supplementary Table S1). Thus, in response to E2, AR binds to many sites correlated with ER regulation.

Finally we compared AR and ER binding following E2 treatment and found that 75% of E2-induced AR binding sites overlapped with ER binding sites (Figure 4f). Notably, ER genome binding was more strongly inhibited by Enza or MJC13 at these overlapping sites compared to non-overlapping sites (Supplementary Figure S3d-e), suggesting that AR might be facilitating ER binding at these loci. Taken together, these data demonstrate that in response to E2, AR and ER bind a significant number of overlapping loci and suggest that new generation anti-androgens which inhibit AR nuclear localization decrease ER activity and E2-mediated tumor growth by diminishing ER genome binding.

Enza synergizes with anti-estrogens

Because Enza inhibited baseline and E2-induced growth by a different mechanism than currently-used anti-estrogens, we hypothesized that it might act synergistically with anti-estrogens such as tam or fulvestrant in ER+/AR+ breast cancer cells. T47D cells were treated with varying concentrations of Enza

and/or tam, and all combinations showed synergistic inhibition of E2-induced growth as determined by Calcusyn (Figure 5a). Enza and tam also showed synergy or additive inhibition of E2-induced proliferation in MCF7 cells (Supplementary Figure S4a), and the combination of Enza plus tam reduced MCF7 growth in soft agar more significantly than either drug alone (Supplementary Figure S4b). We also tested for synergy between Enza and fulvestrant. In BCK4 cells, these drugs showed synergy in 10 of 15 dose combinations (Figure 5b), with similar results also observed in PT12 cells (Figure 5c) and ZR-75-1 cells (Supplementary Figure S4c). Together, this shows that Enza effectively synergizes with anti-estrogens to inhibit both baseline and E2-induced growth of ER+/AR+ cells, likely due to the ability of Enza to inhibit AR as well as to indirectly inhibit ER.

Enza inhibits Tam-resistant tumor growth

Resistance to currently-used endocrine therapies is a common occurrence facing ER+ breast cancer patients. Therefore, we also tested whether Enza could inhibit growth of tam-resistant MCF7 (MCF7-TamR) cells (37). *In vitro*, both Enza and MJC13 significantly decreased growth of MCF7-TamR cells (Figure 6a). Enza also decreased growth of MCF7-TamR cells in soft agar, and the combination of Enza+tam was more effective than Enza alone (Figure 6b).

We next tested whether Enza could inhibit growth of Tam-resistant tumor xenografts *in vivo* using GFP-luciferase labeled MCF7-TamR cells. Once tumors were established, mice were matched into groups to receive CTRL chow, tam pellets, Enza-containing chow, or Enza+tam. 20 days after beginning treatment, the Enza-treated mice demonstrated a significant decrease in tumor viability by IVIS compared to those in the CTRL group (Figure 6c). Each treatment resulted in a significant decrease in tumor weight compared to CTRL-treated tumors, with Enza+tam resulting in the smallest tumors by weight at the end of the experiment (Figure 6d). TUNEL staining revealed increased apoptosis in each of the treatment groups compared to CTRL (Supplementary Figure S5a). Interestingly, the combination resulted in a

significant decrease in ER expression compared to CTRL or either drug alone (Supplementary Figure S5b-c).

AR is expressed in recurrent ER+ breast cancers

To validate the potential clinical utility of anti-androgens as a therapy for advanced ER+ tumors refractory to traditional anti-estrogen directed therapy, we examined AR expression in primary tumors compared to the same patient's local recurrence or metastatic disease. Sections of formalin-fixed paraffin embedded breast tumors from a cohort of 192 female patients (median age of 68 years) diagnosed with breast cancer at the Massachusetts General Hospital (Partners) between 1977 and 1993, treated with adjuvant tamoxifen and followed through 1998 were stained for AR (14). Of 49 patients with ER+/AR+ primary tumors that developed local recurrence, 96% retained AR positivity (>1% cells positive) in the recurrence. Further, in more than half of these cases the ratio of AR to ER expression (percent cells positive) was higher in the recurrence compared to the primary tumor.

Of 55 patients that developed distant metastasis, 67% retained AR positivity in the metastatic lesion. Notably, one patient with an ER+/AR- primary tumor developed an ER-/AR+ metastasis. Nearly half of these metastases showed an increased ratio of AR to ER expression compared to the primary tumor. Two examples of cases in which the recurrence or metastasis displayed increased percent cells positive for AR, but decreased percent cells positive for ER compared to the primary tumor are shown in Figure 6e. Our findings are consistent with other studies demonstrating that AR status is highly conserved in recurrences and metastases (38), and that AR is more highly expressed in metastases than ER and PR (39). Collectively, this suggests that anti-androgens may be a useful therapeutic strategy for patients with anti-estrogen refractory disease, since AR is frequently expressed in recurrences and metastases, often at even higher levels than in the primary tumor.

Enza Inhibits Primary and Metastatic Tumor Growth *in vivo*

To assess the effect of Enza on E2- and DHT-induced growth *in vivo*, we utilized AR+/ER+ PT12 cells, recently cultured from a patient-derived xenograft and expressing GFP-luciferase (16). Cells were injected orthotopically in mice implanted with either E2 or DHT pellets, and once tumors were established, mice were matched based on tumor burden to receive either Enza-containing or control chow. Although E2 induced more rapid tumor growth, DHT also stimulated tumor growth (Figure 7a-b). This demonstrates that DHT, in the absence of E2, promotes ER+/AR+ tumor growth *in vivo*, similar to our previous finding with MCF7 xenografts (14). As shown in Figure 7a, enza significantly reduced the growth rate of E2-driven tumors when compared to E2 alone (difference between treatment groups, $F(1,23) = 37.41$, $p < 0.0001$; and group*time interaction, $F(3,23) = 13.75$, $p < 0.0001$). Enza also significantly reduced growth rate of DHT-driven tumors compared to DHT alone (difference between treatment groups, $F(1,8) = 27.80$, $p=0.001$; and group*time interaction, $F(3,24) = 11.34$, $p < 0.0001$). In E2-driven tumors, BrdU staining demonstrated that Enza significantly decreased proliferation (Figure 7c), but had no effect on apoptosis (not shown). Conversely, in DHT-driven tumors Enza significantly increased apoptosis as measured by cleaved caspase 3 staining (Figure 7d), but had no effect on proliferation.

To identify the molecular mechanisms by which Enza decreased E2-induced tumor growth, we performed RNA-seq on PT12 tumors from E2 treated mice. Enza significantly altered 484 genes ($p<.05$, fold change > 1.2); 144 upregulated and 340 downregulated compared to E2 alone (Supplementary Table S2). Of these, 107 (22.1%) of the genes affected by Enza were previously identified as regulated by estradiol in the original PT12 xenograft model (Supplementary Figure S6b) (16). Metacore analysis of the 484 genes altered by Enza treatment identified AR and ER as among the transcription factors most highly implicated as upstream regulators (Supplementary Table S3a). Gene set over-representation analysis also identified AR regulation as a highly-enriched pathway, as well as the HIF-1α and HIF-2α networks (Supplementary Table S3b), which have previously been associated with AR in prostate cancer

(40). Finally, of the 340 genes downregulated by Enza in PT12 tumors, 56 were also identified in our AR ChIP-seq experiment as being the nearest gene to sites bound by AR in response to E2 treatment in MCF7 cells. Notably, several genes decreased by Enza are reported to be both ER targets and critical for ER activity including *GREB1*, an E2-responsive ER co-activator (41), and the histone demethylases *KDM3A* and *KDM4B*, which mediate ER binding to target gene promoters (42,43). Together, these data confirm our *in vitro* observations and show that Enza alters expression of ER target genes *in vivo*.

Finally, since we found that AR is frequently expressed in metastases of ER+ breast cancers, we tested whether Enza could inhibit metastatic growth *in vivo*. PT12 cells were injected intracardially into mice implanted with E2 pellets, and mice were randomized onto control chow or chow containing Enza. Mice were monitored weekly by IVIS imaging of luciferase over 12 weeks in both the supine and prone positions. Tumors in the enza-treated group were significantly smaller at week 12 ($z=-3.82$, $p=0.0001$, two-sided test) (Figure 7e). Next we analyzed IVIS signal of mice at week 2 (first detectable luciferase signal) versus week 12 (Figure 7f). While control mice showed a significant increase in tumor burden over time, there was no significant increase in tumor burden in the Enza treated mice (Figure 7f and 7g). This held true whether IVIS signal was measured in the supine (shown) or prone position (not shown) or both added together. These data demonstrate clearly, in a model of ER+/AR+ breast cancer recently derived from a patient, that Enza is effective in reducing the growth of metastatic disease.

DISCUSSION

AR was previously thought to antagonize ER activity because androgens such as DHT diminished the transcriptional and proliferative response of breast cancer cells to E2 (2), likely because AR and ER compete for some of the same binding sites on chromatin. However, our previous and present studies indicate that DHT is proliferative in the context of no E2, as would be the case in a postmenopausal woman treated with aromatase inhibitors (14). The AR antagonist bicalutamide has also been shown to increase E2-induced ER activity (2). But unlike bicalutamide, Enza and MJC13 are newer-generation anti-androgens that inhibit AR nuclear localization, and this is the first study to test the effects of new-generation AR inhibitors on ER chromatin binding. By inhibiting AR nuclear localization or decreasing AR expression by shRNA, we have discovered that AR supports ER genome binding and activity in breast cancer.

In response to E2, AR translocated to the nucleus in ER+ cell lines and bound chromatin at sites that overlap with ER binding sites and are enriched for EREs. Inhibiting nuclear localization of AR with Enza or MJC13 dramatically decreased E2-induced ER chromatin binding, with the greatest effects observed at sites also bound by AR. Both the AR antagonist Enza and AR knockdown decreased baseline and E2-induced breast cancer cell proliferation *in vitro*, and Enza decreased both DHT- and E2-stimulated growth of ER+/AR+ xenografts as well as metastatic burden *in vivo*.

These results further underscore the crosstalk between AR and ER in dual-positive breast cancer cells. There is evidence that DHT metabolites can have estrogenic effects and stimulate breast cancer growth through ER activation (44). However, Enza inhibits growth differently in E2-driven tumors, where it decreases proliferation, compared to DHT-driven tumors, where it increases apoptosis. This suggests that DHT-driven growth in ER+/AR+ xenografts is not mediated through ER, but rather directly through AR. Conversely, the expression of the AR cofactor ARA70 can result in E2 having a weak agonist effect on

AR (45,46), which could explain how AR is translocated to the nucleus in response to E2 in our studies. Another possibility is that AR is activated by growth factor pathways subsequent to ER activation. However, E2 only drove nuclear localization of AR in ER+ cell lines, suggesting an ER-dependent mechanism. Further studies are ongoing to determine the mechanism of AR nuclear translocation in response to E2, and whether ARA70 is necessary for AR DNA binding in response to E2.

Although our findings may seem contradictory to prior studies, in actuality they are not mutually exclusive. Ligand-bound AR interfered with E2-mediated ER activity (2) and diminished E2-induced upregulation of a subset of ER target genes (35), likely due to competition between AR and ER for some of the same genome binding sites, this is consistent with our observation that AR can bind to ER binding sites in the genome. Additionally, a recent study using AI-resistant MCF7 cells found that ER and AR cooperate on known androgen- and estrogen-responsive gene promoters (10).

We propose that in ER+/AR+ breast cancer cells, AR supports ER nuclear localization and genome binding, possibly by increasing chromatin availability of ER bound loci (47), by stabilizing ER binding to chromatin, and/or interacting directly with ER or as part of an ER-containing complex, as the proximity ligation assay suggests. While this challenges the current view of AR as antagonizing ER activity, a similar effect has been observed with retinoic acid receptor-α (RARα), which interacts with ER binding sites in an ER-dependent manner in ER+ breast cancer cells (48). This interaction is required for E2-induced proliferation and ER transcriptional activity (48). Additionally, glucocorticoid receptor (GR), which is highly similar to AR (49,50) increases chromatin availability and subsequent ER binding at response elements bound by both receptors, a mechanism termed “assisted loading” (47). Similarly, our data show that ER chromatin binding is most inhibited by anti-androgens at sites where E2 induces binding of AR and ER. Thus, even though androgen-bound AR can diminish E2-stimulated ER activity, we show that

anti-androgens that prevent AR nuclear translocation have the same effect—suppression of ER activity—via an entirely different molecular mechanism.

Importantly, the assays herein were performed using endogenous AR and ER in cells that naturally express both receptors. In light of recent data from our lab and others suggesting that the ratio of AR:ER protein expression is a predictor of response to traditional ER-directed endocrine therapy (14) and DCIS progression (51), it is likely that the interplay of these receptors may depend on their relative expression level, the levels of their respective ligands in circulation and within tumors, and levels of shared co-factors such as FOXA1. Our data show that across multiple cell lines and preclinical models of ER+/AR+ breast cancer, AR antagonists such as Enza and MJC13 that inhibit AR nuclear translocation also inhibit ER activity indirectly. This combined effect on AR and ER may account for the synergy demonstrated between Enza and the anti-estrogens tam and fulvestrant *in vitro*. Further analysis of these data is ongoing to determine the mechanisms of this synergy.

Collectively, these data strongly suggest that in the most common form of breast cancer—ER+/AR+ disease—primary tumors and recurrent disease may become reliant on AR and that AR may serve as an effective therapeutic target either in combination with traditional ER-directed therapies (particularly in tumors that have a high AR:ER protein ratio) or upon resistance to ER-directed therapies. Our present and prior (14) studies on the role of AR in ER+ breast cancer contribute to a deeper understanding of the complex molecular interplay between the two most widely expressed hormone receptors in breast cancer (AR and ER), and have already led to clinical trials testing the efficacy of enzalutamide in combination with the aromatase inhibitor exemestane in patients with advanced ER+ disease (NCT02007512) and in combination with fulvestrant (NCT01597193).

Finally, our data demonstrate that Enza effectively inhibits growth of ER+/AR+ metastases *in vivo*. A recent study of ER- PDX models that metastasize from the orthotopic site found that AR mRNA was

increased in circulating tumor cells and micrometastases compared to the primary tumors (52), indicating AR may be an important target for inhibition of metastasis. Likewise, we show in clinical specimens of patient-matched ER+/AR+ primary tumors compared to local or distant recurrences occurring during tamoxifen treatment, AR expression is often maintained, and sometimes increased, in breast cancers refractory to anti-estrogen therapy. We are actively investigating the specific role that AR plays in facilitating the process of metastasis in both ER+ and ER- breast cancer.

ACKNOWLEDGEMENTS

The authors thank A. Protter at Medivation Inc. for comments on the manuscript. We thank Dr. Marc Cox for graciously providing MJC13 for these studies. We thank Active Motif Inc. for their assistance with AR and ER ChIPseq experiments. The authors also acknowledge the Genomics and Microarray Core and other Shared Resources of Colorado's NIH/NCI Cancer Center Support Grant P30CA046934.

REFERENCES

1. Collins LC, Cole KS, Marotti JD, Hu R, Schnitt SJ, Tamimi RM. Androgen receptor expression in breast cancer in relation to molecular phenotype: results from the Nurses' Health Study. Mod Pathol 2011;24(7):924-31.
2. Peters AA, Buchanan G, Ricciardelli C, Bianco-Miotto T, Centenera MM, Harris JM, et al. Androgen receptor inhibits estrogen receptor-alpha activity and is prognostic in breast cancer. Cancer research 2009;69(15):6131-40.
3. Vera-Badillo FE, Templeton AJ, de Gouveia P, Diaz-Padilla I, Bedard PL, Al-Mubarak M, et al. Androgen receptor expression and outcomes in early breast cancer: a systematic review and meta-analysis. Journal of the National Cancer Institute 2014;106(1):djt319.
4. Tsang JY, Ni YB, Chan SK, Shao MM, Law BK, Tan PH, et al. Androgen receptor expression shows distinctive significance in ER positive and negative breast cancers. Annals of surgical oncology 2014;21(7):2218-28.
5. Panet-Raymond V, Gottlieb B, Beitel LK, Pinsky L, Trifiro MA. Interactions between androgen and estrogen receptors and the effects on their transactivational properties. Molecular and Cellular Endocrinology 2000;167:139-50.
6. Dees EC, Carey LA. Improving endocrine therapy for breast cancer: it's not that simple. Journal of clinical oncology : official journal of the American Society of Clinical Oncology 2013;31(2):171-3.
7. Giuliano M, Schifp R, Osborne CK, Trivedi MV. Biological mechanisms and clinical implications of endocrine resistance in breast cancer. Breast 2011;20 Suppl 3:S42-9.
8. Harvell DM, Richer JK, Singh M, Spoelstra N, Finlayson C, Borges VF, et al. Estrogen regulated gene expression in response to neoadjuvant endocrine therapy of breast cancers: tamoxifen agonist effects dominate in the presence of an aromatase inhibitor. Breast Cancer Res Treat 2008.
9. Harvell DM, Spoelstra NS, Singh M, McManaman JL, Finlayson C, Phang T, et al. Molecular signatures of neoadjuvant endocrine therapy for breast cancer: characteristics of response or intrinsic resistance. Breast Cancer Res Treat 2008.
10. Rechoum Y, Rovito D, Iacopetta D, Barone I, Ando S, Weigel NL, et al. AR collaborates with ERalpha in aromatase inhibitor-resistant breast cancer. Breast cancer research and treatment 2014;147(3):473-85.
11. De Amicis F, Thirugnansampanthan J, Cui Y, Selever J, Beyer A, Parra I, et al. Androgen receptor overexpression induces tamoxifen resistance in human breast cancer cells. Breast cancer research and treatment 2010;121(1):1-11.
12. Gallicchio L, Macdonald R, Wood B, Rushovich E, Helzlsouer KJ. Androgens and musculoskeletal symptoms among breast cancer patients on aromatase inhibitor therapy. Breast cancer research and treatment 2011;130(2):569-77.
13. Morris KT, Toth-Fejel S, Schmidt J, Fletcher WS, Pommier RF. High dehydroepiandrosterone-sulfate predicts breast cancer progression during new aromatase inhibitor therapy and stimulates breast cancer cell growth in tissue culture: a renewed role for adrenalectomy. Surgery 2001;130(6):947-53.
14. Cochrane DR, Bernales S, Jacobsen BM, Cittelly DM, Howe EN, D'Amato NC, et al. Role of the androgen receptor in breast cancer and preclinical analysis of enzalutamide. Breast cancer research : BCR 2014;16(1):R7.

15. Jambal P, Badtke MM, Harrell JC, Borges VF, Post MD, Sollender GE, et al. Estrogen switches pure mucinous breast cancer to invasive lobular carcinoma with mucinous features. Breast Cancer Res Treat 2013;137(2):431-48.
16. Kabos P, Finlay-Schultz J, Li C, Kline E, Finlayson C, Wisell J, et al. Patient-derived luminal breast cancer xenografts retain hormone receptor heterogeneity and help define unique estrogen-dependent gene signatures. Breast cancer research and treatment 2012;135(2):415-32.
17. Recchione C, Venturelli E, Manzari A, Cavalleri A, Martinetti A, Secreto G. Testosterone, dihydrotestosterone and oestradiol levels in postmenopausal breast cancer tissues. The Journal of steroid biochemistry and molecular biology 1995;52(6):541-6.
18. Peters AA, Ingman WV, Tilley WD, Butler LM. Differential effects of exogenous androgen and an androgen receptor antagonist in the peri- and postpubertal murine mammary gland. Endocrinology 2011;152(10):3728-37.
19. Ni M, Chen Y, Lim E, Wimberly H, Bailey ST, Imai Y, et al. Targeting androgen receptor in estrogen receptor-negative breast cancer. Cancer cell 2011;20(1):119-31.
20. Barton VN, D'Amato NC, Gordon MA, Lind HT, Spoelstra NS, Babbs BL, et al. Multiple molecular subtypes of triple-negative breast cancer critically rely on androgen receptor and respond to enzalutamide in vivo. Mol Cancer Ther 2015;14(3):769-78.
21. Chou TC. Theoretical basis, experimental design, and computerized simulation of synergism and antagonism in drug combination studies. Pharmacological reviews 2006;58(3):621-81.
22. Carpenter AE, Jones TR, Lamprecht MR, Clarke C, Kang IH, Friman O, et al. CellProfiler: image analysis software for identifying and quantifying cell phenotypes. Genome biology 2006;7(10):R100.
23. Zhang Y, Liu T, Meyer CA, Eeckhoute J, Johnson DS, Bernstein BE, et al. Model-based analysis of ChIP-Seq (MACS). Genome biology 2008;9(9):R137.
24. Liu X, Brutlag DL, Liu JS. BioProspector: discovering conserved DNA motifs in upstream regulatory regions of co-expressed genes. Pacific Symposium on Biocomputing Pacific Symposium on Biocomputing 2001:127-38.
25. Hertz GZ, Stormo GD. Identifying DNA and protein patterns with statistically significant alignments of multiple sequences. Bioinformatics 1999;15(7-8):563-77.
26. Trapnell C, Williams BA, Pertea G, Mortazavi A, Kwan G, van Baren MJ, et al. Transcript assembly and quantification by RNA-Seq reveals unannotated transcripts and isoform switching during cell differentiation. Nature biotechnology 2010;28(5):511-5.
27. Wu TD, Nacu S. Fast and SNP-tolerant detection of complex variants and splicing in short reads. Bioinformatics 2010;26(7):873-81.
28. Fioretti FM, Sita-Lumsden A, Bevan CL, Brooke GN. Revising the role of the androgen receptor in breast cancer. Journal of molecular endocrinology 2014;52:R257-65.
29. KUMAR MV, LEO ME, TINDALL DJ. Modulation of Androgen Receptor Transcriptional Activity by the Estrogen Receptor. Journal of Andrology 1994;15:534-42.
30. Greeve MA, Allan RK, Harvey JM, Bentel JM. Inhibition of MCF-7 breast cancer cell proliferation by 5alpha-dihydrotestosterone; a role for p21(Cip1/Waf1). J Mol Endocrinol 2004;32(3):793-810.
31. Garay JP, Karakas B, Abukhdeir AM, Cosgrove DP, Gustin JP, Higgins MJ, et al. The growth response to androgen receptor signaling in ERalpha-negative human breast cells is dependent on p21 and mediated by MAPK activation. Breast cancer research : BCR 2012;14(1):R27.
32. Hurtado A, Holmes KA, Ross-Innes CS, Schmidt D, Carroll JS. FOXA1 is a key determinant of estrogen receptor function and endocrine response. Nature genetics 2011;43:27-33.
33. Tran C, Ouk S, Clegg NJ, Chen Y, Watson PA, Arora V, et al. Development of a second-generation antiandrogen for treatment of advanced prostate cancer. Science 2009;324(5928):787-90.

34. De Leon JT, Iwai A, Feau C, Garcia Y, Balsiger HA, Storer CL, et al. Targeting the regulation of androgen receptor signaling by the heat shock protein 90 cochaperone FKBP52 in prostate cancer cells. Proc Natl Acad Sci U S A 2011;108(29):11878-83.
35. Need EF, Selth LA, Harris TJ, Birrell SN, Tilley WD, Buchanan G. Research resource: interplay between the genomic and transcriptional networks of androgen receptor and estrogen receptor alpha in luminal breast cancer cells. Mol Endocrinol 2012;26(11):1941-52.
36. Robinson JLL, MacArthur S, Ross-Innes CS, Tilley WD, Neal DE, Mills IG, et al. Androgen receptor driven transcription in molecular apocrine breast cancer is mediated by FoxA1. The EMBO Journal 2011;30:3019-27.
37. Fagan DH, Uselman RR, Sachdev D, Yee D. Acquired resistance to tamoxifen is associated with loss of the type I insulin-like growth factor receptor: implications for breast cancer treatment. Cancer research 2012;72(13):3372-80.
38. Grogg A, Trippel M, Pfaltz K, Ladrach C, Droeser RA, Cihoric N, et al. Androgen receptor status is highly conserved during tumor progression of breast cancer. BMC cancer 2015;15:872.
39. Lea OA, Kvinnsland S, Thorsen T. Improved measurement of androgen receptors in human breast cancer. Cancer research 1989;49(24 Pt 1):7162-7.
40. Boddy JL, Fox SB, Han C, Campo L, Turley H, Kanga S, et al. The androgen receptor is significantly associated with vascular endothelial growth factor and hypoxia sensing via hypoxia-inducible factors HIF-1a, HIF-2a, and the prolyl hydroxylases in human prostate cancer. Clin Cancer Res 2005;11(21):7658-63.
41. Mohammed H, D'Santos C, Serandour AA, Ali HR, Brown GD, Atkins A, et al. Endogenous purification reveals GREB1 as a key estrogen receptor regulatory factor. Cell Rep 2013;3(2):342-9.
42. Gaughan L, Stockley J, Coffey K, O'Neill D, Jones DL, Wade M, et al. KDM4B is a master regulator of the estrogen receptor signalling cascade. Nucleic acids research 2013;41(14):6892-904.
43. Wade MA, Jones D, Wilson L, Stockley J, Coffey K, Robson CN, et al. The histone demethylase enzyme KDM3A is a key estrogen receptor regulator in breast cancer. Nucleic acids research 2015;43(1):196-207.
44. Sikora MJ, Cordero KE, Larios JM, Johnson MD, Lippman ME, Rae JM. The androgen metabolite 5alpha-androstane-3beta,17beta-diol (3betaAdiol) induces breast cancer growth via estrogen receptor: implications for aromatase inhibitor resistance. Breast cancer research and treatment 2009;115(2):289-96.
45. Thin TH, Kim E, Yeh S, Sampson ER, Chen YT, Collins LL, et al. Mutations in the helix 3 region of the androgen receptor abrogate ARA70 promotion of 17beta-estradiol-induced androgen receptor transactivation. The Journal of biological chemistry 2002;277(39):36499-508.
46. Yeh S, Miyamoto H, Shima H, Chang C. From estrogen to androgen receptor: a new pathway for sex hormones in prostate. Proc Natl Acad Sci U S A 1998;95(10):5527-32.
47. Voss TC, Schiltz RL, Sung MH, Yen PM, Stamatoyannopoulos JA, Biddie SC, et al. Dynamic exchange at regulatory elements during chromatin remodeling underlies assisted loading mechanism. Cell 2011;146(4):544-54.
48. Ross-Innes CS, Stark R, Holmes KA, Schmidt D, Spyrou C, Russell R, et al. Cooperative interaction between retinoic acid receptor-alpha and estrogen receptor in breast cancer. Genes & development 2010;24:171-82.
49. Arora VK, Schenkein E, Murali R, Subudhi SK, Wongvipat J, Balbas MD, et al. Glucocorticoid receptor confers resistance to antiandrogens by bypassing androgen receptor blockade. Cell 2013;155(6):1309-22.
50. Wright AP, Zilliacus J, McEwan IJ, Dahlman-Wright K, Almlof T, Carlstedt-Duke J, et al. Structure and function of the glucocorticoid receptor. J Steroid Biochem Mol Biol 1993;47(1-6):11-9.

51. Tumedei MM, Silvestrini R, Ravaioli S, Massa I, Maltoni R, Rocca A, et al. Role of androgen and estrogen receptors as prognostic and potential predictive markers of ductal carcinoma in situ of the breast. The International journal of biological markers 2015:0.
52. Lawson DA, Bhakta NR, Kessenbrock K, Prummel KD, Yu Y, Takai K, et al. Single-cell analysis reveals a stem-cell program in human metastatic breast cancer cells. Nature 2015;526(7571):131-5.

FIGURE LEGENDS

***Figure 1* – AR inhibition decreases ER+/AR+ breast cancer growth.** (a) Proliferation of MCF7 cells treated with increasing concentrations of Enza was monitored by IncuCyte. (b) MCF7 cells were grown in soft agar with Enza or tam and colony size was measured by ImageJ. (c) Immunoblotting for AR, ER, and Tubulin in MCF7 cells expressing a non-targeting (shNeg) or AR-targeting (shAR15 and shAR17) shRNA constructs (upper). Proliferation was monitored by IncuCyte (lower). (d) MCF7 cells were grown in media with CSS for 72 hrs then treated with vehicle (Veh), E2, or E2 + Enza or MJC13 and cell number was measured by crystal violet. (e) MCF7 cells were grown in media with CSS for 72hrs then treated with Veh, E2, or E2+Enza for 24hrs followed by cell cycle analysis. (f) MCF7 cells expressing shNeg, shAR15, or shAR17 were cultured in media with CSS for 72 hrs then treated with veh or E2 and growth was measured by crystal violet. Error bars represent standard error of the mean. * p<.05, **** p<.0001 by ANOVA with Dunnett's Multiple Comparison Test.

***Figure 2* – AR inhibitors diminish ER genomic binding.** ChIP-seq for ER in MCF7 cells grown in CSS for 3 days then treated with E2 +/- Enza or MJC-13. (a) Heat map of ER binding. The heat map is shown with a horizontal window of +/- 2kb. (b) The number of binding sites identified by MACS2, using vehicle treatment as the control. (c) The ER ChIP-seq signal at individual sites with E2 alone (x-axis) versus E2 + Enza (blue) or MJC13 (red) (y-axis). (D-E) ChIP-qPCR (d) and ChIP-seq read depth (e) at well-characterized ER binding sites. Error bars represent standard error of the mean. ** p<.01, *** p<.001, **** p<.0001 by ANOVA with Dunnett's Multiple Comparison Test except.

***Figure 3* – AR and ER co-localize in the nucleus in response to E2.** (a) MCF7 cells were grown in media with CSS for 72 hr then pre-treated with veh, 10 uM Enza, or 1 uM bicalutamide (bic). Following pre-treatment, cells were treated with veh or 10nM E2 +/- Enza or bic as shown for an additional 3 hr. Cells were then fixed and ICC was performed for AR (green) and ER (red). (b,c) MCF7 cells were grown in media with CSS for 72hrs then treated with the indicated treatment for 3 hrs, and nuclear extracts were immunoblotted for AR and TOPO1. (d) ER+/AR+ ZR-75-1 or (e) ER-/AR+ MDA-453 cells were grown in media with CSS for 72hrs, then pre-treated for 3 hr with Enza or vehicle control. Following pre-treatment, cells were treated with veh, 10nM DHT, or 10nM E2 +/- Enza as shown for 3 additional hrs. Nuclear extracts were then obtained and subjected to western blotting for AR and TopoI. (f) MCF7 cells were grown in media with CSS for 72hrs then treated with E2 +/- Enza for 1 h followed by fixation and PLA staining for AR and ER (red). Nuclei were stained with DAPI (blue). (g) Fluorescent intensity per nuclei was measured by CellProfiler. Error bars represent standard error of the mean. ****p <0.0001 by ANOVA with Dunnett's Multiple Comparison Test.

Figure 4* – *E2 induces AR genome binding that overlaps with ER binding. ChIP-seq for AR in MCF7 cells grown in CSS for 3 days then treated with E2 for 1 h or DHT for 4 h. (a) Heat map of binding showing a horizontal window of +/- 2kb and enriched motifs from each category. (b) The number of binding sites identified by MACS2, using vehicle treatment as the control. (c) The number of AR binding sites that are unique to DHT (red), unique to E2 (blue), or shared (overlap) are shown. (d,e) ChIP-qPCR (d) and ChIP-seq read depth (e) results show AR binding at well-characterized ER binding sites following E2 treatment. (f) The percentage of AR binding sites in response to DHT (left) or E2 (right) that were also identified as ER binding sites (blue) is shown.

***Figure 5* – *Enza synergizes with tam and fulvestrant* in vitro.** (a) T47D cells were grown in media with complete serum and Enza and/or tam, and cell number was monitored by IncuCyte. Percent inhibition was compared to vehicle after 5 days, and synergy was calculated using Calcusyn software. A Combination Index (CI) value < 1 is indicative of synergy (yellow). (b-c) BCK4 or PT12 cells were grown in phenol red-free media with CSS for 1 day then treated with E2 with Enza and/or fulvestrant and cell number was monitored by Incucyte.

Figure 6* – *Enza inhibits tamoxifen-resistant tumor growth* in vitro *and* in vivo*, and AR is expressed in recurrent breast cancers. (a) Growth of MCF7-TamR cells treated with vehicle, Tam, Enza, or MJC13 for 7 days. (b) MCF7-TamR cells were plated in soft agar and the number of colonies was counted after 14 days. (c-d) MCF7-TamR cells were implanted into the mammary glands of nude mice with estrogen pellets and were matched into groups to receive either control chow (CTRL), tamoxifen pellets (tam), enzalutamide-containing chow (enza), or both (tam+enza). (c) Tumor growth was measured over time by luminescence. (d) Final tumor weights of mice from each group (lower). (e) IHC for AR and ER in clinical samples of patient-matched primary tumor and recurrence 110 months later. (f) IHC for AR and ER in clinical samples of patient-matched primary tumor and metastasis 167 months later (400x). * p<.05, *** p<.001, **** p<.0001 by ANOVA with Dunnett's Multiple Comparison Test.

Figure 7* –*Enza decreases hormone driven growth of PT12 primary tumors and metastases. (a-d) $1x10^6$ GFP-luciferase expressing PT12 cells were injected orthotopically into the mammary fat pad of NOD-SCID-IL2Rgc–/– mice followed by implantation of either an E2 or DHT pellet. When tumors reached an average of 39 mm^3, mice were randomized into the following groups: E2 with control chow (n=10) or enza chow (n=10), or DHT with control chow (n=5) or enza chow (n=5). Tumor viability was measured by IVIS for mice with E2 pellets (a) or DHT pellets (b). (c) BrdU staining of tumors from mice with E2 pellets. (d) Cleaved caspase staining of tumors from mice with DHT pellets. (e) PT12 GFP-luciferase cells were injected intracardially in NOD-SCID-IL2Rgc–/– mice. Metastatic burden of mice treated with E2 or E2+Enza was monitored using IVIS (photons/second) over 12 weeks (total signal supine+prone). (f) IVIS signal from mice in supine position at 2 weeks versus 12 weeks in E2 versus E2+Enza mice. (g) IVIS image of mice in the supine position in the E2 (n=11) or E2+Enza (n=12) groups after 12 weeks, red denotes high IVIS signal. Error bars represent SEM. *p<0.05, ***p<0.001, ****p <0.0001 by repeated measures mixed model approach for (a-b), ANOVA with Bonferroni's Multiple Comparison Test for (c-d), and Wilcoxon rank sum test for (e).

Figure 1

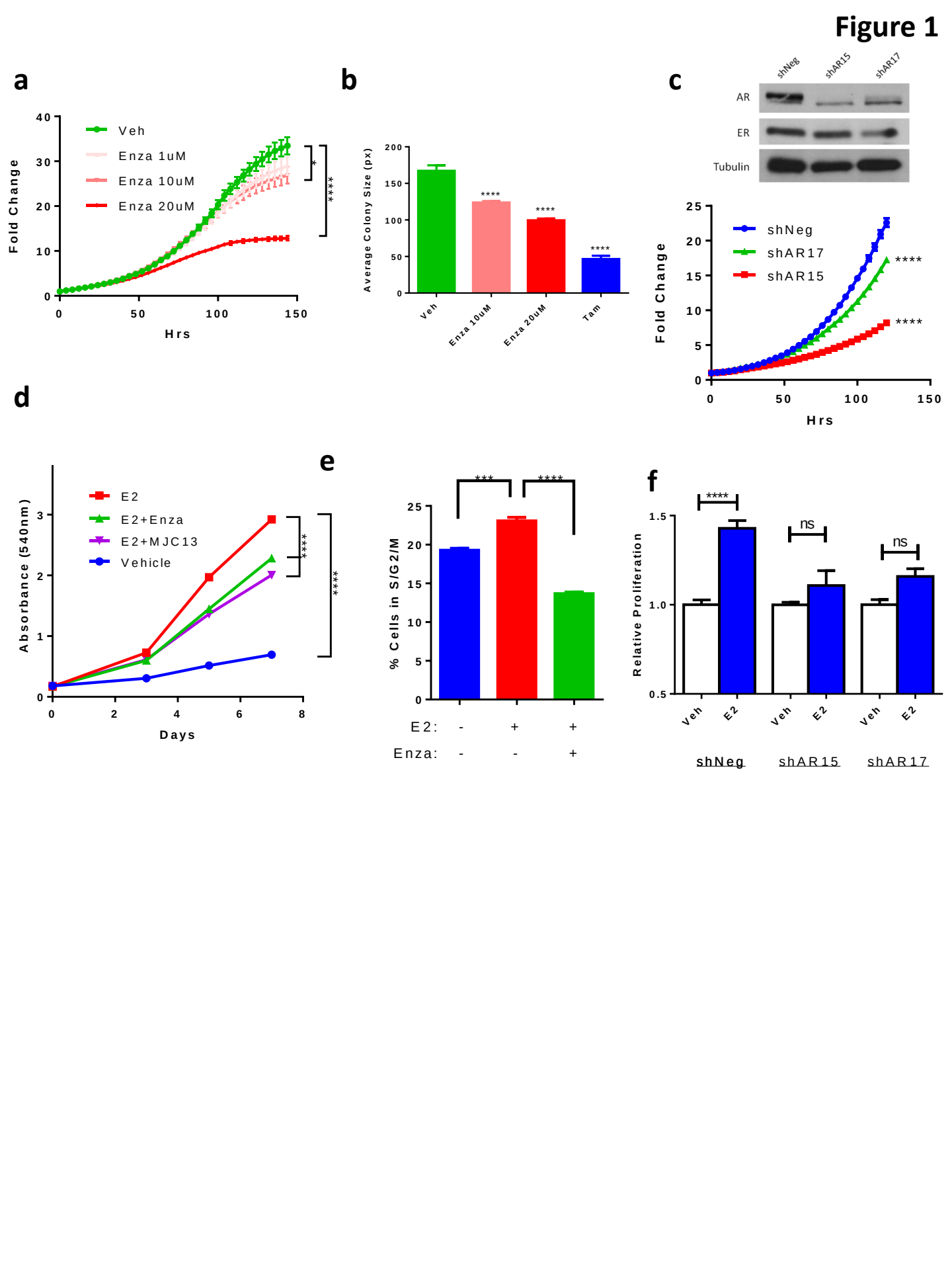
a
Fold Change
Hrs
Veh
Enza 1uM
Enza 10uM
Enza 20uM
*
****
b
Average Colony Size (px)
Veh
Enza 10uM
Enza 20uM
Tam
****
c
shNeg
shAR15
shAR17
AR
ER
Tubulin
Fold Change
Hrs
shNeg
shAR17
shAR15
****
d
Absorbance (540nm)
Days
E2
E2+Enza
E2+MJC13
Vehicle
****
e
% Cells in S/G2/M
***
****
E2:
Enza:
f
Relative Proliferation
****
ns
ns
Veh
E2
shNeg
shAR15
shAR17

Figure 2

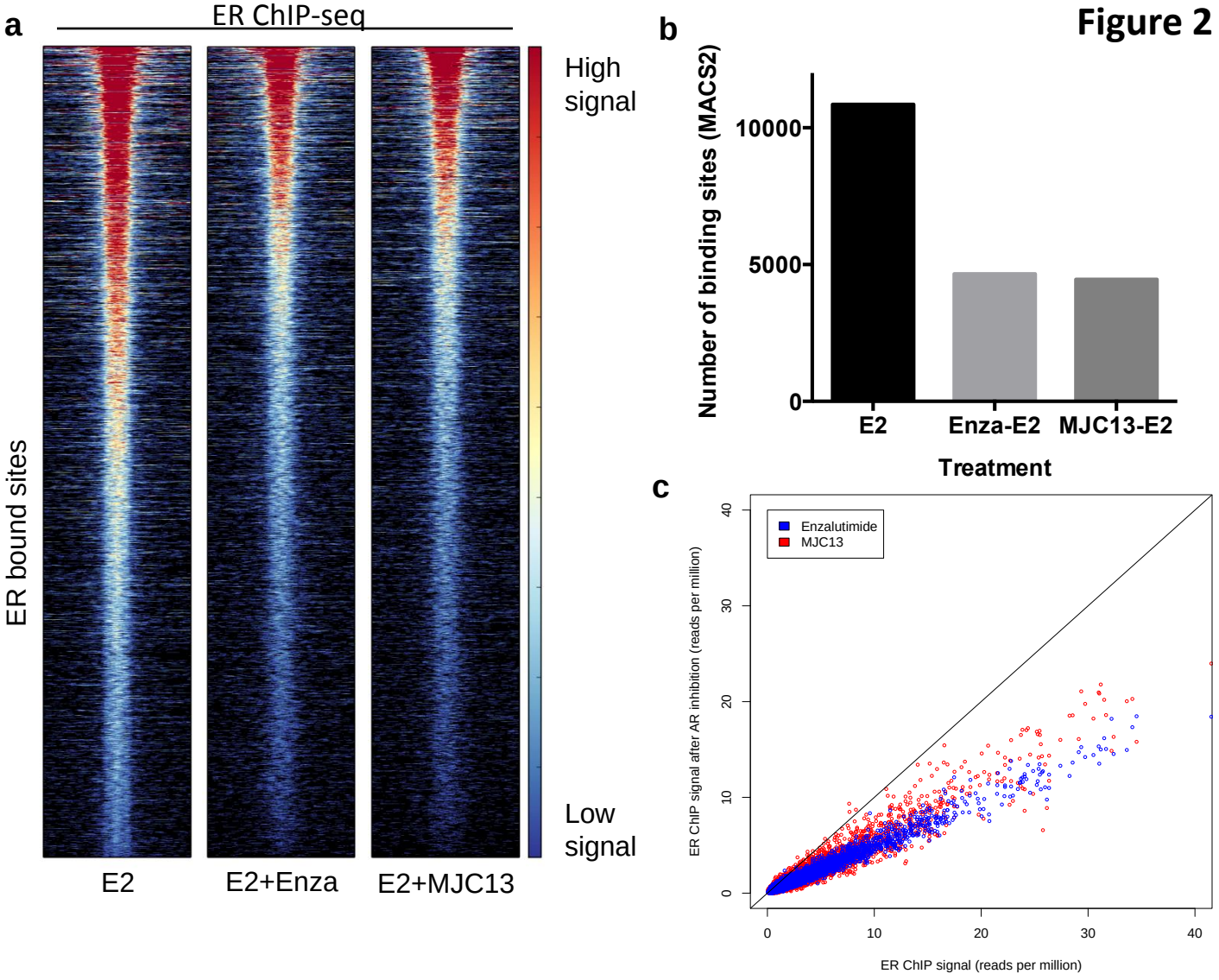
a
ER ChIP-seq
High signal
Low signal
ER bound sites
E2
E2+Enza
E2+MJC13
b
Number of binding sites (MACS2)
10000
5000
0
E2
Enza-E2
MJC13-E2
Treatment
c
Enzalutimide
MJC13
ER ChIP signal after AR inhibition (reads per million)
ER ChIP signal (reads per million)
0
10
20
30
40

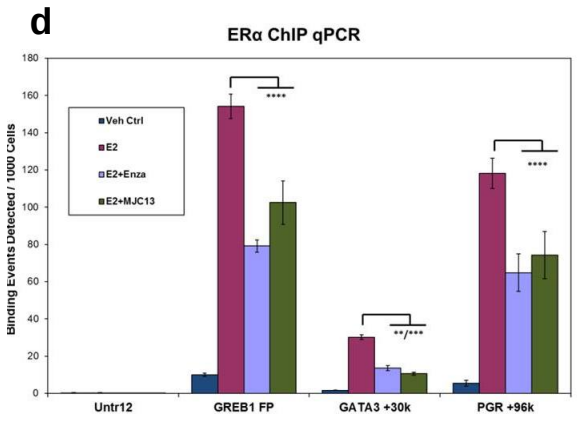
d
ERα ChIP qPCR
Binding Events Detected / 1000 Cells
Veh Ctrl
E2
E2+Enza
E2+MJC13
****
/*
Untr12
GREB1 FP
GATA3 +30k
PGR +96k

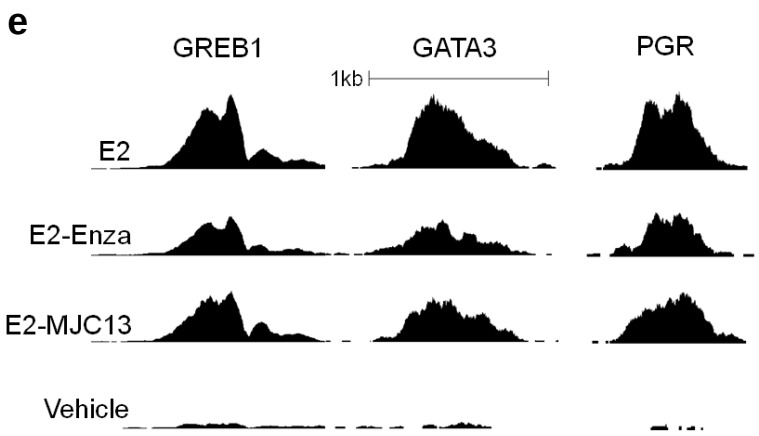
e
GREB1
GATA3
PGR
1kb
E2
E2-Enza
E2-MJC13
Vehicle

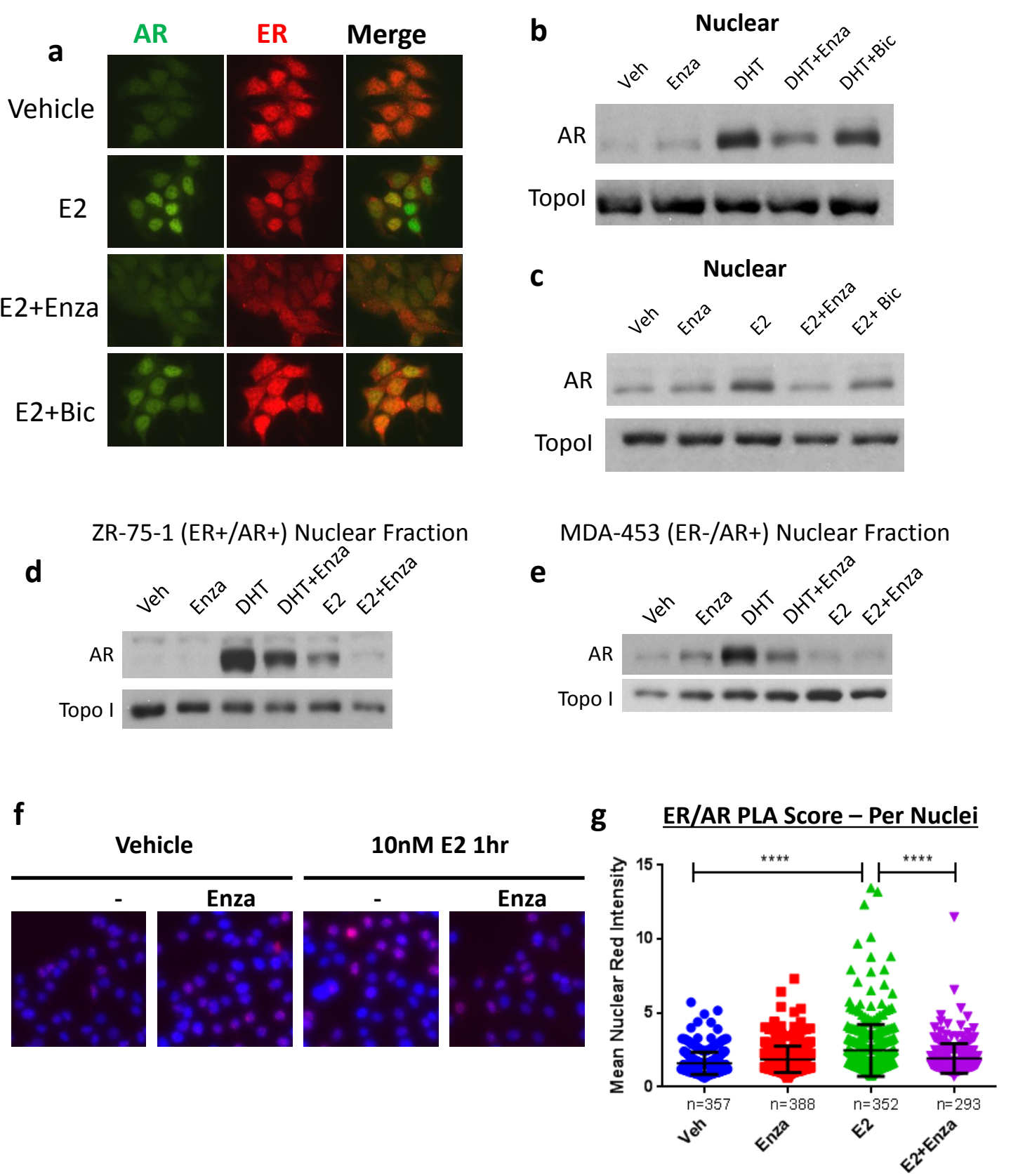
a
AR
ER
Merge
Vehicle
E2
E2+Enza
E2+Bic
b
Nuclear
Veh
Enza
DHT
DHT+Enza
DHT+Bic
AR
TopoI
c
Nuclear
Veh
Enza
E2
E2+Enza
E2+ Bic
AR
TopoI
ZR-75-1 (ER+/AR+) Nuclear Fraction
d
Veh
Enza
DHT
DHT+Enza
E2
E2+Enza
AR
Topo I
MDA-453 (ER-/AR+) Nuclear Fraction
e
Veh
Enza
DHT
DHT+Enza
E2
E2+Enza
AR
Topo I
f
Vehicle
10nM E2 1hr
-
Enza
-
Enza
g
ER/AR PLA Score – Per Nuclei
Mean Nuclear Red Intensity
15
10
5
0
****
****
n=357
n=388
n=352
n=293
Veh
Enza
E2
E2+Enza

Figure 3

Figure 4

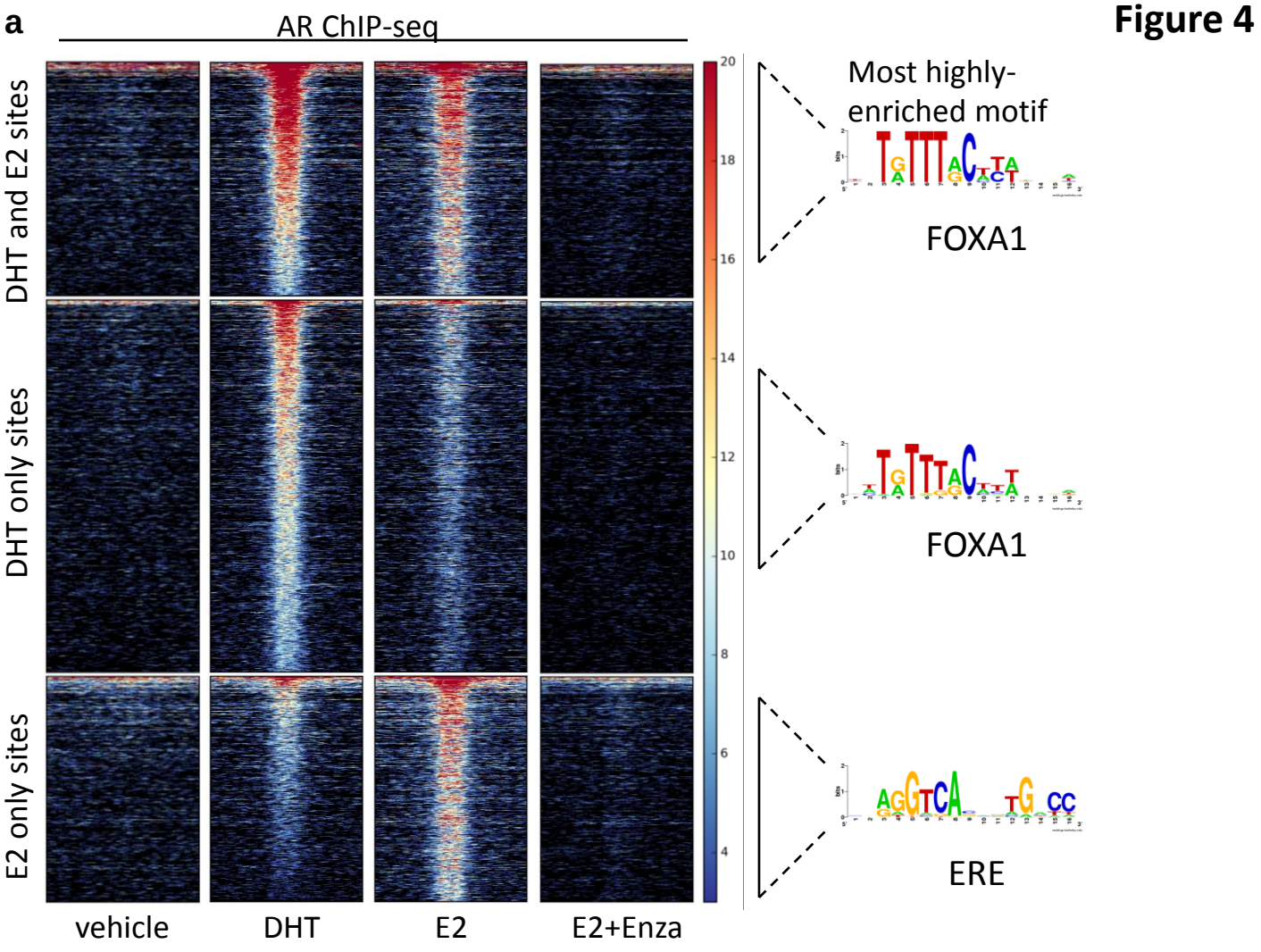
a
AR ChIP-seq
DHT and E2 sites
DHT only sites
E2 only sites
vehicle
DHT
E2
E2+Enza
Most highly-enriched motif
FOXA1
FOXA1
ERE

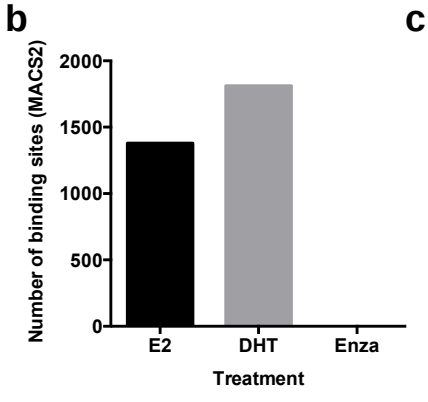
b
Number of binding sites (MACS2)
Treatment
E2
DHT
Enza

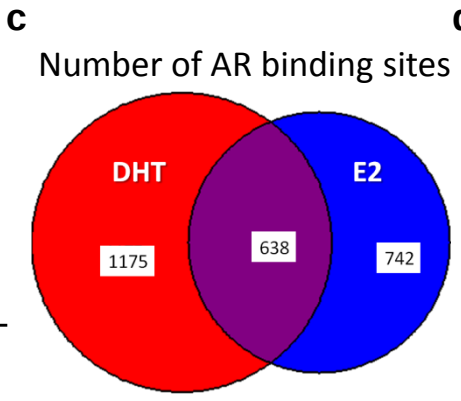
c
Number of AR binding sites
DHT
E2
1175
638
742

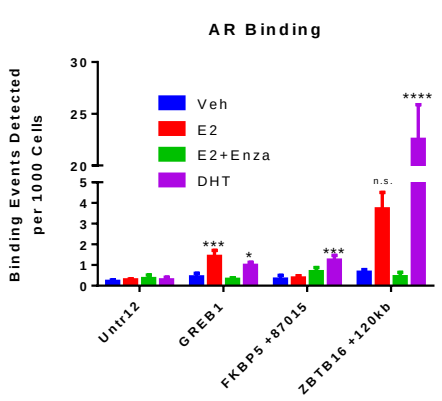
d
AR Binding
Binding Events Detected per 1000 Cells
Veh
E2
E2+Enza
DHT
Untr12
GREB1
FKBP5 +87015
ZBTB16 +120Kb

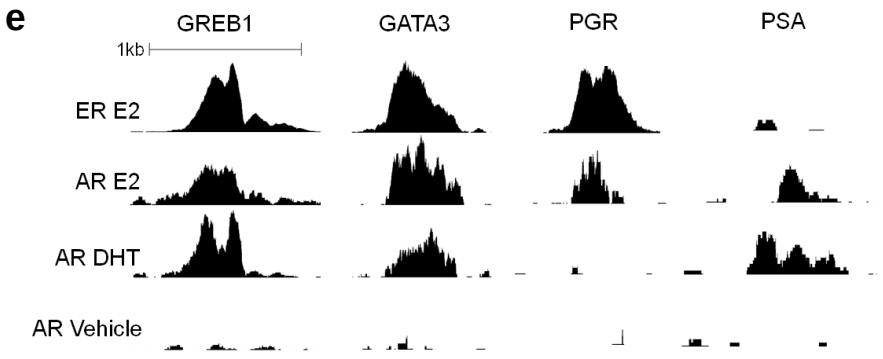
e
GREB1
GATA3
PGR
PSA
1kb
ER E2
AR E2
AR DHT
AR Vehicle

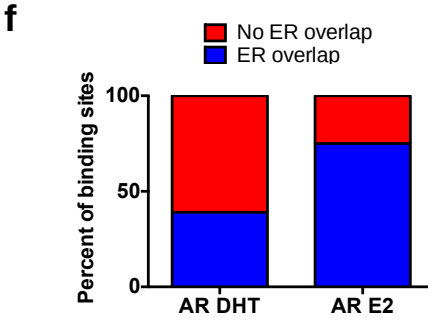
f
No ER overlap
ER overlap
Percent of binding sites
AR DHT
AR E2

Figure 5

a

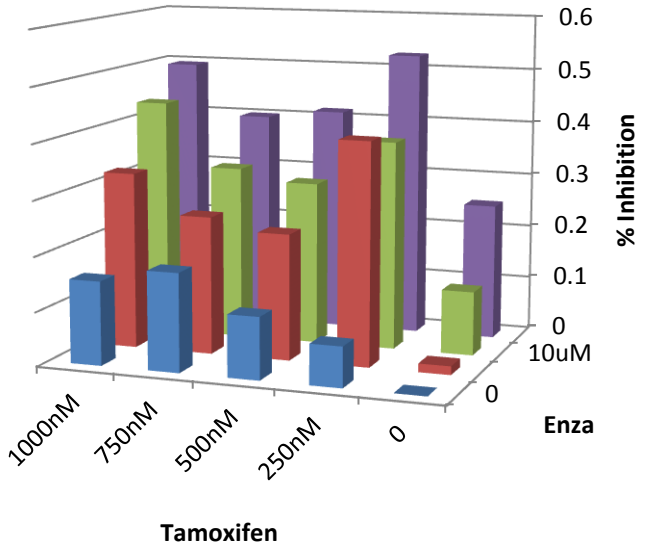

b

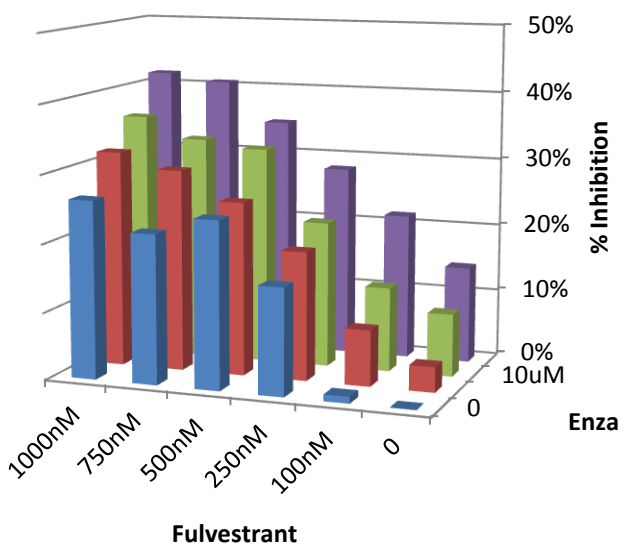

Combination Index

Tamoxifen

Enza	250nM	500nM	750nM	1000nM
5uM	0.244	0.593	0.659	0.544
10uM	0.466	0.675	0.710	0.529
20uM	0.656	0.867	0.947	0.781

Combination Index

Fulvestrant

Enza	100nM	250nM	500nM	750nM	1000nM
5uM	0.831	0.652	0.838	1.027	1.238
10uM	0.882	0.745	0.768	1.015	1.171
20uM	0.835	0.8	0.876	0.938	1.119

c

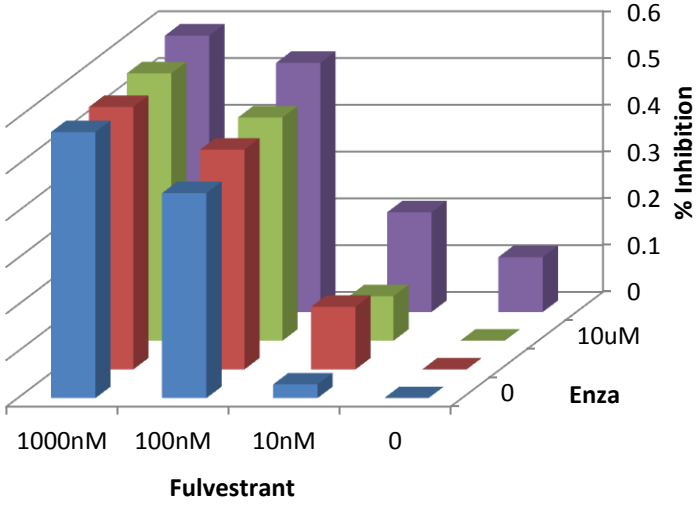

Combination Index

Fulvestrant

Enza	10nM	100nM	1000nM
1uM	0.244	0.283	1.812
10uM	0.53	0.275	1.721
20uM	0.159	0.211	1.565

Figure 6

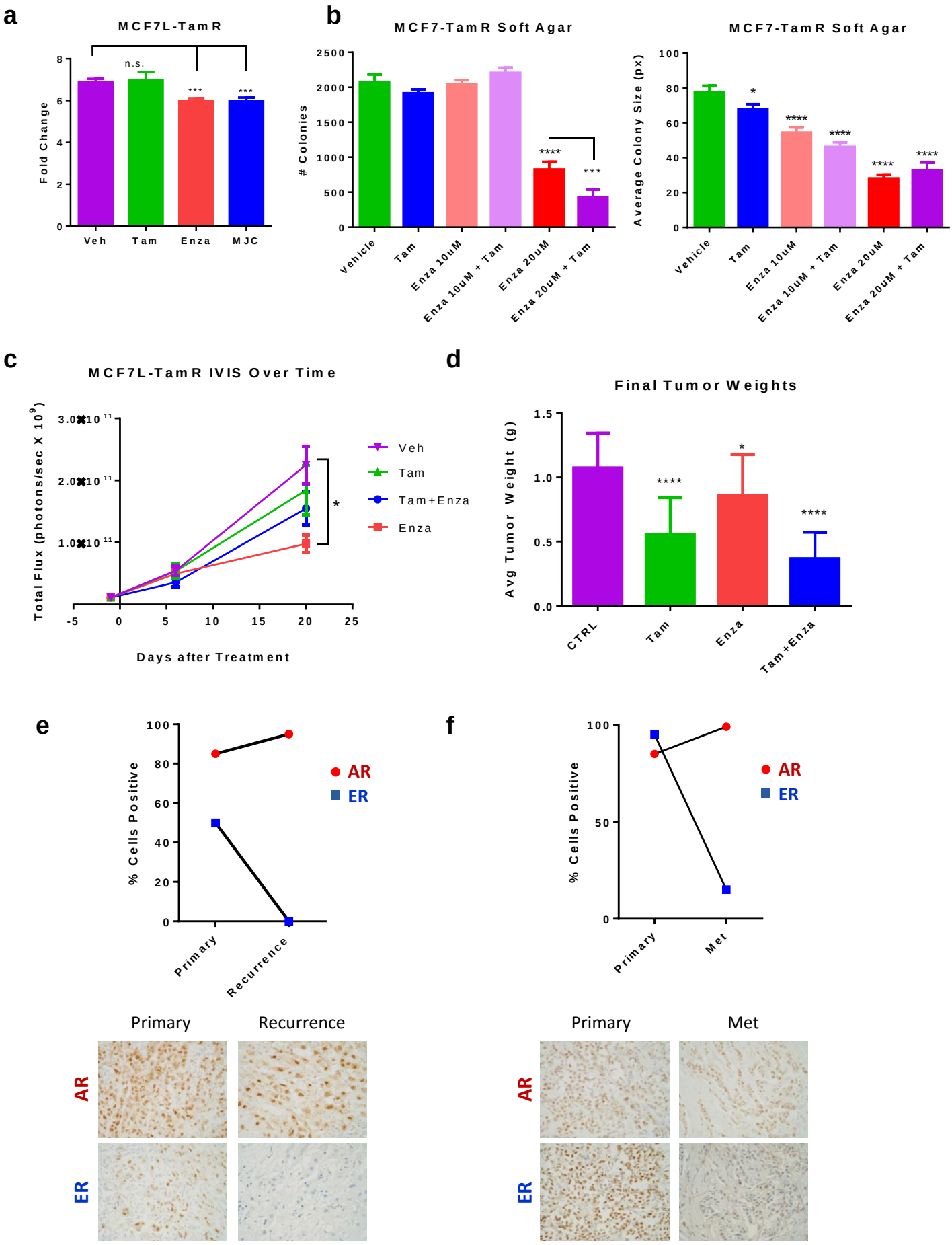
a
MCF7L-TamR
Fold Change
n.s.
***
***
Veh
Tam
Enza
MJC
b
MCF7-TamR Soft Agar
Colonies
****
***
Vehicle
Tam
Enza 10uM
Enza 10uM + Tam
Enza 20uM
Enza 20uM + Tam
MCF7-TamR Soft Agar
Average Colony Size (px)
*
****
****
****
****
Vehicle
Tam
Enza 10uM
Enza 10uM + Tam
Enza 20uM
Enza 20uM + Tam
c
MCF7L-TamR IVIS Over Time
Total Flux (photons/sec X 10^9)
3.0X10^11
2.0X10^11
1.0X10^11
*
Veh
Tam
Tam+Enza
Enza
-5
0
5
10
15
20
25
Days after Treatment
d
Final Tumor Weights
Avg Tumor Weight (g)
1.5
1.0
0.5
0.0
****
*
****
CTRL
Tam
Enza
Tam+Enza
e
% Cells Positive
100
80
60
40
20
0
AR
ER
Primary
Recurrence
f
% Cells Positive
100
50
0
AR
ER
Primary
Met
Primary
Recurrence
AR
ER
Primary
Met
AR
ER

Figure 7

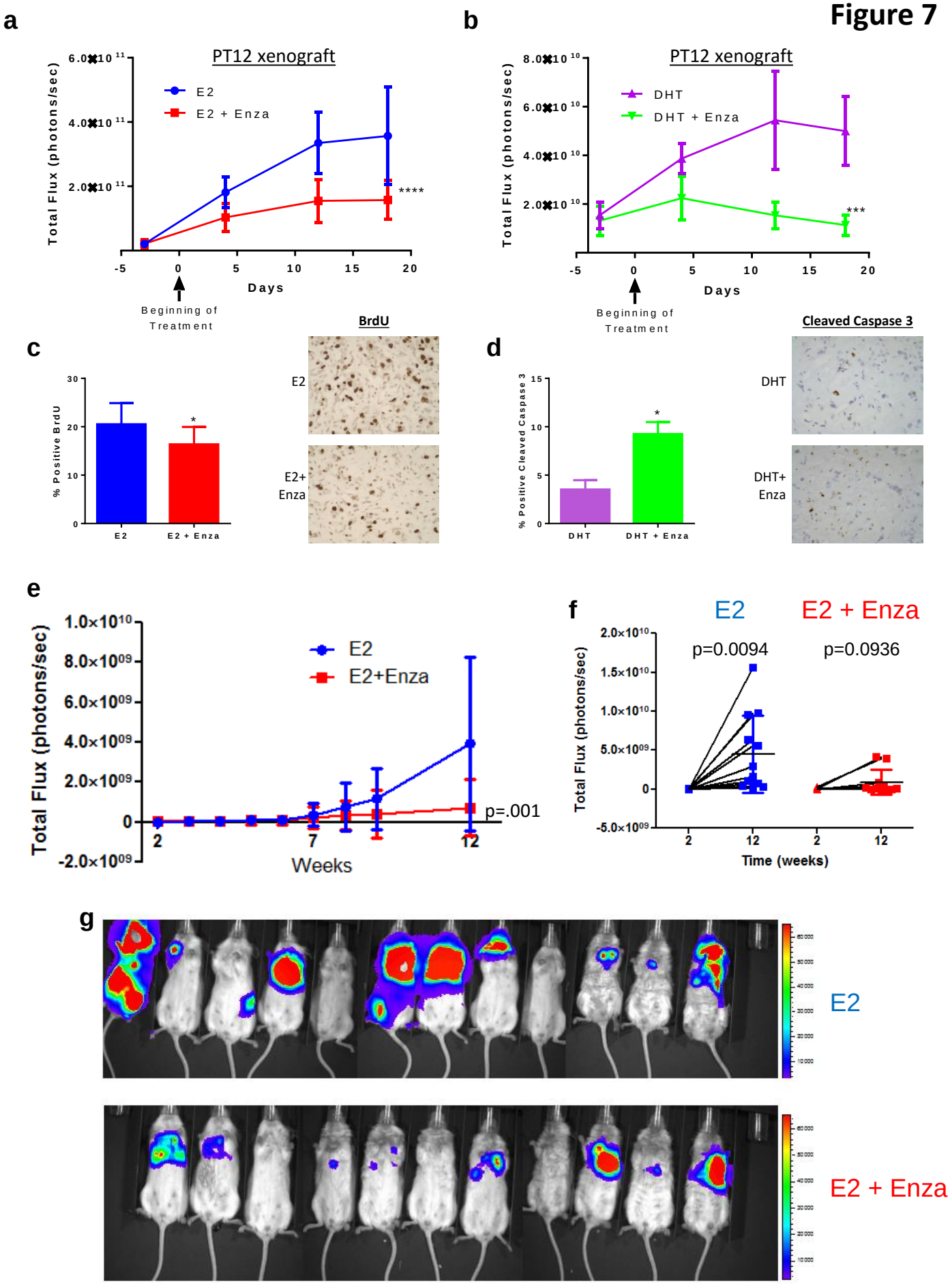
a
PT12 xenograft
Total Flux (photons/sec)
E2
E2 + Enza
****
Days
Beginning of Treatment
b
PT12 xenograft
Total Flux (photons/sec)
DHT
DHT + Enza
***
Days
Beginning of Treatment
c
BrdU
% Positive BrdU
E2
E2 + Enza
E2
E2+ Enza
d
Cleaved Caspase 3
% Positive Cleaved Caspase 3
DHT
DHT + Enza
DHT
DHT+ Enza
e
Total Flux (photons/sec)
E2
E2+Enza
p=.001
Weeks
f
E2
E2 + Enza
p=0.0094
p=0.0936
Total Flux (photons/sec)
Time (weeks)
g
E2
E2 + Enza

SUPPLEMENTARY DATA LEGENDS

Supplementary Table S1 *– E2 induces AR binding at sites that overlap with ER binding.* Genes near AR binding sites in response to E2 or DHT were identified using GREAT, and gene set over-representation analysis was subsequently performed using ConsensusPathDB(44). The top 5 over-enriched pathways from Pathway Interaction Database are shown for binding sites that were found in response to both DHT and E2 separately, E2 only, or DHT only.

Supplementary Table S2 *– Enza alters expression of E2-regulated genes in PT12 xenograft tumors.* List of genes with altered expression in tumors from mice receiving control chow compared to Enza chow by as determined by RNA-seq ($p<.05$, fold change >1.2). Genes previously described as E2-regulated in PT12 PDX model are highlighted in red.

Supplementary Table S3 *– Pathway analysis of Enza-regulated genes in PT12 xenograft tumors.* (a) Metacore analysis revealed that genes differentially expressed between Enza and CTRL-treated PT12 tumors are enriched in both ER and AR target genes. (a) Gene set over-representation analysis was performed using ConsensusPathDB and over-enriched pathways from Pathway Interaction Database are shown.

Supplementary Figure S1 *– Enza or AR knockdown decrease baseline and E2-induced proliferation of breast cancer cells in vitro.* (a) ER+/AR+ T47D or ZR-75-1 cells were grown in complete media with the indicated concentration of Enza and cell number was monitored by Incucyte live cell imaging. Growth is expressed as fold change compared to t=0. (b) T47D cells were grown in soft agar in the indicated concentration of Enza or tam for 15 days. Plates were photographed and colony size was measured by ImageJ. $p<.05$ by unpaired student t-test. (c) T47D and ZR-75-1 cells were grown in media with CSS for 72hrs, and PT12 cells were grown in media with CSS for 24hrs, then cells were treated with Veh, 10nM E2, or E2+Enza at the indicated concentrations and cell number was monitored by Incucyte live cell imaging. Growth is expressed as fold change compared to t=0. (d) MCF7 or T47D cells were grown in media with CSS with 10nM E2 and the indicated concentration of Enza. After 8 days, cell viability was measured by CellTiter-Glo assay and EC50 was calculated. (e) T47D cells were grown in media with CSS for 72hrs then treated with Veh, 10nM E2, or E2+Enza for 24hrs followed by fixation and cell cycle analysis. Error bars represent standard error of the mean. * $p<.05$, ** $p<.01$, **** $p<.0001$ by ANOVA with Bonferroni's Multiple Comparison Test except (F) by unpaired student t-test.

Supplementary Figure S2 *– E2 induces and Enza inhibits AR nuclear localization.* (a) ER-/AR+ MDA-MB-231 cells were grown in media with CSS for 72hrs, then pre-treated for 3 hr with Enza or vehicle control. Following pre-treatment, cells were treated with veh, 10nM DHT, or 10nM E2 +/- Enza as shown for 3 additional hrs. Nuclear and cytosolic extracts were then obtained and subjected to western blotting for AR, TopoI, and α-Tubulin. (b) T47D cells were grown in media with CSS for 72hrs then treated with veh or E2 +/- Enza for 1 hr followed by fixation and PLA staining for AR and ER. (c) The number of fluorescent foci per nucleus was determined by CellProfiler. (d) The number of nuclei with greater than 20 foci (per 100 nuclei). Error bars represent standard error of the mean. ** $p<.01$, *** $p<.001$, **** $p<.0001$ by ANOVA with Bonferroni's Multiple Comparison Test.

Supplementary Figure S3 ***– AR and ER binding in MCF7 cells.*** (a) Venn diagram illustrating overlap between DHT-induced AR binding in MDA-453 cells (light blue), LNCAP prostate cancer cells (yellow) and MCF7 cells (pink). (b) Percentage of AR binding sites in response to DHT, E2, or either ligand that match the consensus palindromic ARE sequence. (c) Percentage of AR binding sites in response to DHT, E2, or either ligand that match the consensus palindromic ERE sequence. (d-e) Scatter plot of ER ChIP signal intensity with E2 alone (X-axis) or E2+Enza (e) or E2+MJC13 (e) on the Y-axis. Blue points are ER binding loci that were also bound by AR in response to E2, while red points represent loci not bound by AR in response to E2.

Supplementary Figure S4 ***– Enza synergizes with anti-estrogens.*** (a) MCF7 cells were grown in phenol red-free media with CSS for 3 days then treated with 10 nM E2 with the indicated concentrations of Enza and/or fulvestrant and cell number was monitored by Incucyte. Percent inhibition compared to vehicle control was calculated for each treatment, and the Combination Index (CI) was calculated by Calcusyn software. A CI less than 1 is indicative of synergistic inhibitory activity. (b) MCF7 cells were grown in soft agar with 1 uM tam and/or 20 uM enza for 14 days. Colonies were photographed and quantified using ImageJ. (c) ZR-75-1 cells were cultured in media with CSS for 72 hr, then treated with 10 nM E2 plus the indicated concentrations of enza and/or fulvestrant. Percent inhibition compared to vehicle control was calculated for each treatment, and the CI was calculated by Calcusyn. Error bars represent standard error of the mean. * p<.05, *** p<.001, **** p<.0001 by ANOVA with Bonferroni's Multiple Comparison Test.

Supplementary Figure S5 ***– The combination of Enza plus tam reduces ER.*** (a) Whole cell extracts from MCF7L and MCF7L-TamR cells were subjected to immunoblotting for AR, ER, FOXA1, and Tubulin. (b) Quantification of TUNEL staining in MCF7-TamR xenograft tumors. Error bars represent standard error of the mean. (c) Quantification and (d) representative images of IHC for ER in MCF7-TamR xenograft tumors. Error bars represent standard error of the mean. *p<.05, ***p < 0.001 by ANOVA with Bonferroni's Multiple Comparison Test.

Supplementary Figure S6 ***–PT12 cells are AR+ and Enza alters expression of E2-regulated genes in PT12 xenograft tumors.*** (a) First passage of PT12 PDX stained with AR antibody SP107. AR staining was detected using DAB. (b) Immunoblot for AR, ER, and Tubulin on lysates from a panel of cell lines including PT12 cells demonstrating AR and ER expression. (c) Venn diagram of genes altered (p<.05, fold change >1.2) in Enza-treated PT12 xenograft tumors in E2-treated mice compared to all E2-regulated genes previously identified in the PT12 PDX model (16).

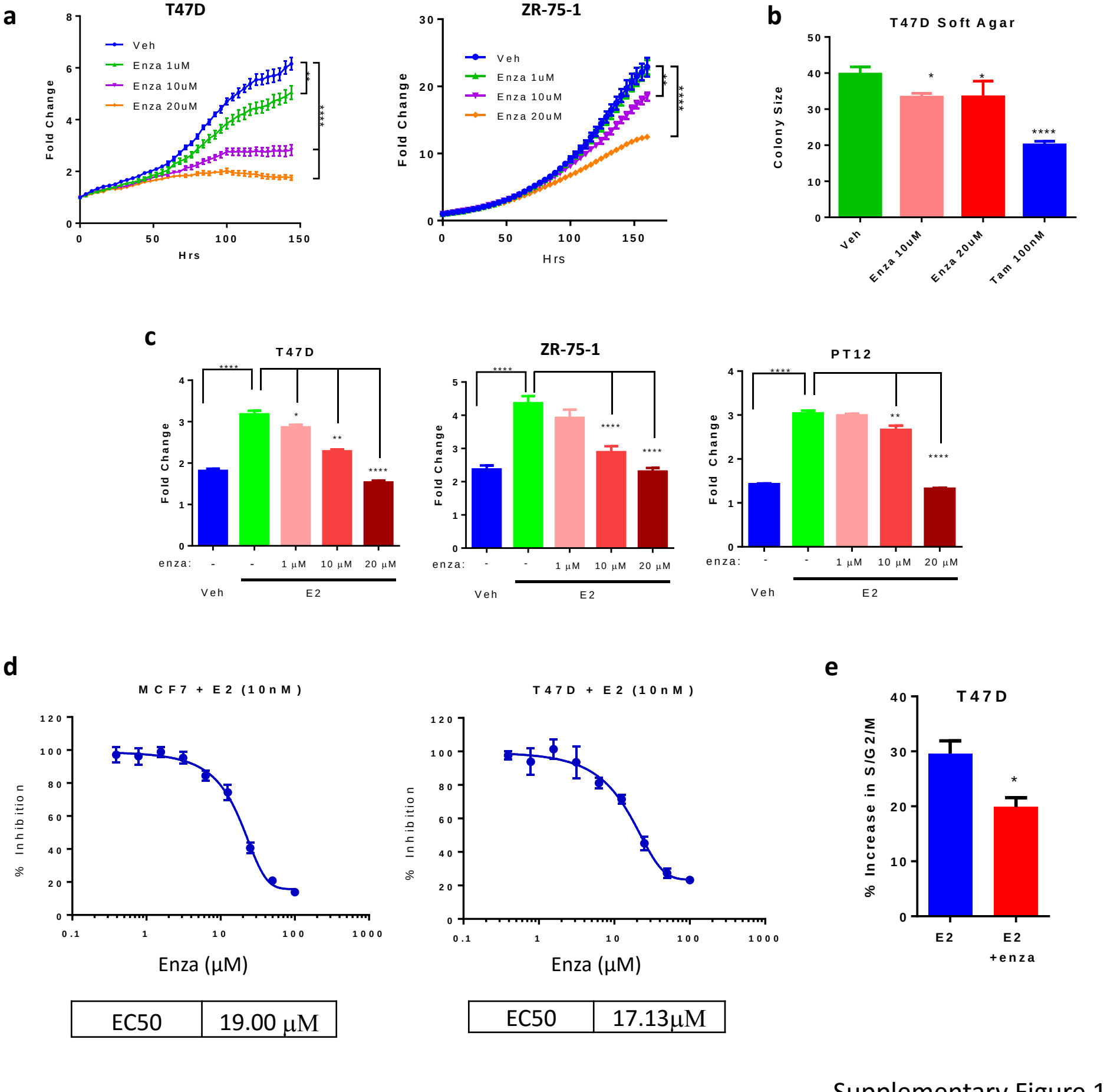

Supplementary Figure 1

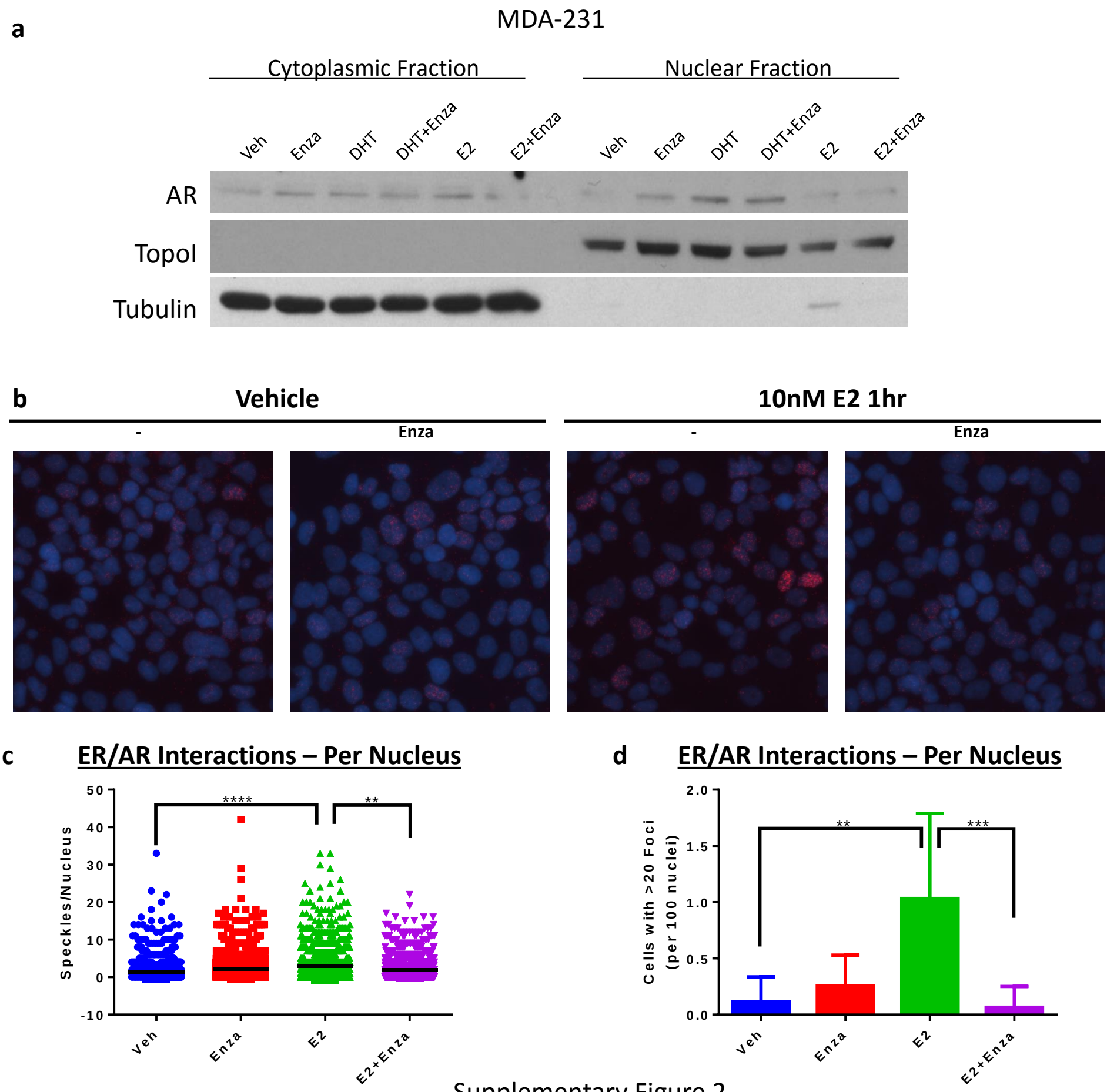

Supplementary Figure 2

a

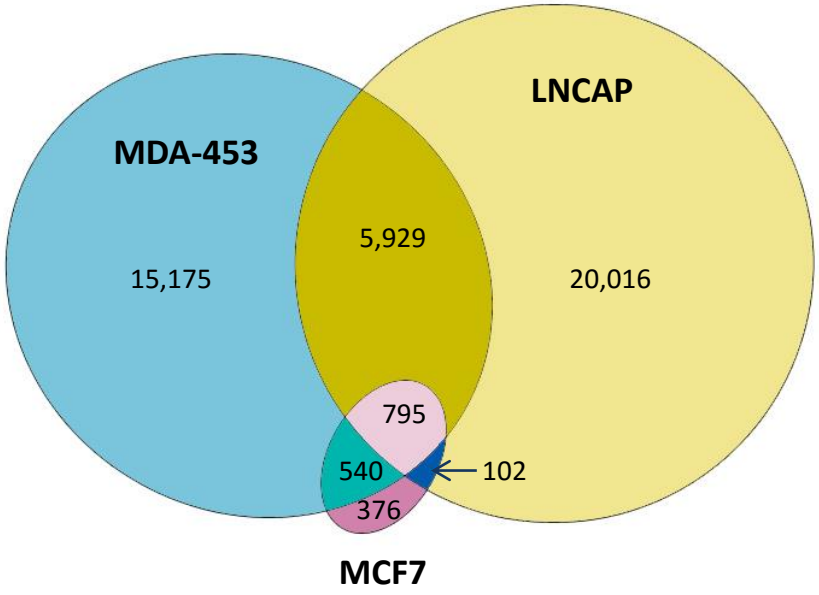

b

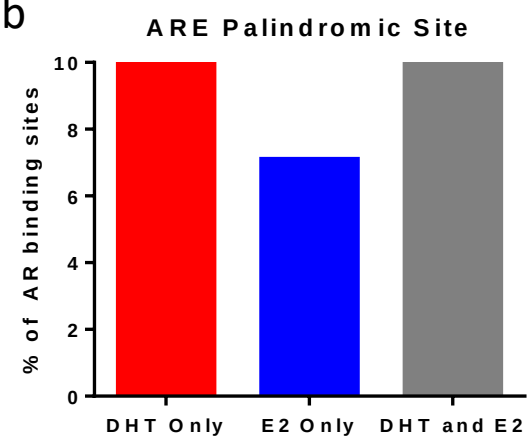

c

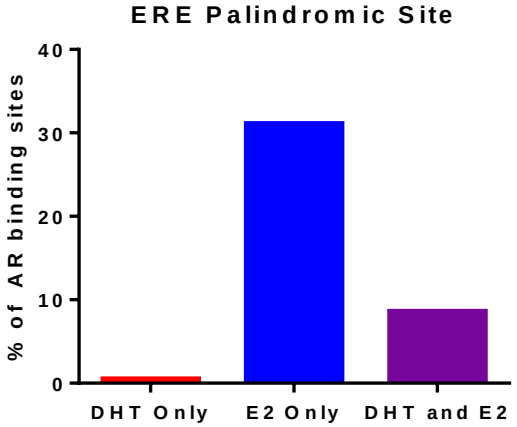

d

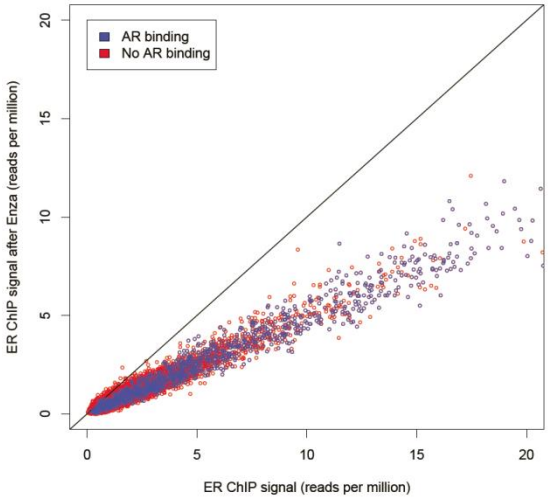

e

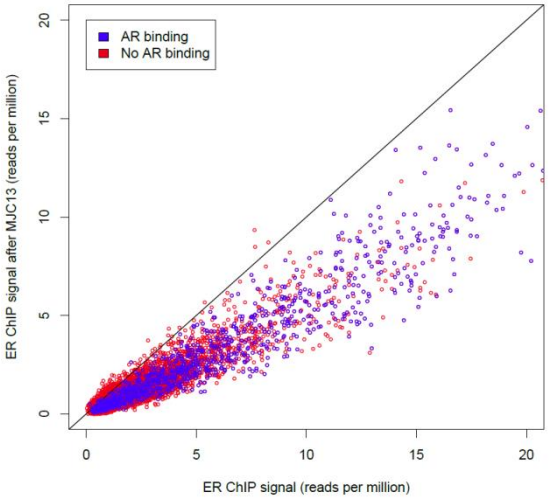

Supplementary Figure 3

a

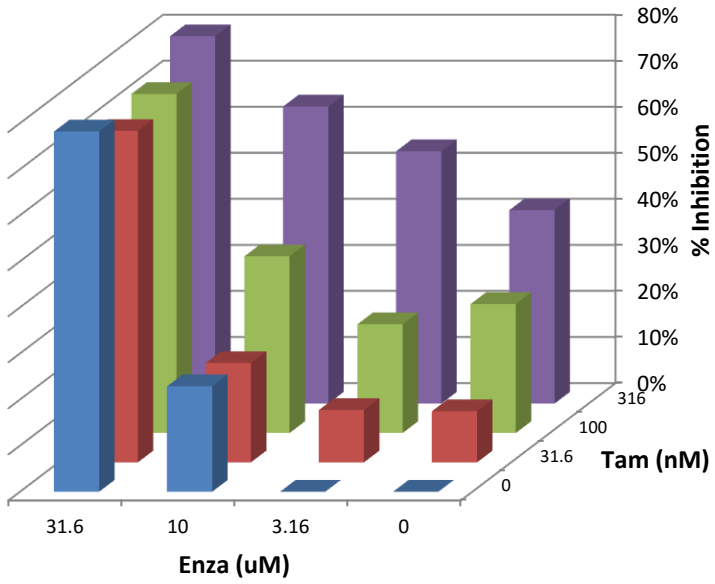

Combination Index

Enza \ Tam	10nM	100nM	1000nM
3.16uM	1.286	1.261	0.722
10.0uM	0.982	0.956	0.791
31.6uM	1.396	1.420	1.420

b

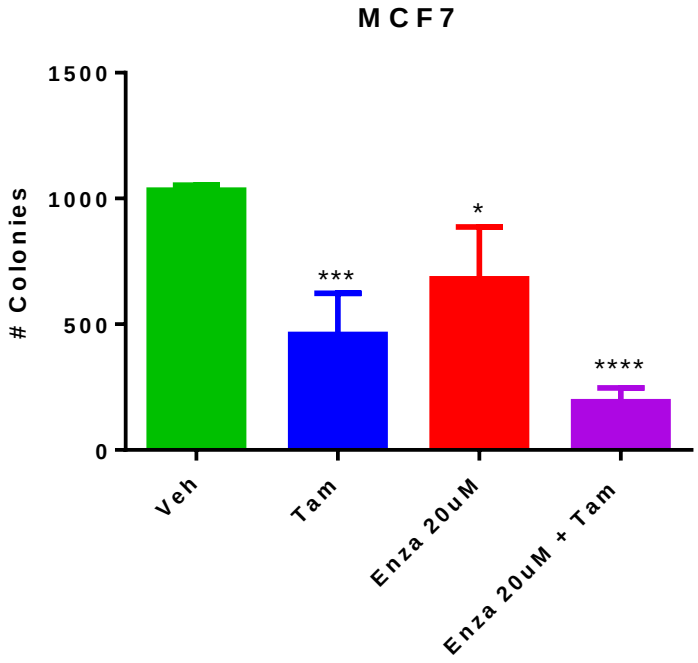

c

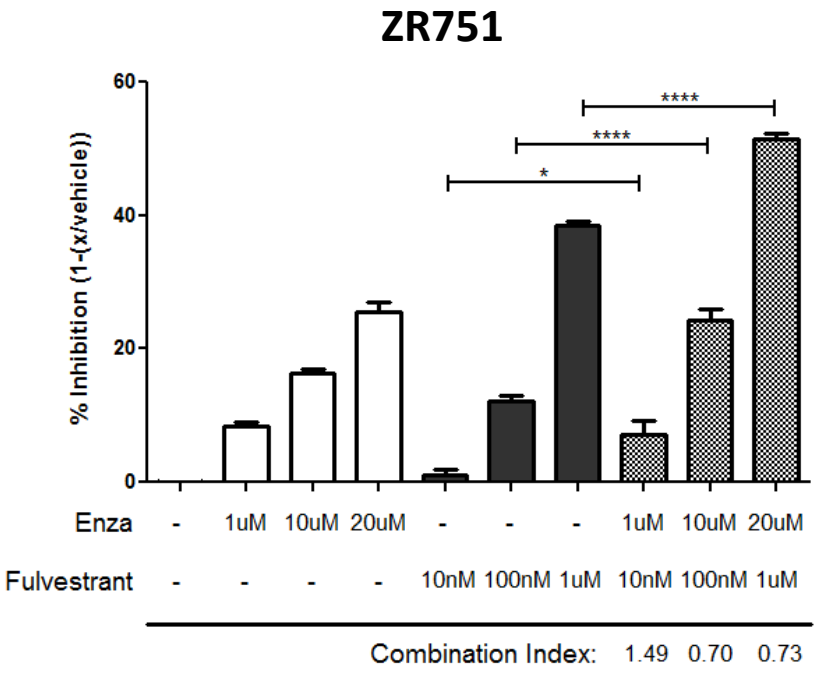

Supplementary Figure 4

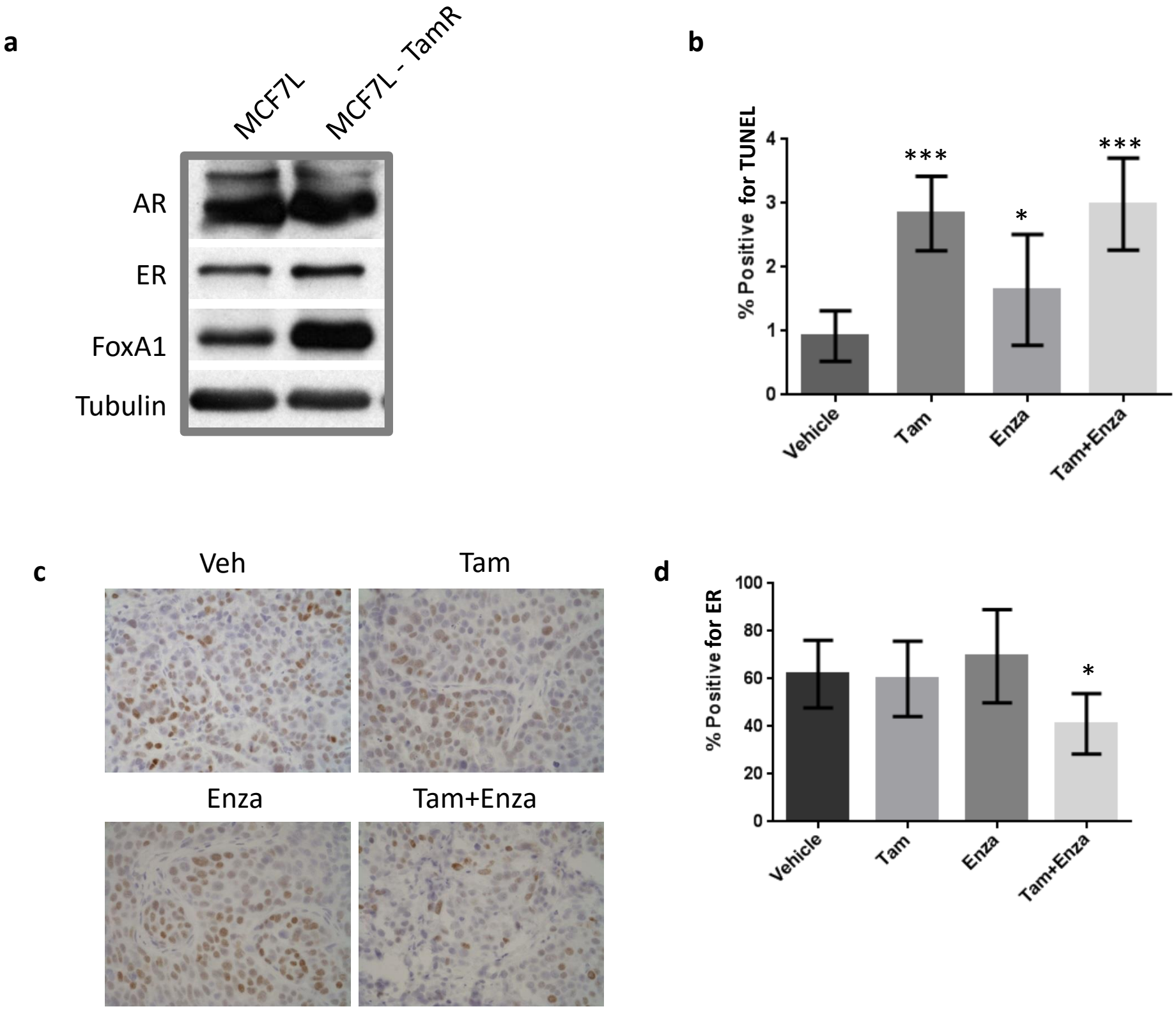

Supplementary Figure 5

a

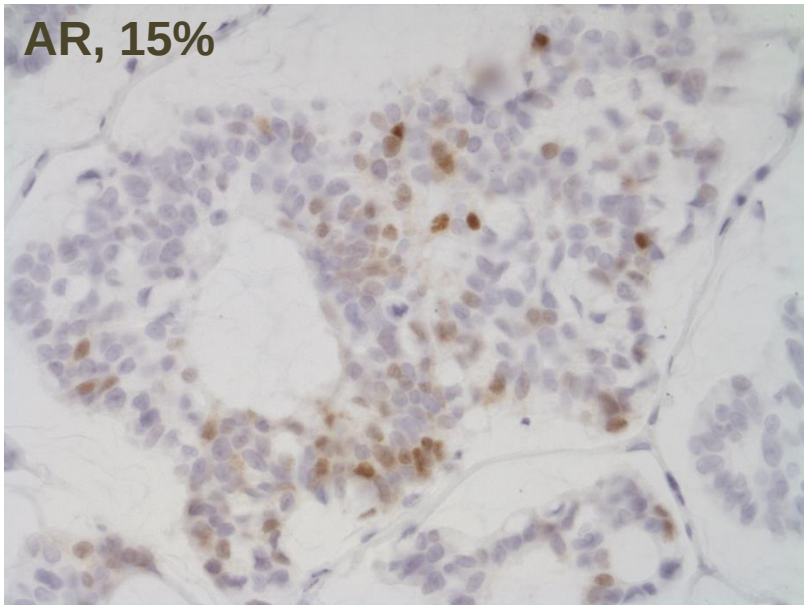

b

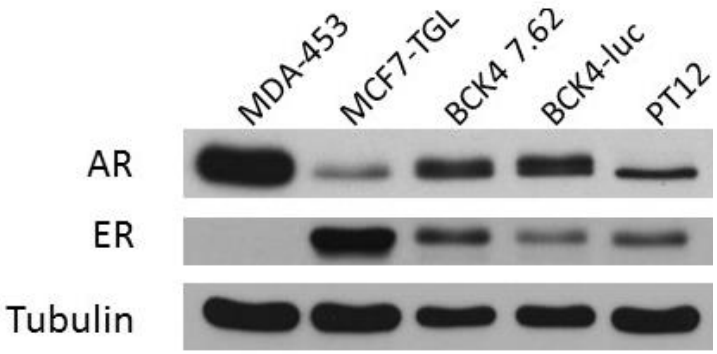

c

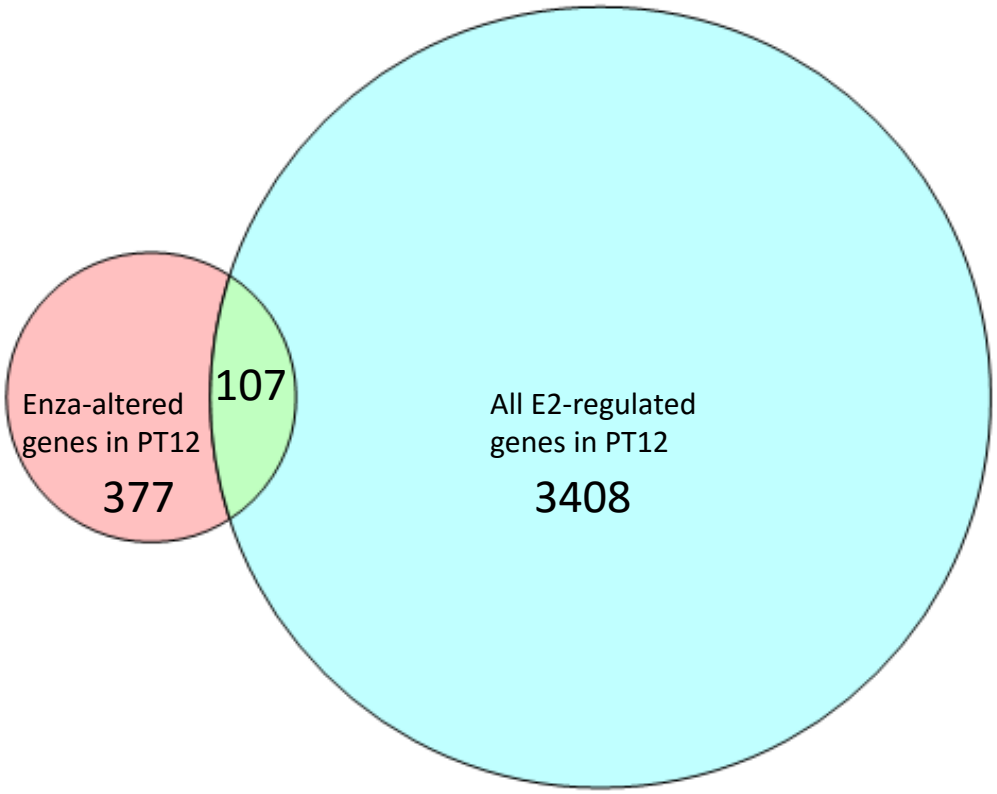

Supplementary Figure 6

ANDROGEN RECEPTOR SUPPORTS A CANCER STEM CELL-LIKE POPULATION IN TRIPLE-NEGATIVE BREAST CANCER

Valerie N. Barton, Jessica L. Christenson, Thomas J. Rogers, Kiel Butterfield, Beatrice Babbs, Nicole S. Spoelstra, Nicholas C. D'Amato, Anthony Elias, Jennifer K. Richer[1]

University of Colorado Anschutz Medical Campus
Department of Pathology
12800 E. 19th Ave.
Aurora, CO 80045

Valerie.Barton@ucdenver.edu
Jessica.Christenson@ucdenver.edu
Thomas.Rogers@ucdenver.edu
Kiel.Butterfield@ucdenver.edu
Beatrice.Babbs@ucdenver.edu
Nicole.Spoelstra@ucdenver.edu
Nicholas.Damato@ucdenver.edu
Jennifer.Richer@ucdenver.edu

[1] Corresponding author

ABSTRACT (350 words)

Background Triple-negative breast cancer (TNBC) is an aggressive breast cancer subtype lacking estrogen and progesterone receptors, and human epidermal growth factor receptor 2 (HER2). While to date there are no approved targeted therapies for TNBC, preclinical and early clinical trials indicate that up to 50% express some degree of positivity for androgen receptors (AR) and are sensitive to AR targeted therapy. However, the function of AR in TNBC and the mechanisms by which AR targeted therapy reduces tumor burden in preclinical and clinical settings are unknown. We hypothesized that AR maintains a cancer stem cell-like (CSC) tumor initiating population and that it serves as an anti-apoptotic factor that facilitates anchorage independence. **Methods** Anchorage independence/anoikis resistance was assessed on poly-Hema coated tissue culture plates used to achieve forced suspension culture and apoptosis was measured with cleaved caspase 3 antibody. AR was inhibited using the AR inhibitor Enzalutamide (Enza) or shRNAs targeting AR. CSC populations were assessed in vitro using ultra low attachment plates, CD44/CD24 staining, the ALDEFLUOR assay, and single cell mammosphere formation efficiency (MFE) assays in TNBC cell lines SUM159PT and MDA-MB-453.. In vivo, tumor-initiating capacity was assessed using a limiting dilution assay of SUM159PT cells pre-treated with or without Enza. Lastly, the efficacy of combination Enza and chemotherapy was assessed by caliper measurement and intravital imaging of TNBC xenografts in mice treated with Enza and paclitaxel. **Results** AR transcript ($P<0.05$), protein, and transcriptional activity ($P<0.01$) increased in tumor cells in suspension culture compared to attached conditions. Cells that expressed AR protein resisted detachment-induced apoptosis. The CSC population increased in suspension culture by ALEDFLUOR staining ($P<0.01$), CD44/CD24 staining ($P<0.001$), and MFE ($P<0.05$). AR inhibition decreased ADLH staining ($P<0.001$), increased CD24 staining ($P<0.05$), and decreased MFE($P<0.01$). In vivo, pre-treatment with Enza decreased the tumor-initiating capacity of TNBC cells in a limiting

dilution assay ($P<0.05$). Enza significantly decreased tumor volume and viability when administered during or after chemotherapy in vivo ($P<0.05$) and simultaneous treatment significantly reduced tumor recurrence. **Conclusions** AR supports anchorage independence, maintenance of CSCs, tumor initiation and regrowth following chemotherapy in a TNBC preclinical model. Thus AR targeted therapies may enhance the efficacy of chemotherapy even in TNBC with very few cells positive for AR, perhaps by targeting a different cell population.

KEYWORDS

Androgen receptor, triple-negative breast cancer, cancer stem-like cells, chemotherapy

BACKGROUND

Triple-negative breast cancer (TNBC) is an aggressive breast cancer (BC) subtype and currently no effective targeted therapies are available. A study of over 1600 invasive breast carcinomas found that women with TNBC have a peak risk of recurrence between 1-3 years, an increased likelihood of distal recurrence, and a majority of deaths occurring in the first five years compared to other BC subtypes [1]. While most metastatic TNBC initially respond to cytotoxic chemotherapy, the majority of patients experience recurrence following treatment [2]. Studies suggest that survival of chemotherapy-resistant cancer cells with stem-like properties (CSC) may repopulate the tumor [3-6]. Therapies that target CSCs in combination with chemotherapy may prevent tumor recurrence.

Androgen receptor (AR) is expressed in 12-55% of TNBC [7-15] and results of clinical trials targeting AR are promising [16]. However, little is known about the function of AR in TNBC and the mechanisms by which AR antagonists improve TNBC outcomes. There is recent evidence that progesterone supports the expansion of breast cancer tumor-initiating cells [17] and that estrogen and progesterone expand the normal mouse mammary stem cell population, even though it is thought that the stem cells themselves lack estrogen and progesterone receptors (ER, PR) [18, 19]. Interestingly, PR and AR can recognize identical consensus DNA response elements [20] and regulate many of the same genes [21], and AR in TNBC cells binds to chromatin at sites more similar to ER in ER+ BC than AR in prostate cancer [22]. Recent studies suggest that AR may regulate genes associated with CSCs in prostate cancer [23, 24]. Finally, we

previously demonstrated that the AR-antagonist Enzalutamide (Enza) significantly decreased anchorage-independent growth of multiple TNBC lines [7].

Based on these data, we hypothesized that in the absence of ER and PR, AR supports a CSC population in TNBC. Identification of AR as a target that maintains a tumor-initiating population may alter the clinical treatment strategy of AR antagonists in TNBC from a targeted therapy that inhibits only AR+ tumor cells to a stem cell-targeted therapy that inhibits expansion of a chemotherapy-resistant CSC population. Our research demonstrates that both AR and CSC populations are upregulated in suspended conditions, AR inhibition decreases CSC populations in vitro and tumor initiation in vivo, and Enza enhances the efficacy of chemotherapy and reduces recurrence in a preclinical model.

METHODS

Cell Culture

All cell lines were authenticated by short tandem repeat analysis and verified free of mycoplasma. SUM159PT cells were purchased from the University of Colorado Cancer Center Tissue Culture Core in August of 2013 and were grown in Ham's F-12 with 5% fetal bovine serum, penicillin/streptomycin, hydrocortisone, insulin, HEPES and L-glutamine supplementation. BT549 cells, purchased from ATCC in 2008, were grown in RPMI Medium 1640 with 10% fetal bovine serum, penicillin/streptomycin and insulin. MDA-MB-453 (MDA453) cells, purchased from ATCC in 2012, were grown in DMEM Medium with 10% fetal bovine serum and penicillin/streptomycin.

SUM159PT-TGL cells were generated by stable retroviral transduction with a SFG-NES-TGL vector, encoding a triple fusion of thymidine kinase, green fluorescent

protein and luciferase and sorted for green fluorescent protein. SUM159PT and MDA453 AR knockdown cells were generated by lentiviral transduction of shRNAs targeting AR (pMISSION VSV-G, Sigma Aldrich; St Louis, MO), including AR shRNA 3715 (shAR15) and AR shRNA 3717 (shAR17). Lentiviral transduction of pMISSION shRNA NEG (shNEG) was used as a non-targeting control. Plasmids were purchased from the University of Colorado Functional Genomics Core Facility.

Cellular Assays and Reagents

Cells were treated with 20 μM Enza (Medivation; San Francisco, CA) and 10 nM dihydrotestosterone (DHT, Sigma Aldrich). 20 μM Enza approximates the IC_{50} of the cell lines studied and is a clinically achievable concentration. Circulating plasma C_{max} values for Enza and its active metabolite (N-desmethyl enzalutamide) are 16.6 μg/ml (23% CV) and 12.7 μg/ml (30% CV) respectively (Enza package insert Exposure Rationale), which is equivalent to approximately 60 μM total active drug in plasma at steady state.

Forced Suspension Culture

Ply-2-hydroxyethyl methacrylate (poly-HEMA, Sigma) was reconstituted in 95% ethanol to 12 mg/ml. Ethanol was allowed to evaporate overnight, and plates were washed with PBS prior to use.

For mammosphere formation assays, single cells were plated in 96-well ultra-low attachment plates in 200 μl per well of Mammocult media (Stem Cell Technologies; Vancouver, BC, Canada). After incubating for one week, the number of mammospheres present was determined by microscopy. Mammosphere criteria included at least five cells and a length of at least 50 μm. The mammosphere formation efficiency (MFE) was

calculated as number of mammospheres formed divided by the number of single cells plated. CD24/CD44 (BD Biosciences; San Jose, CA) staining was conducted per the manufacturer's protocol by flow analysis. The ALDEFLUOR^{TM} assay (Stem Cell Technologies) was performed per the manufacturer's protocol.

Luciferase Reporter Activity

The AR luciferase reporter, PRE/ARE2-tata-luc [30] generously provided by Dr. Kate Horwitz (University of Colorado Denver) was transiently transfected with SV40 Renilla in BT549 cells using Lipofectamine (Thermo Fisher Scientifics; Waltham, MA). Transfected cells were then incubated at 37°C for 24 hours. Reporter activation was determined using the Dual-Luciferase Assay System (Promega) according to the manufacturer's protocol. Briefly, cells were lysed for 15 minutes at room temperature and centrifuged at 14,000 rpm for 15 minutes at 4C to eliminate cellular debris. The supernatant was used immediately for determination of luciferase activity. AR reporter activity was normalized to SV40 Renilla reporter activity to control for differences in transfection efficiency.

Immunohistochemistry and Immunofluorescence

Tissues were fixed in 10% neutral buffered formalin, and the UC Denver Tissue Biobanking and Processing Core performed tissue processing and paraffin embedding. Slides were deparaffinized in a series of xylenes and ethanols, and antigens were heat retrieved in either 10mM citrate buffer, pH 6.0, or 10mM Tris/1mM EDTA, pH 9.0. Antibodies used were AR clone 441 (Dakocytomation; Carpinteria, CA) or AR clone SP107 (Cell Marque; Rocklin, CA). The Vectastain Elite ABC kit (Vector Laboratories

Inc., Burlingame, CA) or Envision horseradish peroxidase (Dakocytomation) were used for detection.

Tumor Studies

Xenograft experiments were approved by the University of Colorado Institutional Animal Care and Use Committee (IACUC protocol 83614(01)1E). All animal experiments were conducted in accordance with the National Institutes of Health Guidelines for the Care and Use of Laboratory Animals. For the limiting dilution study, a range of 10^2-10^6 SUM159PT-TGL cells were mixed with Matrigel (BD Biosciences; Franklin Lakes, New Jersey) and bilaterally injected into the mammary fat pads of five female, athymic nu/nu mice (Taconic; Germantown, NY) per dilution and treatment group. Cells were treated before injection with 20 μM Enza or Vehicle control (??% DMSO) for 72 hours. Tumor burden was assessed by luciferase activity and by caliper measurements (tumor volume was calculated as volume = (length × width^2)/2). Mice were euthanized by carbon dioxide asphyxiation followed by cervical dislocation, and the tumors were harvested.

For the Enza and Paclitaxel (Pac) study, 10^6 SUM159PT-TGL cells were mixed with Matrigel (BD Biosciences) and bilaterally injected into the mammary fat pads of female, athymic nu/nu mice (Taconic). Tumor burden was assessed by luciferase activity and by caliper measurements (tumor volume was calculated as volume=(length × width^2)/2). Once tumors were established, mice were matched into groups based on the total tumor burden as assessed by in vivo imaging and by caliper measurements. Mice were administered Enza in their chow (approximately a 50 mg/kg daily dose). Enza was mixed with ground mouse chow (Research Diets Inc.; New Brunswick, NJ) at 0.43 mg/g chow.

The feed was irradiated and stored at 4°C before use. Mice in the control group received the same ground mouse chow but without Enza. Mice were given free access to either Enza formulated chow or control chow throughout the study period. Mice were given Pac (LTK Labs; St Paul, MN) i.p. at a dose of 10 mg/kg/d for five consecutive days. Stock Pac was prepared in 50% ethanol and 50% Kolliphor EL (Sigma), then diluted in PBS to a concentration of 1 mg/ml. Mice were euthanized by carbon dioxide asphyxiation followed by cervical dislocation, and the tumors were harvested.

Immunoblotting

Whole cell protein extracts (50 μg) were denatured, separated on SDS-PAGE gels and transferred to polyvinylidene fluoride membranes. After blocking in 3% bovine serum albumin in Tris-buffered saline–Tween, membranes were probed overnight at 4°C. Primary antibodies utilized include: AR (PG-21, 1:500 dilution; EMD Millipore, Darmstadt, Germany), GR (1:1000 dilution; Cell Signaling), and α-TUBULIN (clone B-5-1-2, 1:30,000 dilution; Sigma Aldrich). Following secondary antibody incubation, results were detected using Western Lightning Chemiluminescence Reagent Plus (Perkin Elmer; Waltham, MA).

Real-time quantitative polymerase chain reaction

RNA was isolated by Trizol (Invitrogen; Grand Island, NY) and cDNA was synthesized from 1 μg total RNA, using M-Mulv reverse transcriptase enzyme (Promega; Fitchburg, WI). SYBR green quantitative gene expression analysis was performed using the following primers: *AR* forward, 5'-CTCACCAAGCTCCTGGACTC-3' and *AR* reverse, 5'-CAGGCAGAAGACATCTGAAAG-3'; *GR* forward, 5'-ACTGCCCCAAGTGAAAACAGA-3' and *GR* reverse, 5'-

ATGAACAGAAATGGCAGACATTT-3'; *βACTIN* forward, 5′-CTGTCCACCTTCCAGCAGATG-3′ and *βACTIN* reverse, 5′-CGCAACTAAGTCATAGTCCGC-3′; and *RPL13A* forward, 5′-CCTGGAGGAGAAGAGGAAAGAGA-3′ and *RPL13A* reverse, 5′-TTGAGGACCTCTGTGTATTTGTCAA-3′. Relative gene expression was calculated using the comparative cycle threshold method and values were normalized to *β-ACTIN* or *RPL13A*.

Gene Expression Array Analysis

BT549 cells were grown in either attached or forced suspension condition on poly-HEMA coated plates in quadruplicate for 24 hours. RNA was harvested using the Trizol method, and hybridized onto Affymetrix Human Gene 1.0ST arrays at the University of Colorado Denver Genomics and Microarray Core, following the manufacturer's instructions.

Microarray analysis was performed using Parktek Genomics Suite (Partek, Inc.) and Ingenuity Pathway Analysis software (Qiagen, Inc.). One-way ANOVA analysis was performed to determine differentially expressed genes between the two treatment groups. Significantly differentially expressed genes were imported to Ingenuity for pathway analysis, including identification of altered canonical pathways.

Statistical Significance

Statistical significance was evaluated using a two-tailed student's t-test or ANOVA with GraphPad Prism software. Binomial probability was used to calculate significance of MFE assays. Extreme limiting dilution analysis (ELDA) was used to calculate stem cell frequency and significance of tumor initiation frequency of the

limiting dilution assay. A P-value of less than 0.05 was considered statistically significant.

RESULTS

Androgen receptor transcript, protein, and transcriptional activity are upregulated in forced suspension culture compared to adherent conditions

To determine what genes may have a role in the ability of cells to resist anoikis and survive in suspension (mimicking survival in-transit during metastasis), gene expression microarray analysis was conducted on BT549 cells in adherent or forced suspension conditions for 24 hours. Metacore and Ingenuity Pathway analysis of this data (genes significantly altered by more than 1.5 fold in BT549 in attached versus suspension culture for 24 hrs) revealed that AR is one of the top predicted upstream regulators of the genes altered in suspension culture (Fig. 1A). When MDA-MB-453, SUM159PT, and BT549 triple-negative breast cancer cell lines were placed in forced suspension or adherent culture conditions AR and GR mRNA transcripts were measured and AR transcript significantly increased in all three cell lines after 48 hours in forced suspension compared to the attached condition in all 3 cell lines, while GR protein did not (Fig. 1B). An increase in AR, but not GR protein was confirmed by western blot (Fig. 1C) and immunohistochemistry (Fig. 1D). Indeed, culture of BT549 cells in the attached verus suspended culture over time 24-96 hours showed enrichment for AR positive cells in suspension culture over time (Supplemental Fig 1)

AR transcriptional activity as measured using a consensus response element luciferase reporter, significantly increased in suspended compared to attached culture in

SUM159PT and BT549 cell lines and this effect was attenuated in cells transduced with shRNAs targeting AR (Fig. 1E).

*AR+ cells are resistant to apoptosis*Since AR increased in forced suspension culture, we hypothesized that AR might protect against anoikis (detachment-induced cell death). We had previously reported that the anti-androgen enzalutamide caused a greater than 80% reduction in growth on soft agar **(ref Val's first paper)**. Cleaved caspase 3 (red) increased in MDA-MB-453 and BT549 following 48 hours in forced suspension culture, as did AR protein positivity (green) (Fig 2A). Higher magnification of the BT549 line demonstrates the mutually exclusive nature of the red apoptotic cells and the green AR positive cells (Fig 2B). Percent cells positive for red (cleaved caspase), green (AR) or both was evaluated in BT549 cells Image analysis of BT549 suspended cells and the number of dual positive cells was found to be less than 1% indicating that cells positive for AR do not undergo apoptosis in suspension (Fig 2C).

A population of cancer stem-like cells increases in forced suspension conditions

The ability to survive in suspension is a characteristic of CSCs. Therefore, the CSC population will likely increase in forced suspension culture conditions. As expected, a 3-day forced suspension culture of SUM159PT cells increased the population of ALDH+ cells from 40% to 60% (Fig 3A, $P<0.01$). Likewise, in a mammosphere formation efficiency (MFE) assay, SUM159PT cells suspended 3 days prior to plating exhibited a 5-fold increase in MFE (Fig. 3B, $P<0.001$). These findings were confirmed in a second cell line, MDA453. As MDA453 does not express ALDH, $CD44^{+}/CD24^{-}$ staining was used to identify CSCs. Although there were no changes in CD44 staining (data not shown), CD24 staining decreased by 2-fold following suspension culture,

suggesting a less luminal phenotype (Fig. 3C, $P<0.001$). A 2-fold increase in MFE was also observed in MDA453 cells placed in suspension culture for five days prior to plating the mammosphere assay (Fig. 3D, $P<0.05$).

Androgen receptor inhibition decreases the cancer stem cell-like population in vitro

Given the data that both AR and CSCs are increased in suspension, it was hypothesized that inhibiting AR would decrease the CSC population. In SUM159PT cells, AR knockdown decreased the percentage of ALDH+ cells from 55% to approximately 40% (Fig. 4A, $P<0.001$). A 4-fold decrease in MFE was also observed (Fig. 4B, $P<0.05$) following AR knockdown. Finally, treatment with the AR antagonist Enza decreased MFE by nearly 2-fold (Fig. 4C, $P<0.01$). These results were recapitulated in the MDA453 cell line. AR knockdown led to a decrease in the $CD44^{+}/CD24^{-}$ cell population, indicative of a more luminal phenotype (Fig. 4D, $P<0.05$). Similarly, AR knockdown decreased MFE in MDA453 by 2-fold (Fig. 4E, $P<0.05$). Treatment with Enza resulted in a 9-fold decrease in MFE in MDA453 (Fig 4F, $P<0.001$). Although there were trends of decreased mammosphere length following AR inhibition, these changes did not reach statistical significance.

Pre-treatment with Enzalutamide decreases tumor initiation frequency in vivo

To evaluate the stem cell-like property of tumor initiation, an in vivo limiting dilution assay was performed. tTo determine if AR inhibition would affect tumor initiation frequency luciferase-tagged SUM159PT cells were pretreated for 3 days with either Veh or Enza and mice received bilateral orthotopic injections of these cells ranging from 10^2-10^6 cells and tumor initiation frequency was measured by palpation and total flux.(Fig. 5A). By both palpation and total flux analyses, pretreatment with Enza

significantly decreased the tumor initiation frequency by approximately 2.5-fold (Fig. 5C, $P<0.05$).

Combination Enzalutamide and Paclitaxel is more effective than Paclitaxel alone

CSCs are resistant to chemotherapy and may repopulate the tumor following treatment [3-6]. Given that AR inhibition decreases the CSC population in vitro and in vivo (Fig. 4-5), AR inhibition in combination with chemotherapy may be more effective than chemotherapy alone. In vitro, both Enza and Pac inhibit SUM159PT cell growth more than 50% $P<0.001$). However, the combination of drugs inhibits cell growth by 25%, $P<0.01$) (Supplemental Fig 2). To determine whether the combination of drugs is more effective in vivo, three treatment groups were compared: Pac alone, Pac + Enza Group 1 (received Enza simultaneous with with Pac (Sim), and Pac + Enza Group 2 (received Enza sequentially after treatment with Pac (Seq)) (see Supplemental Fig 2 for experimental design). (Figure 6B) and randomization e by caliper measurements and total flux, respectively. Tumor viability measured by IVIS imaging demonstrated that he addition of Enza (whether simultaneous or sequential) significantly decreased tumor viability at the end of the study (Day 49) (Fig 6A and B). Tumor volume was also significantly smaller in both groups that got pac plus Enza compared to Pac alone ($P<0.05$) (Fig. 6C and D).. In addition, the simultaneous Pac+Enza Group 1 (sim) was more statistically significant than the Pac+Enza Group 2 sequential (seq) treatment group at end of study by both total flux measuring tumor viability and tumor volume. . In a comparison of individual change in total flux following the last day of Pac versus the end of study by paired t-test, only the Pac+Enza simultaneous treatment (sim) showed a statistically significant reduction in tumor viability (Fig. 6E), indicating that only this

group did not exhibit recurrance. These findings suggest that Enza may more effectively reduce recurrance following cessation of chemotherapy if given simultaneously with chemotherapy.

DISCUSSION

For the first time, these data suggest that AR transcript, protein, and transcriptional activity is upregulated in TNBC lines in forced suspension compared to attached conditions. Our previously published data demonstrate that, in multiple TNBC cell lines, Enza dramatically reduces growth on soft agar, a classic measure of anchorage independence [7]. The data presented here also indicate that AR is anti-apoptotic and particularly, because it increases in suspension culture, protects against cell death under anchorage independent conditions (forced suspension culture). This data is consistent with previous studies demonstrating that AR+ tumors retain AR expression in metastatic disease [31, 32]. Interestingly, Lawson et al. recently reported single cell sequencing of circulating tumor cells from breast cancer patient-derived xenografts (PDX) and found many genes upregulated in low burden metastatic cells compared to primary tumor cells, including AR (21.5-fold) [33] a.. Increased AR expression found in ciruclating tumor cells, along with our data on AR in forced suspension, and clinical data showing retention of AR in metastatic disease [31, 32], suggest that AR is supporting survival in transit during metastasis.

In a comparison of genes upregulated in circulating tumor cells in the TNBC PDX model reported by Lawson et al [33] and in our suspended culture conditionsboth ,

transforming growth factor beta 2 (TGFB2) and AR increased in both datasets. Metacore analysis predicted that AR is transcriptionally active in suspension and that TGFB2 may be an AR regulated gene. Indeed transforming growth factor beta receptor 2 (TGFBR2, 43-fold) and transforming growth factor beta receptor 3 (TGFBR3, 3.4-fold), were also highly expressed in circulating tumor cells from TNBC PDX models [33] andare associated with dormancy of tumor-disseminated cells [34, 35]. There is evidence that AR regulates TGFB2 expression in prostate cancer associated fibroblasts [36] and the TGFB2 gene has an androgen response element adjacent to its transcription start site (published?). Additionally, transforming growth factor beta 1 (TGFB1) plays a role in mammary stem cell maintenance [37]. Together, these data imply that one mechanism by which AR may support survival in suspension and metastasis is upregulation of TGFB2. Indeed we find that activated SMAD3 is more abundant in TNBC in forced suspension culture.

The present data also demonstrate, both in vitro and in vivo, that AR inhibition decreases a CSC like population. This finding challenges the prior dogma that AR targeted therapies will be most effective in tumors with high AR expression [38-40]. Indeed, preliminary data from the Phase II trial of Enza in TNBC demonstrates that the degree of AR immunostaining itself was not the best predictor of who will receive the most benefit from AR targeted therapy, but rather a signature of genes indicative of AR activity [16]. If AR targeted therapies decrease a CSC population capable of repopulating the tumor, then even patients with relatively low AR expression may benefit from this treatment, since even a low percentage of AR+ cells may be supporting CSCs that can survive chemotherapy and repopulate a tumor. The finding that patients with low levels

of a hormone receptor may benefit from targeted therapy is not unprecidented, as breast cancer patients with as low as 1% ER+ cells can receive benefit from ER targeted therapies . Estrogen and progesterone expand the stem cell population in the normal mammary gland and breast cancer [18, 19] and in AR+ TNBC, AR is known to bind to many of the same sites on chromatin as ER does in ER+ BC **(put in Robinson reference**). In immortal mammary epithelial cells, amphiregulin (AREG), transcriptionally regulated by ER, supports the expansion of stem cells [18, 19, 41]. Our previously published data demonstrate that activation of AR increases AREG secretion while treatment with Enza decreases *AREG* expression in TNBC cell lines [7]. AR+ cells may support a CSC population through a similar paracrine mechanism or may themselves have stem-like properties. Further studies are needed to elucidate the mechanisms by which AR supports a CSC population, or whether the AR+ cells themselves are the CSC tumor initiating population. In either case, these data show that AR inhibition decreaseses mammosphere formation frequency in vitro and tumor initiation in vivo.

CONCLUSIONS

Given the success of the Phase II trial of Enza (Xtandi) in metastatic TNBC [16], there is great clinical interest in the efficacy of Enza in combination with standard of care chemotherapy. The need for improved chemotherapy among AR+ TNBC tumors is highlighted in a study by Masuda et al. demonstrating that AR+ TNBCs (luminal AR subtype) have a poor pathologic complete response compared to other subtypes [43]. This may be because AR+ tumors proliferate more slowly and are therefore less responsive to chemotherapeutic agents. Enza may increase the efficacy of chemotherapy by decreasing the CSC population that is both insensitive to chemotherapy and that is thought to

repopulate the tumor post-chemotherapy to cause relapse [3-6]. Using a preclinical model, the present study indicates that the combination of Enza and chemotherapy is more effective than chemotherapy alone. Although both Enza plus chemotherapy regimens (simultaneous and sequential) were more effective than chemotherapy alone, the combination of Enza given simultaneously with chemotherapy, rather than following chemotherapy, yielded better preclinical outcomes (more significant decrease in tumor volume and viability and less tumor regrowth upon cessation of chemotherapy). This study provides preclinical evidence supporting chemotherapy combination trials with Enza, and it shows promise that the addition of a targeted therapy may improve outcomes for patients with TNBC. The first clinical trial (give trial number), showed an impressive clinical benefit rate when given to women with metastatic disease where the majority of patients had already received chemotherapy (REF ASCO talk). The next trial with Enza in AR+ disease will likely involve Enza plus chemotherapy compared to chemotherapy alone as adjuvant therapy in metastatic, then non-metastatic disease. Indeed, if AR targeted therapies continue to be successful in the clinic, they may become the first successful targeted therapy forTNBC.

DECLARATIONS

List of Abbreviations

ALDH	Aldehyde dehydrogenase
AR	Androgen receptor
AREG	Amphiregulin
BC	Breast cancer
CSC	Cancer stem-like cells

344	DHT	Dihydrotestosterone
345	EGFR	Epidermal growth factor receptor
346	ELDA	Extreme limiting dilution analysis
347	Enza	Enzalutamide
348	ER	Estrogen receptor α
349	GR	Glucocorticoid receptor
350	HER2	Human epidermal growth factor receptor 2
351	IHC	Immunohistochemistry
352	MFE	Mammosphere formation efficiency
353	MDA453	MDA-MB-453
354	qRT-PCR	quantitative real-time polymerase chain reaction
355	Pac	Paclitaxel
356	PDX	Patient-derived xenografts
357	Poly-HEMA	Ply-2-hydroxyethyl methacrylate
358	PR	Progesterone receptor
359	shAR15	AR shRNA 3715
360	shAR17	AR shRNA 3717
361	TGFB	Transforming growth factor β
362	TGFB2	Transforming growth factor β 2
363	TGFBR2	Transforming growth factor β receptor 2
364	TGFBR3	Transforming growth factor β receptor 3
365	TNBC	Triple-negative breast cancer
366	Veh	Vehicle control

Ethics approval and consent to participate

Animal studies in this manuscript were approved by the University of Colorado Institutional Animal Care and Use Committee (IACUC protocol 83614(01)1E). All animal experiments were conducted in accordance with the National Institutes of Health Guidelines for the Care and Use of Laboratory Animals.

Consent for publication

Not applicable.

Availability of data and materials

All datasets on which the conclusions in the manuscripts rely are presented in the main paper or additional supporting files.

Competing interests

The authors declare no competing interests.

Funding

This study was funded by DOD XXX to JKR, RO1 to JKR, and F31 XXX to VNB.

Authors' contributions

Valerie Barton-data collection, data analysis, manuscript preparation

Jessica Christenson-data collection, data analysis, manuscript preparation

Thomas Rogers-data collection, data analysis

Kiel Butterfield-data collection, data analysis

Beatrice Babbs-data collection, data analysis

Nicholas D'Amato-data collection, data analysis

Jennifer Richer-data analysis, manuscript preparation

Acknowledgements

XXX

REFERENCES

1. Dent, R., et al., *Triple-negative breast cancer: clinical features and patterns of recurrence.* Clin Cancer Res, 2007. **13**(15 Pt 1): p. 4429-34.
2. Liedtke, C., et al., *Response to neoadjuvant therapy and long-term survival in patients with triple-negative breast cancer.* J Clin Oncol, 2008. **26**(8): p. 1275-81.
3. Kabos, P., et al., *Cytokeratin 5 positive cells represent a steroid receptor negative and therapy resistant subpopulation in luminal breast cancers.* Breast Cancer Res Treat, 2011. **128**(1): p. 45-55.
4. Al-Hajj, M., et al., *Prospective identification of tumorigenic breast cancer cells.* Proc Natl Acad Sci U S A, 2003. **100**(7): p. 3983-8.
5. Li, X., et al., *Intrinsic resistance of tumorigenic breast cancer cells to chemotherapy.* J Natl Cancer Inst, 2008. **100**(9): p. 672-9.
6. Bhola, N.E., et al., *TGF-beta inhibition enhances chemotherapy action against triple-negative breast cancer.* J Clin Invest, 2013. **123**(3): p. 1348-58.
7. Barton, V.N., et al., *Multiple molecular subtypes of triple-negative breast cancer critically rely on androgen receptor and respond to enzalutamide in vivo.* Mol Cancer Ther, 2015. **14**(3): p. 769-78.
8. Micello, D., et al., *Androgen receptor is frequently expressed in HER2-positive, ER/PR-negative breast cancers.* Virchows Arch, 2010. **457**(4): p. 467-76.
9. Collins, L.C., et al., *Androgen receptor expression in breast cancer in relation to molecular phenotype: results from the Nurses' Health Study.* Mod Pathol, 2011. **24**(7): p. 924-31.
10. Mrklic, I., et al., *Expression of androgen receptors in triple negative breast carcinomas.* Acta Histochem, 2013. **115**(4): p. 344-8.
11. Safarpour, D., S. Pakneshan, and F.A. Tavassoli, *Androgen receptor (AR) expression in 400 breast carcinomas: is routine AR assessment justified?* Am J Cancer Res, 2014. **4**(4): p. 353-68.
12. Thike, A.A., et al., *Loss of androgen receptor expression predicts early recurrence in triple-negative and basal-like breast cancer.* Mod Pathol, 2014. **27**(3): p. 352-60.
13. Qi, J.P., et al., *Expression of the androgen receptor and its correlation with molecular subtypes in 980 chinese breast cancer patients.* Breast Cancer (Auckl), 2012. **6**: p. 1-8.
14. Gucalp, A., et al., *Phase II trial of bicalutamide in patients with androgen receptor-positive, estrogen receptor-negative metastatic Breast Cancer.* Clin Cancer Res, 2013. **19**(19): p. 5505-12.
15. Traina, T., *Stage I results from MDV3100-11: a 2 stage study of enzalutamide (Enza), an androgen receptor (AR) inhibitor, in advanced AR+ triple-negative breast cancer (TNBC).* 2014.

16. Traina TA, M.K., Yardley DA, O'Shaughnessy J, Cortes J, Awarda A, Kelly CM, Trudeau ME, Schmid P, Gianni L, Garcia-Estevez L, Nanda R, Ademuyiwa FO, Chan S, Steinberg JL, Blaney ME, Tudor TC, Uppal H, Peterson AC, Hudis CA, *Results from a phase 2 study of enzalutamide (ENZA), an androgen receptor (AR) inhibitor, in advanced AR+ triple-negative breast cancer (TNBC).* 2015.
17. Horwitz, K.B., et al., *Rare steroid receptor-negative basal-like tumorigenic cells in luminal subtype human breast cancer xenografts.* Proc Natl Acad Sci U S A, 2008. **105**(15): p. 5774-9.
18. Graham, J.D., et al., *DNA replication licensing and progenitor numbers are increased by progesterone in normal human breast.* Endocrinology, 2009. **150**(7): p. 3318-26.
19. Asselin-Labat, M.L., et al., *Control of mammary stem cell function by steroid hormone signalling.* Nature, 2010. **465**(7299): p. 798-802.
20. Beato, M., P. Herrlich, and G. Schutz, *Steroid hormone receptors: many actors in search of a plot.* Cell, 1995. **83**(6): p. 851-7.
21. Cloke, B., et al., *The androgen and progesterone receptors regulate distinct gene networks and cellular functions in decidualizing endometrium.* Endocrinology, 2008. **149**(9): p. 4462-74.
22. Robinson, J.L., et al., *Androgen receptor driven transcription in molecular apocrine breast cancer is mediated by FoxA1.* EMBO J, 2011. **30**(15): p. 3019-27.
23. Wang, Q., et al., *Androgen receptor regulates a distinct transcription program in androgen-independent prostate cancer.* Cell, 2009. **138**(2): p. 245-56.
24. Yu, J., et al., *An integrated network of androgen receptor, polycomb, and TMPRSS2-ERG gene fusions in prostate cancer progression.* Cancer Cell, 2010. **17**(5): p. 443-54.
25. Recchione, C., et al., *Testosterone, dihydrotestosterone and oestradiol levels in postmenopausal breast cancer tissues.* J Steroid Biochem Mol Biol, 1995. **52**(6): p. 541-6.
26. Peters, A.A., et al., *Differential effects of exogenous androgen and an androgen receptor antagonist in the peri- and postpubertal murine mammary gland.* Endocrinology, 2011. **152**(10): p. 3728-37.
27. Ni, M., et al., *Targeting androgen receptor in estrogen receptor-negative breast cancer.* Cancer Cell, 2011. **20**(1): p. 119-31.
28. Gallicchio, L., et al., *Androgens and musculoskeletal symptoms among breast cancer patients on aromatase inhibitor therapy.* Breast Cancer Res Treat, 2011. **130**(2): p. 569-77.
29. Sedelaar, J.P. and J.T. Isaacs, *Tissue culture media supplemented with 10% fetal calf serum contains a castrate level of testosterone.* Prostate, 2009. **69**(16): p. 1724-9.
30. Tung, L., et al., *Mapping the unique activation function 3 in the progesterone B-receptor upstream segment. Two LXXLL motifs and a tryptophan residue are required for activity.* J Biol Chem, 2001. **276**(43): p. 39843-51.
31. Cimino-Mathews, A., et al., *Androgen receptor expression is usually maintained in initial surgically resected breast cancer metastases but is often lost in end-stage metastases found at autopsy.* Hum Pathol, 2012. **43**(7): p. 1003-11.

32. McNamara, K.M., et al., *Complexities of androgen receptor signalling in breast cancer.* Endocr Relat Cancer, 2014. **21**(4): p. T161-81.
33. Lawson, D.A., et al., *Single-cell analysis reveals a stem-cell program in human metastatic breast cancer cells.* Nature, 2015. **526**(7571): p. 131-5.
34. Bragado, P., et al., *TGF-beta2 dictates disseminated tumour cell fate in target organs through TGF-beta-RIII and p38alpha/beta signalling.* Nat Cell Biol, 2013. **15**(11): p. 1351-61.
35. Kim, R.S., et al., *Dormancy signatures and metastasis in estrogen receptor positive and negative breast cancer.* PLoS One, 2012. **7**(4): p. e35569.
36. Yu, S., et al., *Androgen receptor in human prostate cancer-associated fibroblasts promotes prostate cancer epithelial cell growth and invasion.* Med Oncol, 2013. **30**(3): p. 674.
37. Mani, S.A., et al., *The epithelial-mesenchymal transition generates cells with properties of stem cells.* Cell, 2008. **133**(4): p. 704-15.
38. Doane, A.S., et al., *An estrogen receptor-negative breast cancer subset characterized by a hormonally regulated transcriptional program and response to androgen.* Oncogene, 2006. **25**(28): p. 3994-4008.
39. Farmer, P., et al., *Identification of molecular apocrine breast tumours by microarray analysis.* Oncogene, 2005. **24**(29): p. 4660-71.
40. Lehmann, B.D., et al., *Identification of human triple-negative breast cancer subtypes and preclinical models for selection of targeted therapies.* J Clin Invest, 2011. **121**(7): p. 2750-67.
41. Booth, B.W., et al., *Amphiregulin mediates self-renewal in an immortal mammary epithelial cell line with stem cell characteristics.* Exp Cell Res, 2010. **316**(3): p. 422-32.
42. Zheng, Z., et al., *Correlation between epidermal growth factor receptor and tumor stem cell markers CD44/CD24 and their relationship with prognosis in breast invasive ductal carcinoma.* Med Oncol, 2015. **32**(1): p. 275.
43. Masuda, H., et al., *Differential response to neoadjuvant chemotherapy among 7 triple-negative breast cancer molecular subtypes.* Clin Cancer Res, 2013. **19**(19): p. 5533-40.

FIGURE LEGENDS

Figure 1 Androgen receptor expression increases in suspension culture. A, quantitative real-time PCR (qRT-PCR) for androgen receptor (AR) and glucocorticoid receptor (GR) expression in attached versus forced suspension cell culture conditions at 24 hours. B, Western blot for AR and GR in attached versus forced suspension cell culture conditions at 24 hours. C, Immunohistochemistry for AR in attached versus forced suspension cell culture conditions at 48 hours. Photomicrographs at 400x. *, $P<0.05$; ***, $P<0.001$

Figure 2 AR transcriptional activity is increased in suspension culture. A, Ingenuity analysis of BT549 microarray data found that AR is one of the most upregulated transcription factors in suspended compared to attached conditions. B, AR luciferase reporter assay in attached compared to suspended conditions in cells transduced with a non-targeting control (shNEG) or shRNAs targeting AR (shAR15, shAR17). **, $P<0.01$; ***$P<0.001$

Figure 3 A cancer stem cell-like population is increased in suspension. A, ALDEFLUOR assay of SUM159PT cells placed in suspended conditions for 3 days. DEAB was used as a control to set the gate. B, mammosphere formation efficiency (MFE) assay of SUM159PT cells placed in attached or suspended conditions for 3 days prior to plating. C, CD24 staining of MDA-MB-453 (MDA453) cells following 5 days in suspension culture. D, MFE assay of MDA453 cells placed in attached or suspended conditions for 5 days prior to plating. Statistics include two-tailed t-tests (A, C) and binomial probability (B,D). *, $P<0.05$; **, $P<0.01$; ***, $P<0.001$.

Figure 4 AR inhibition decreases a cancer stem cell-like population. A, ALDEFLUOR assay of SUM159PT cells transduced with a non-targeting control (shNEG) or shRNAs targeting androgen receptor (AR, shAR15 and shAR17). Western blot for AR. αTUBULIN is shown as a loading control. B, mammosphere formation efficiency (MFE) assays of SUM159PT cells transduced with shNEG, shAR15, or shAR17 or C, treated with Enzalutamide (Enza). D, CD24 staining of MDA-MB-453 (MDA453) cells transduced with shNEG, shAR15, or shAR17. Western blot for AR. β-ACTIN is shown as a loading control. E, MFE assays of MDA453 cells transduced with shNEG, shAR15,

or shAR17 or F, treated with Enza. Statistics include two-tailed t-tests (A, D) and binomial probability (B, C, E, F). #, P=0.06; *, P<0.05; **, P<0.01; ***, P<0.001.

Figure 5 Tumor initiation frequency of SUM159PT cells pre-treated with Enzalutamide. A, schematic of experimental design. B, total flux of mice injected with 10^2-10^4 cells pretreated for three days with Vehicle control (Veh) or Enzalutamide (Enza). C, tables displaying number of mice with tumors by palpation (left) or total flux right). P-values and stem cell frequencies were calculated by extreme limiting dilution analysis (ELDA).

Figure 6 Experimental design of combined Paclitaxel and Enzalutamide therapy in vivo. A, proliferation assay of SUM159PT-Luc cells treated three days with vehicle control (DMSO), Enzalutamide (Enza), and/or Paclitaxel (Pac) in vitro. B, timeline schematic of mouse injection, tumor matching, and treatment. C, randomization of tumor burden by caliper measurements. D, randomization of tumor burden by total flux. E, total flux of Enza naïve tumors (Pac and Pac+Enza Group 2) before and after treatment with Pac. Statistic is a two-sided t-test. **, P<0.01; ***, P<0.001

Figure 7 Enzalutamide and Paclitaxel combination therapy is more effective than Paclitaxel alone. A, total flux throughout study by treatment group. B, comparison of total flux on study day 49. C, tumor burden throughout study by treatment group. D, comparison of tumor burden on study day 51. E, total flux (left, paired t-test) and tumor burden (right) per mouse between the final day of Paclitaxel and the end of study. Statistics represent two-tailed t-tests. #, P=0.06; *, P<0.05; **, P,0.01

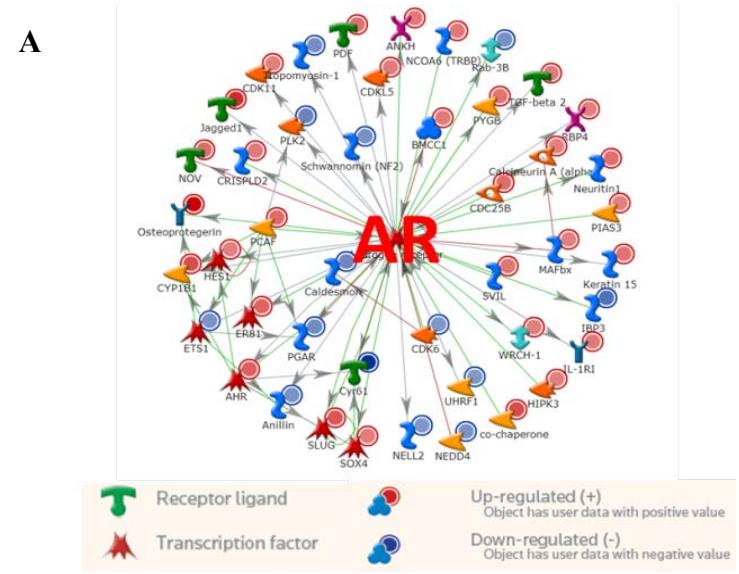
A
AR
Receptor ligand
Transcription factor
Up-regulated (+)
Object has user data with positive value
Down-regulated (-)
Object has user data with negative value

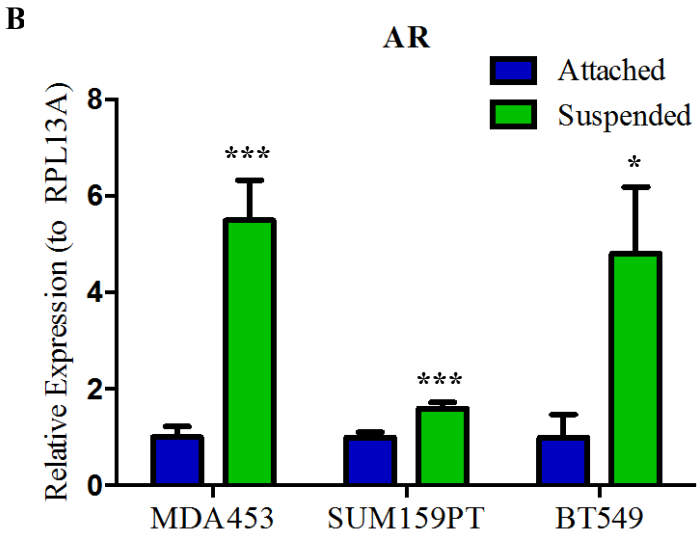
B
AR
Attached
Suspended
Relative Expression (to RPL13A)
MDA453
SUM159PT
BT549

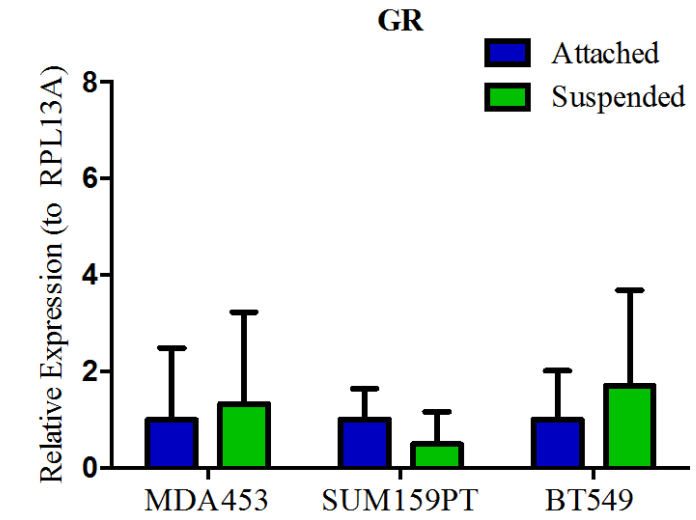
GR
Attached
Suspended
Relative Expression (to RPL13A)
MDA453
SUM159PT
BT549

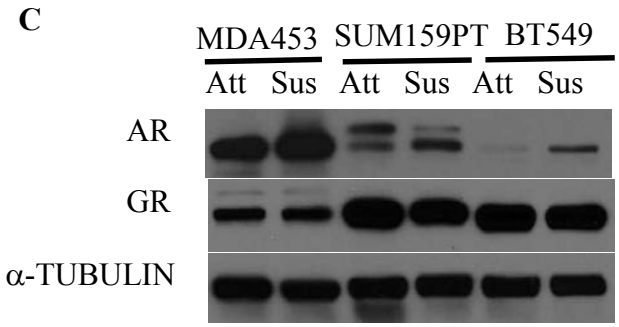
C
MDA453
SUM159PT
BT549
Att
Sus
AR
GR
α-TUBULIN

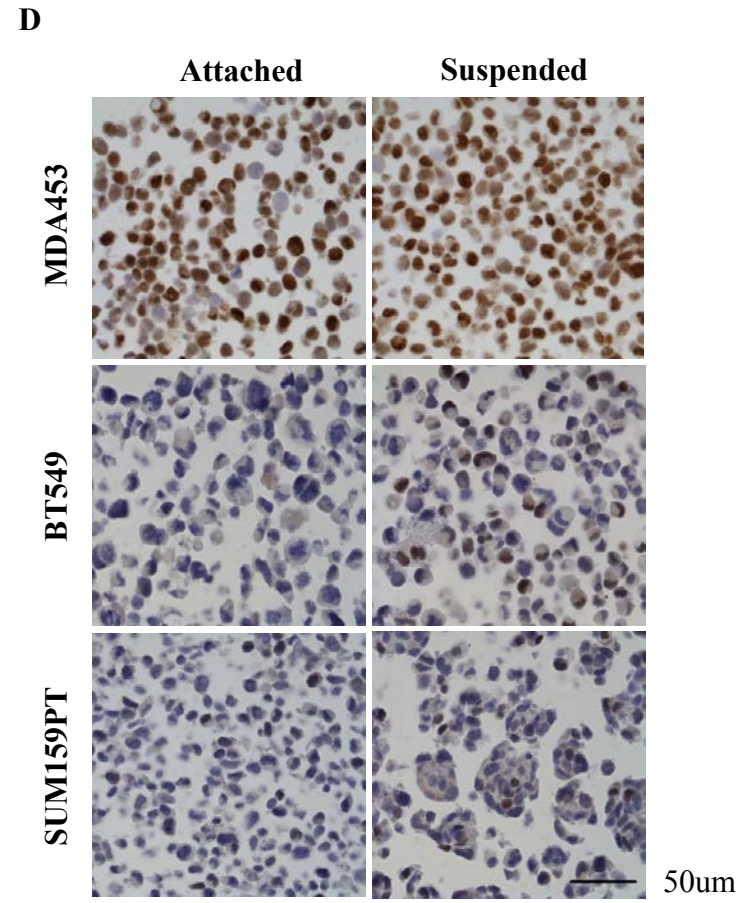
D
Attached
Suspended
MDA453
BT549
SUM159PT
50um

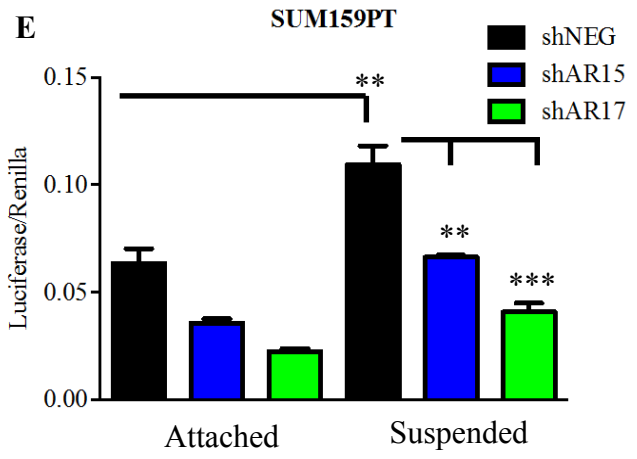
E
SUM159PT
shNEG
shAR15
shAR17
Luciferase/Renilla
Attached
Suspended

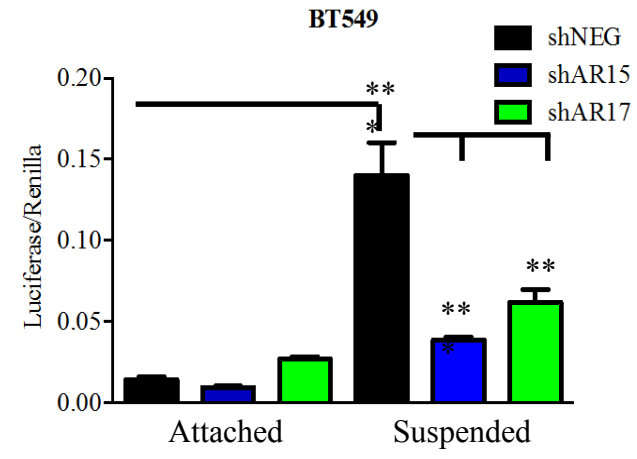
BT549
shNEG
shAR15
shAR17
Luciferase/Renilla
Attached
Suspended

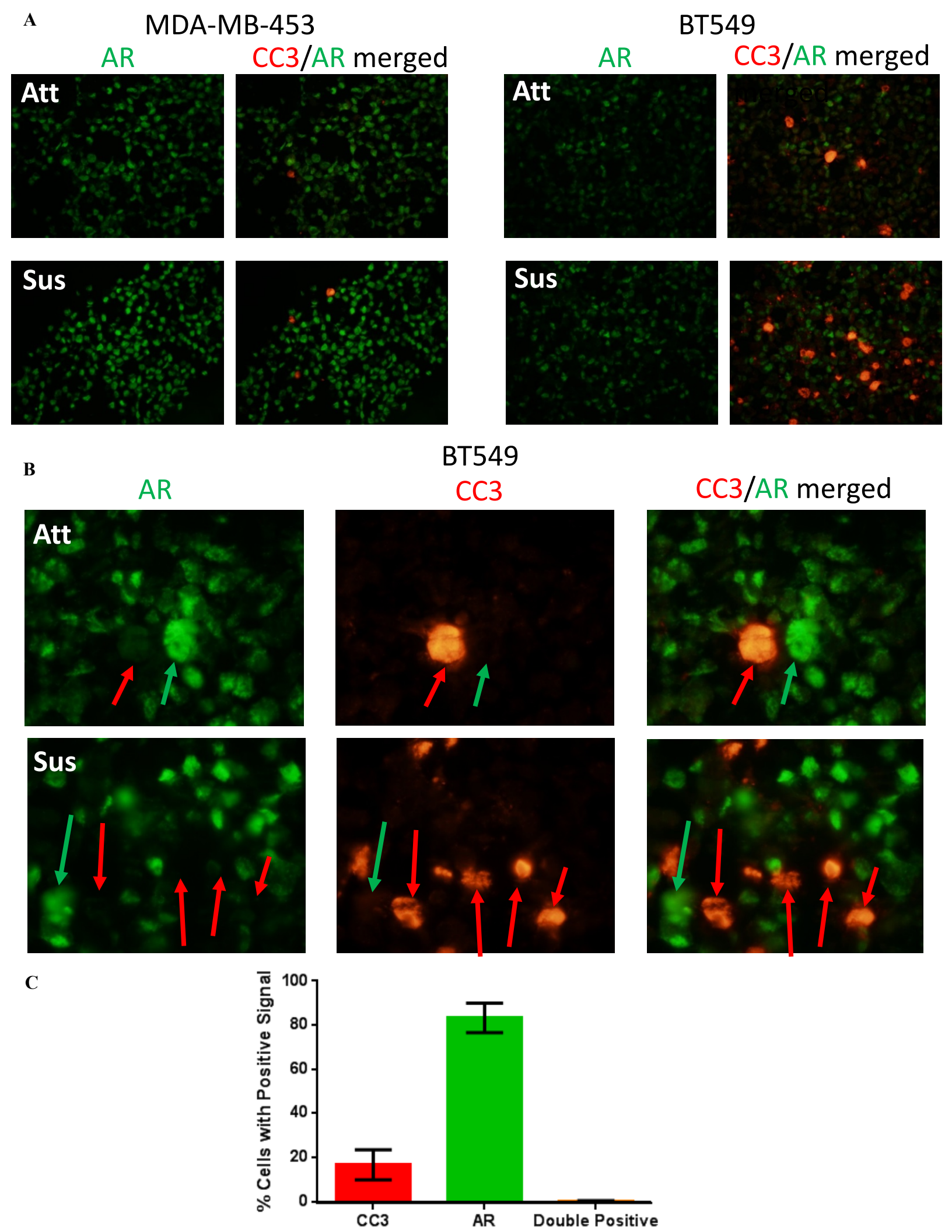
A
MDA-MB-453
AR
CC3/AR merged
Att
Sus
BT549
AR
CC3/AR merged
Att
Sus
B
BT549
AR
CC3
CC3/AR merged
Att
Sus
C
% Cells with Positive Signal
100
80
60
40
20
0
CC3
AR
Double Positive

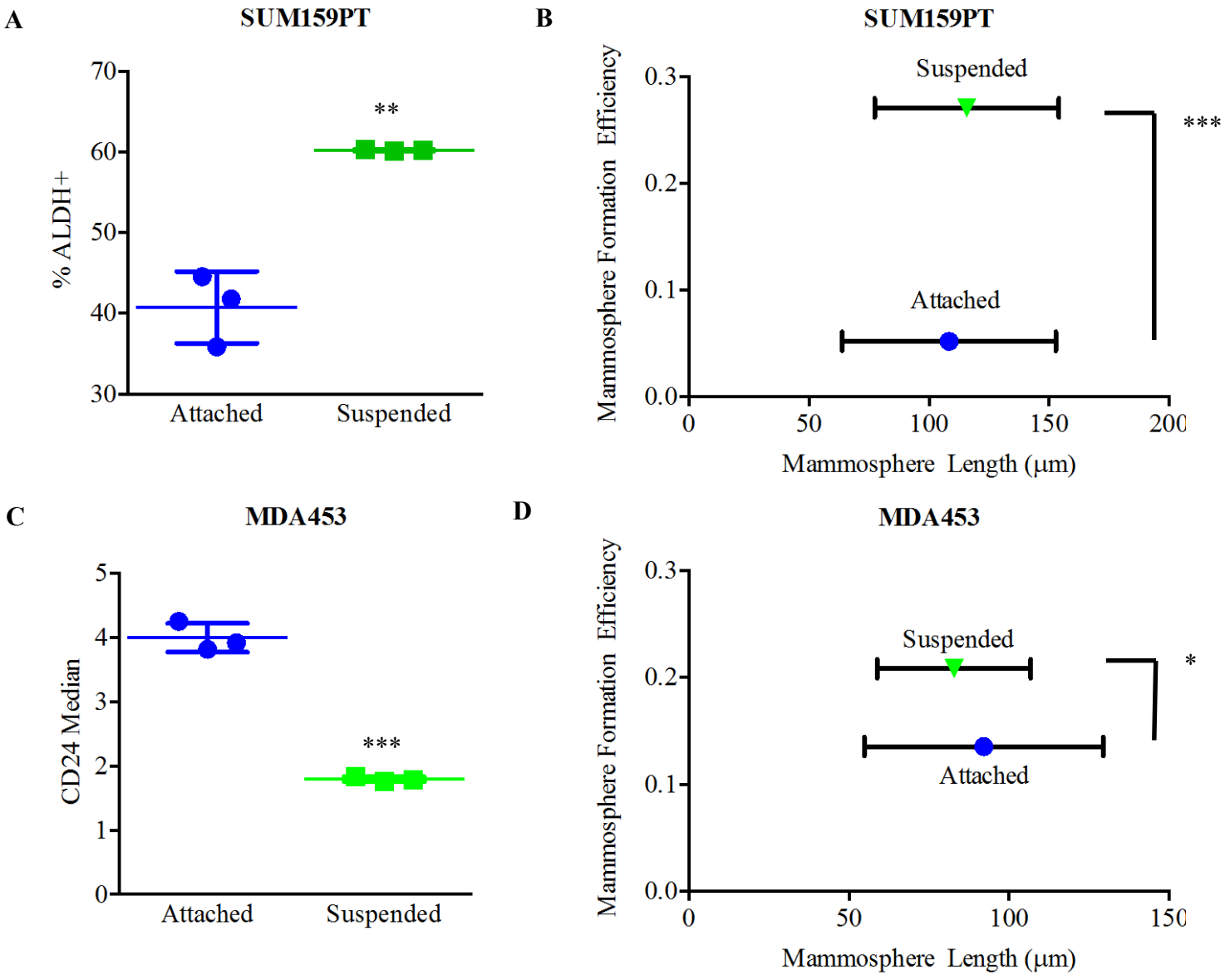
A
SUM159PT
% ALDH+
70
60
50
40
30
**
Attached
Suspended
B
SUM159PT
Mammosphere Formation Efficiency
0.3
0.2
0.1
0.0
Suspended
Attached
***
0
50
100
150
200
Mammosphere Length (μm)
C
MDA453
CD24 Median
5
4
3
2
1
0
***
Attached
Suspended
D
MDA453
Mammosphere Formation Efficiency
0.3
0.2
0.1
0.0
Suspended
Attached
*
0
50
100
150
Mammosphere Length (μm)

Figure 3

Fig 4

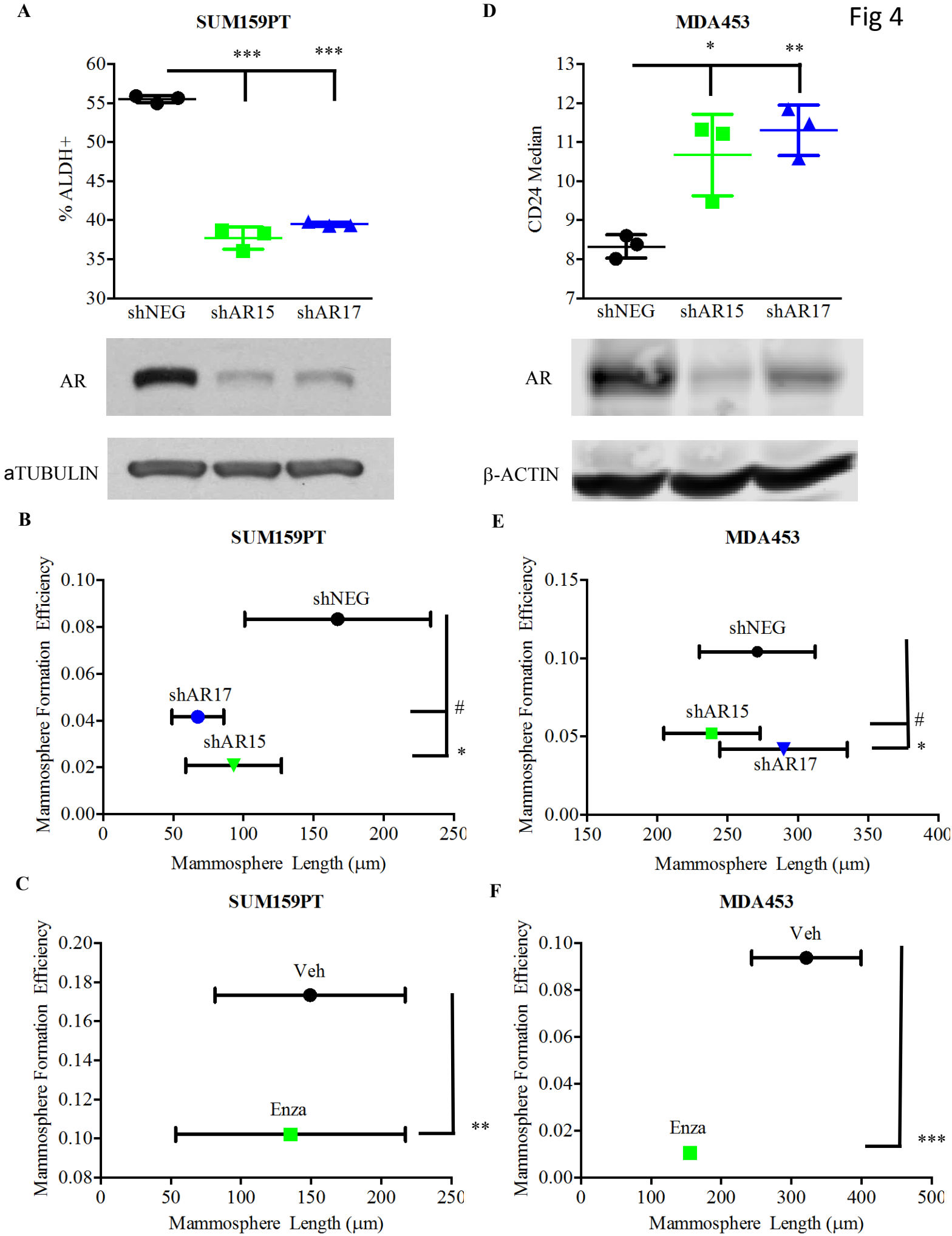
A
SUM159PT
% ALDH+
shNEG
shAR15
shAR17
AR
aTUBULIN
D
MDA453
CD24 Median
shNEG
shAR15
shAR17
AR
β-ACTIN
B
SUM159PT
Mammosphere Formation Efficiency
shNEG
shAR17
shAR15
Mammosphere Length (μm)
E
MDA453
Mammosphere Formation Efficiency
shNEG
shAR15
shAR17
Mammosphere Length (μm)
C
SUM159PT
Mammosphere Formation Efficiency
Veh
Enza
Mammosphere Length (μm)
F
MDA453
Mammosphere Formation Efficiency
Veh
Enza
Mammosphere Length (μm)

A

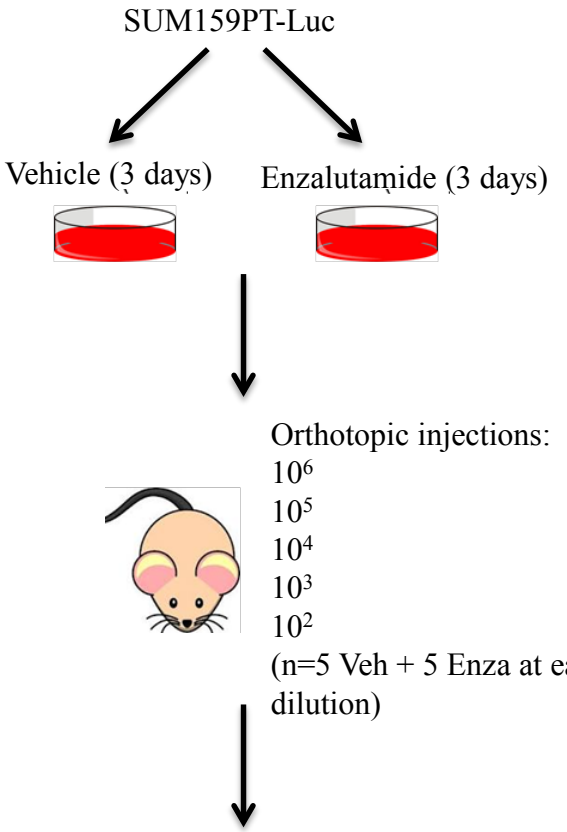

B

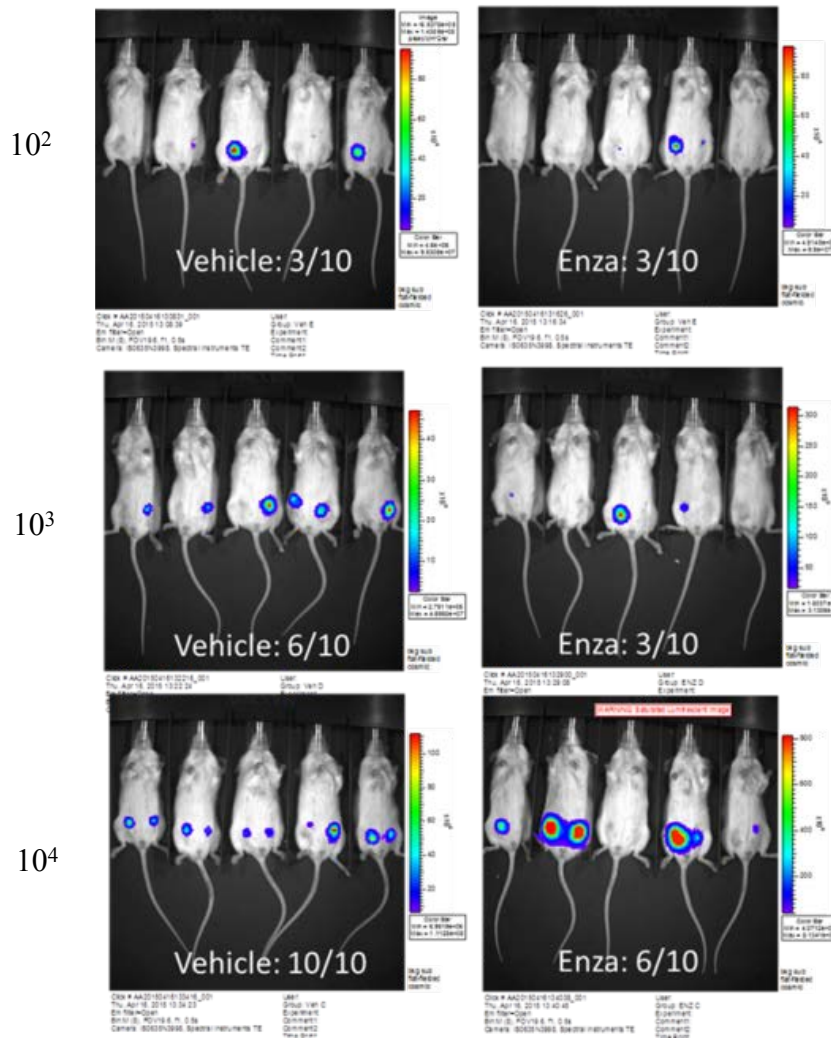

C

Palpable

Cell #	Vehicle	Enza
1,000,000	10/10	10/10
100,000	10/10	10/10
10,000	10/10	10/10
1,000	7/10	4/10
100	6/10	3/10

P-Value	Veh Stem Cell Frequency	Enza Stem Cell Frequency
0.0413	1/463	1/1,221

Total Flux

Cell #	Vehicle	Enza
1,000,000	10/10	10/10
100,000	10/10	10/10
10,000	9/10	7/10
1,000	5/10	3/10
100	2/10	1/10

P-Value	Veh Stem Cell Frequency	Enza Stem Cell Frequency
0.0478	1/2,401	1/5,907

Figure 5

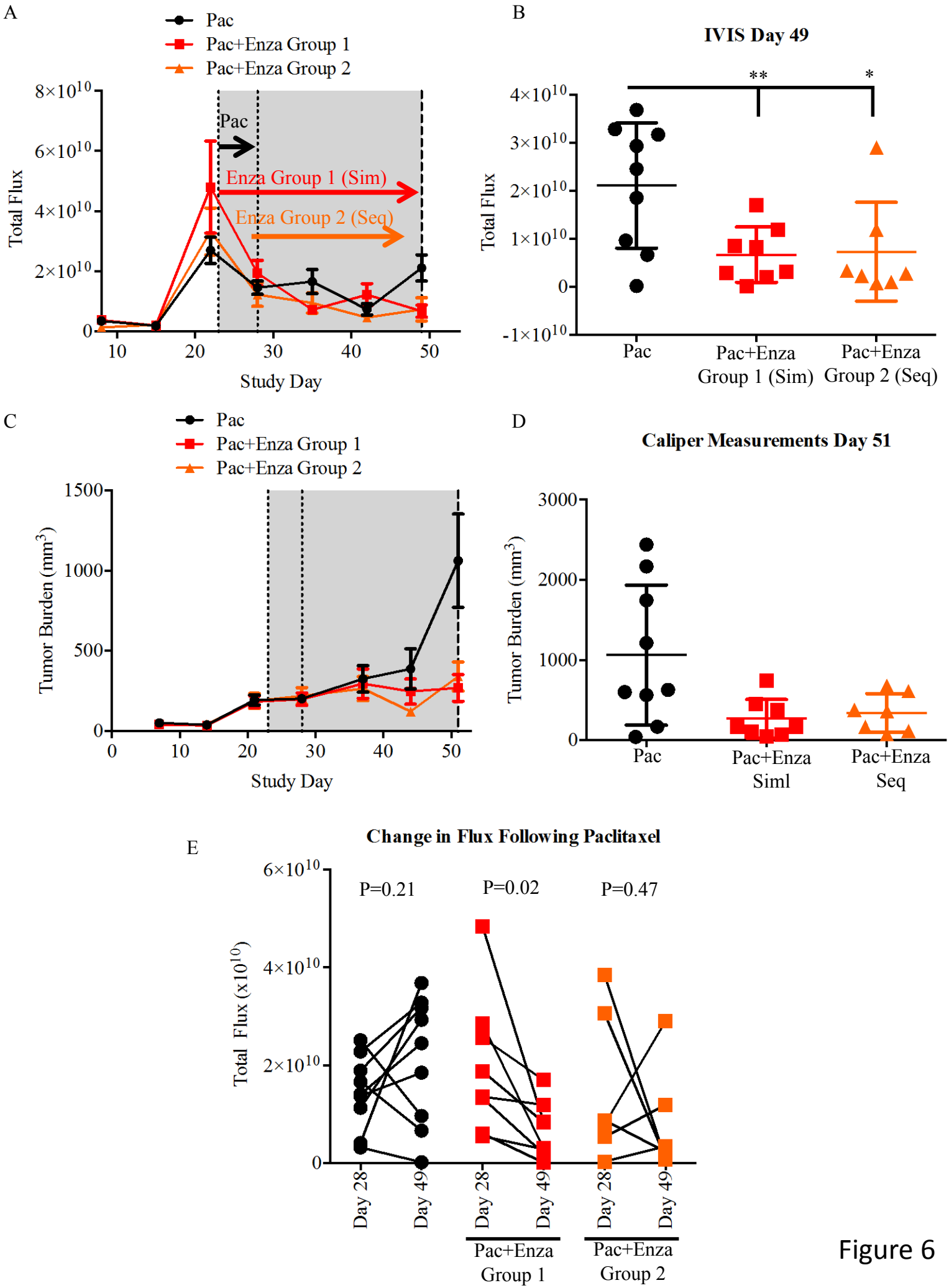
A
Pac
Pac+Enza Group 1
Pac+Enza Group 2
Total Flux
Study Day
Pac
Enza Group 1 (Sim)
Enza Group 2 (Seq)
B
IVIS Day 49
Total Flux
**
*
Pac
Pac+Enza Group 1 (Sim)
Pac+Enza Group 2 (Seq)
C
Pac
Pac+Enza Group 1
Pac+Enza Group 2
Tumor Burden (mm3)
Study Day
D
Caliper Measurements Day 51
Tumor Burden (mm3)
Pac
Pac+Enza Siml
Pac+Enza Seq
E
Change in Flux Following Paclitaxel
Total Flux (x10^10)
P=0.21
P=0.02
P=0.47
Day 28
Day 49
Pac+Enza Group 1
Pac+Enza Group 2

Figure 6

Supplemental Figure 1

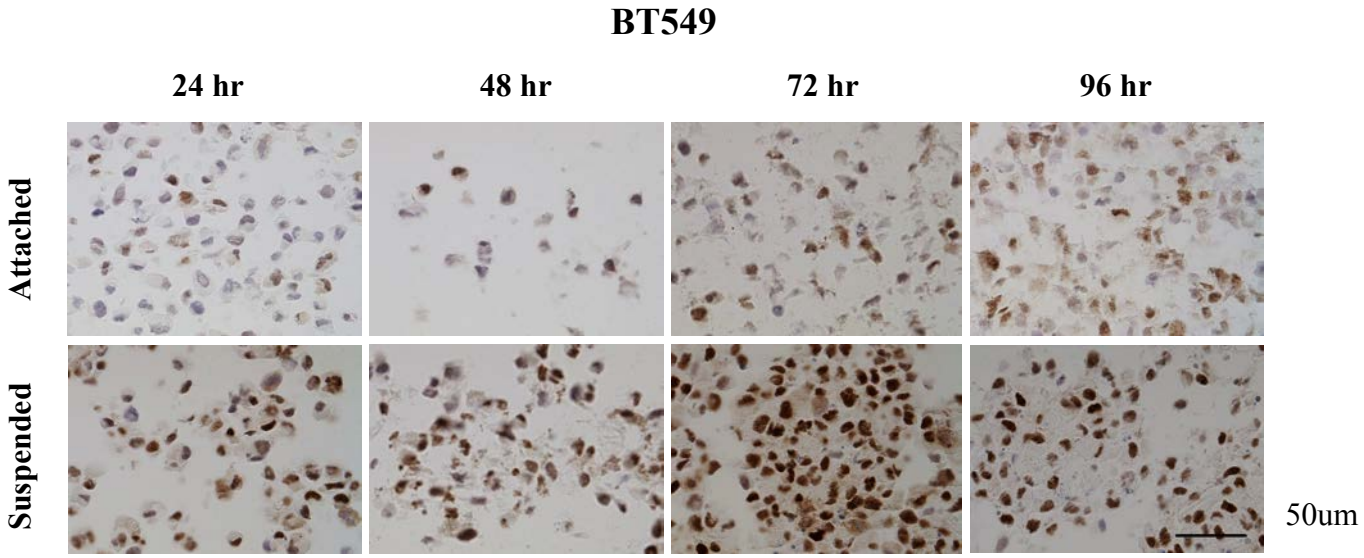

Supplemental Figure 2

A

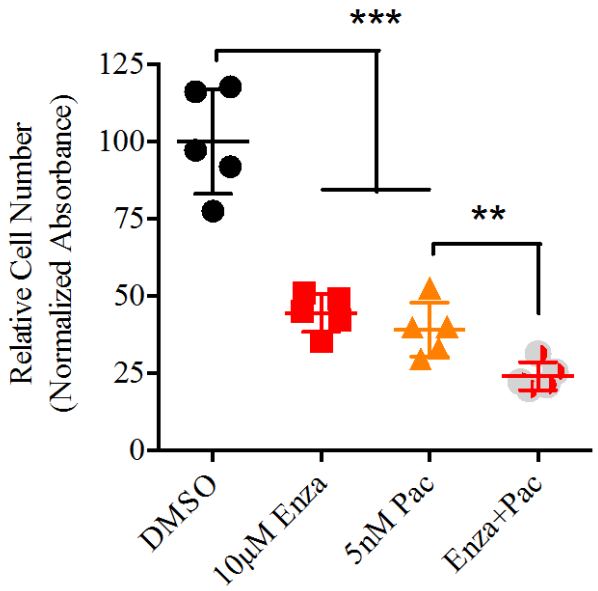

B

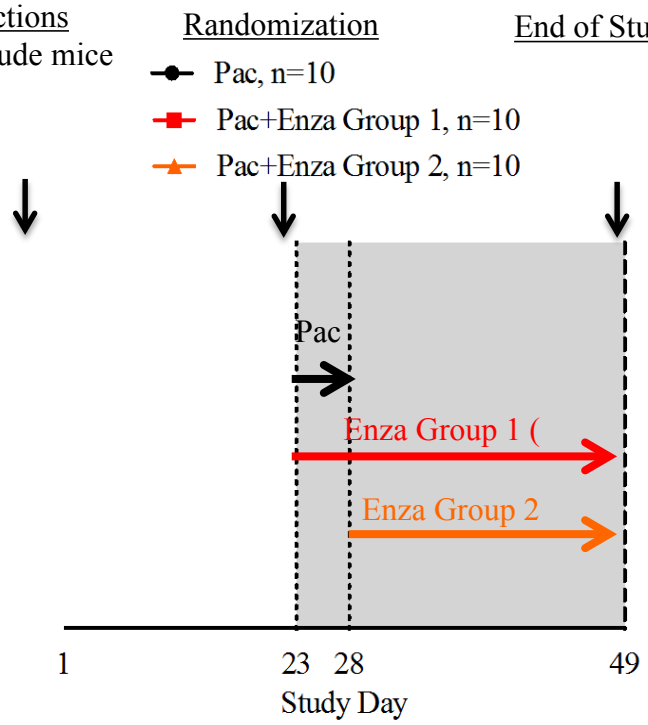

C

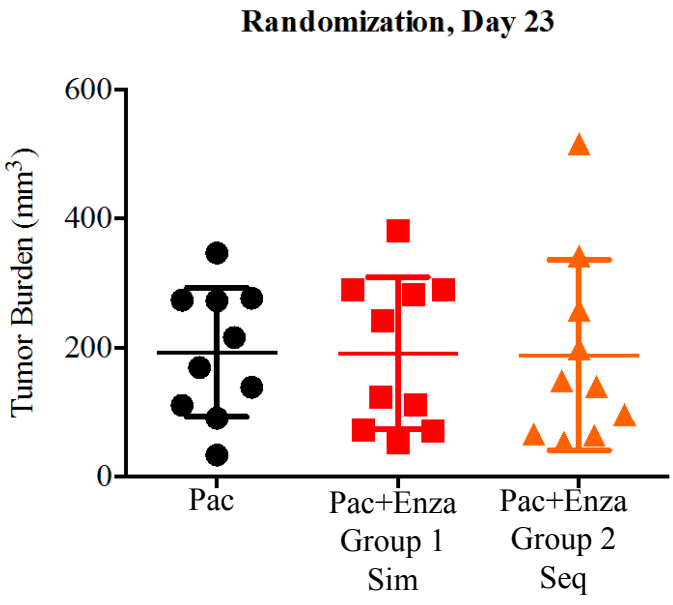

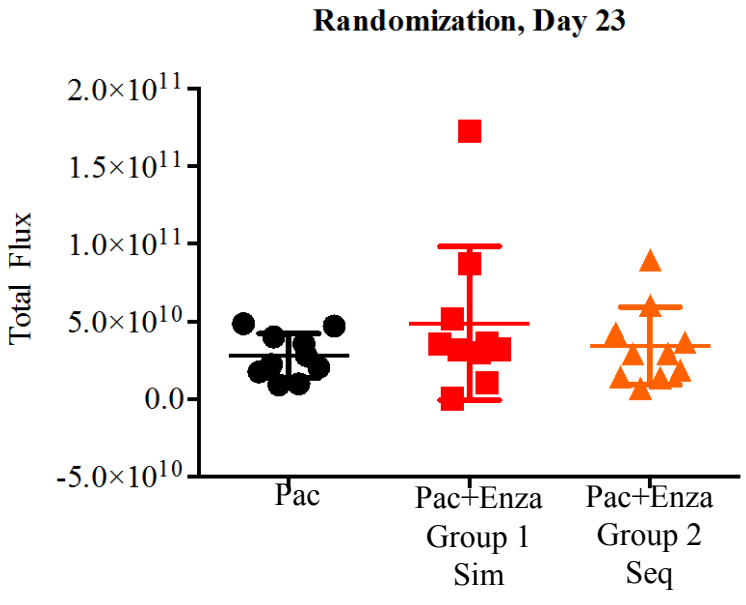

Dual inhibition of androgen receptor and mTOR in breast cancer

Michael A. Gordon[1], Nicholas D'Amato[1], Haihua Gu[1], Beatrice Babbs[1], Kiel Butterfield[1], Bolin Liu[1], Anthony Elias[2], and Jennifer K. Richer[1]

[1]Department of Pathology, University of Colorado Anschutz Medical Campus, [2]Division of Medical Oncology, University of Colorado Anschutz Medical Campus, Aurora, CO USA, [3]Center for Applied Proteomics and Molecular Medicine, George Mason University, Manassas VA USA

Corresponding Author:
Jennifer K. Richer, Ph.D.
Department of Pathology
University of Colorado, Anschutz Medical Campus
12800 E 19th Ave
Aurora, CO 80045, USA
Email: jennifer.richer@ucdenver.edu

INTRODUCTION

The estrogen receptor (ER), progesterone receptor (ER) and human epidermal growth factor receptor 2 (HER2) have been the principal targets of breast cancer (BC) therapies for the last several decades. The androgen receptor (AR) has recently emerged as another promising target in BC. AR is expressed in 77% of all BC and is more widely expressed than estrogen receptor (ER); it is present to varying degrees in all BC subtypes, including luminal A, luminal B, HER2 enriched, and triple negative breast cancers (TNBC)[1]. Recent preclinical studies of AR in BC indicate it is required for survival, and may contribute to metastatic progression. AR drives TNBC tumor growth[2,3], and it interacts with ER in ER+ BC to affect clinical outcome as well as tumor growth in preclinical models (D'Amato et al, in press). A number of AR antagonists currently used for the treatment of prostate cancer are being investigated for use in breast cancer. Recent clinical trials of anti-androgen therapies in breast cancer have demonstrated significant clinical benefit in a variety of disease settings[4,5]. Notably, administration of the AR antagonist enzalutamide (Xtandi, Medivation, Inc) in patients with advanced TNBC results in better than expected survival[5]. Enzalutamide is a second-generation AR inhibitor which functions by preventing AR nuclear localization and has minimal agonist activity. Several other AR antagonists are currently in pre-clinical development, including VT-464 (Seviteronel, Innocrin, Inc). Based on the availability of targeted therapies and the pre-clinical data in BC, AR inhibition has the potential to be widely effective across multiple breast cancer subtypes and disease settings, including those that have become resistant to other therapies.

AR expression has been associated with favorable prognosis in BC[6,7]; however this effect may be subtype-specific[8]. Similarly, ER expression is also associated with a favorable prognosis, which is explained by the observation that ER+ BC are generally well differentiated and more indolent than ER-negative cancers[9,10]; however since these tumors rely on ER for growth, ER-targeted therapies are highly effective. Accumulating evidence suggests that AR may have a similar effect in BC.

The mammalian target of rapamycin (mTOR) is a driver of BC growth and is a potential therapeutic target in a number of solid tumor types. Therapeutic inhibition of mTOR has shown promise in pre-clinical studies[11] and clinical trials. A recent phase III trial of the second-generation mTOR inhibitor everolimus in BC demonstrated significant clinical benefit in patients with ER+/HER2- disease[12], leading to FDA approval of this agent for patients with advanced ER+ breast cancer. However, results have been disappointing in trials of patients with HER2+ disease[13] and TNBC[14]. Given the heavily integrated nature of mTOR signaling, and that it integrates signals from well-established breast cancer targets such as HER2, PI3K, and ER, therapeutic inhibition of mTOR may have unintended compensatory effects within the cell, leading to resistance and continued breast cancer growth. Indeed, this observation was part of the rationale to design clinical trials to dually inhibit mTOR and HER2; however, two phase III clinical trials testing this hypothesis have resulted in only marginal survival improvements[13,15]. Further compounding the issue, molecular markers to reliably predict response or resistance to everolimus remain elusive.

In the current study, we examined the interplay between AR and mTOR in the context of HER2+ BC and TNBC. We sought to determine whether dual inhibition of these pathways would synergistically inhibit BC growth, thus providing the rationale for a new therapeutic combination that could increase the efficacy of mTOR-targeted therapies.

MATERIALS AND METHODS

Cell lines

Breast cancer cell lines BT474, SKBR3, MDAMB453, BT549, HCC1806, and SUM159 were purchased from ATCC. The trastuzumab-resistant cell line BT474-HR20 has been previously described (REF). Cell line molecular subtypes, mutation status, and culture conditions are listed in Supplementary Table 1.

Proliferation and synergy studies

Proliferation was measured using an Incucyte ZOOM Live Cell Imaging System (Essen Biosciences, Inc.) following the manufacturer's protocol. Cells were first stably transfected with a plasmid containing nuclear red-fluorescent protein (RFP) and proliferation was measured either by % confluence, or change in fluorescence over time. Synergy between everolimus and enzalutamide was calculated using CalcuSyn Software (Biosoft Inc), which uses the Chou-Talalay Median Effect method, where a combination index (CI)<0.9 indicated synergy, CI = 0.9-1.1 indicated additivity, and CI>1.1 indicated antagonism. Experiments were performed in biological triplicate.

Patient-derived xenograft sponge culture explants

A patient derived breast cancer xenograft was harvested from a NOD/SCID mouse and cut into $1mm^3$ sections. Sections were placed on dental sponges which were grown in culture dishes with RPMI media containing vehicle, 1uM enzalutamide, 10nM everolimus, or combination. Sponge cultures were grown for 48 hours in the presence of drug, then formalin-fixed and paraffin embedded for immunohistochemistry (IHC).

Western Immunoblotting

For cell lines, cells were lysed in RIPA buffer containing protease inhibitor and phosphatase inhibitor. For xenografts, lysates were generated by first homogenizing tumors with a rotor-stator homogenizer, then lysing in RIPA buffer with protease and phosphatase inhibitor. Whole cell protein lysates were heat-denatured, separated on SDS-PAGE gels, and transferred to polyvinylidene fluoride membranes. Membranes were blocked in 5% BSA in Tris-buffered saline-Tween and then probed overnight at 4°C. The following primary antibodies were used: AR (PG-21, 1:500 dilution, EMD Millipore); phospho-HER2 (Y1248, 1:1000 dilution, Cell Signaling); total-HER2 (D8F12, 1:1000 dilution, Cell Signaling); phospho-HER3 (Y1197, 1:1000 dilution, Cell Signaling); total-HER3 (1B2E, 1:1000 dilution, Cell Signaling); GAPDH (G879S, 1:5000 dilution, Sigma Aldrich); α-tubulin (B-5-1-2; 1:20,000 dilution, Sigma Aldrich). Following incubation in secondary antibody, results were detected using an Odyssey CLx Imager (Licor Inc); densitometry quantification was performed using Image Studio Lite Version 4.0 and reported as a ratio compared with α-tubulin or GAPDH as a loading control.

Quantitative RT-PCR

Total RNA was isolated using the RNeasy Plus Mini Kit (Qiagen) according to manufacturer's instructions. cDNA was synthesized using qScript cDNA SuperMix (Quanta Biosciences) following manufacturer's instructions. qPCR was performed on an ABI 7600 FAST thermal cycler using Absolute Blue qPCR SYBR Green Low ROX Mix (Thermo Scientific). Target gene expression was normalized to either 18s or GAPDH. Experiments were repeated at least twice. qPCR primers were as follows: AR Fwd: 5'…3'; AR Rev: 5'…3'; PIP Fwd: 5'-TCCCAAGTCAGTACGTCCAAA-3'; PIP Rev: 5'-CTGTTGGTGTAAAAGTCCCAG-3'; 18s Fwd: 5'-GTAACCCGTTGAACCCCATT-3'; 18s Rev: 5'-CCATCCAATCGGTAGTAGCG-3'; GAPDH Fwd: 5'-GTCAGTGGTGGACCTGACCT; GAPDH Rev: 5'-AGGGGTCTACATGGCAACTG-3'.

Reverse Phase Protein Array (RPPA)

Tumor xenografts and in vivo *treatments*

Xenograft studies were approved by the University of Colorado Institutional Animal Care and Use Committee (IACUC protocol XXXX). All experiments were conducted in accordance with the NIH Guidelines of Care and Use of Laboratory Animals. Trastuzumab-resistant BT474-HR20 breast cancer cells were stably transfected with the NES-TGL vector, which contains GFP-luciferase. A total of $2x10^6$ trastuzumab-resistant BT474-HR20 cells were mixed in 100uL Matrigel (BD Biosciences) and injected bilaterally into the mammary fat pads of female NOD/SCID mice (Taconic). Tumor growth was measured weekly by caliper and by luciferase signal using an in vivo preclinical imaging system (IVIS).

When tumors reached an average of $50mm^3$, mice were randomized into 4 treatment groups based on caliper measurements and total IVIS signal (Supplementary figure XX). Mice received enzalutamide via their chow (equivalent to 50mg/kg dose). Enzalutamide was mixed with ground mouse chow at a concentration of 0.43 mg/g chow (Research Diets, Inc.). Everolimus was administered intraperitoneally twice weekly at a dose of 2mg/kg. Mice were euthanized by CO_2 asphyxiation and cervical dislocation. Tumors, mammary glands, and colons were harvested for immunohistochemical and gene expression analyses.

Statistical Analyses

To compare the effect of treatment on tumor growth over time, a repeated measures design was used. Assumptions for different types of repeated measures analyses were tested (i.e., normal distribution, equal variances, balanced data, no missing data or unequal time measurements). Normal distributions were determined by graphing the data to check for a symmetrical data distribution without outliers and by the Shapiro-Wilk test. Data failing this assumption were transformed. A repeated measures ANOVA was used if there were no missing data, there were equal numbers in each treatment group, the measurement time points were equal, and there were no missing data points. If this model failed the assumptions of sphericity (Mauchly's Test), either a p-value correction (Huynh-Feldt) was reported or a multivariate ANOVA was used to determine differences in treatment groups over time. If there were missing data, or unbalanced data, or unequal time points, a repeated measures mixed models approach was used. The appropriate covariance structure for the mixed model was tested and the covariance structure leading to the best model fit (lowest Akaike Information Criterion and Bayesian Information Criterion values) was used. Adjusted p-values using Tukeys' method were used to determine differences between individual treatment groups over time. The repeated measures analyses were performed using SAS ver 9.4 (SAS Institute, Cary, NC). Significance was set at $p<0.05$.

RESULTS

mTOR inhibition promotes AR expression and activity

Two breast cancer cell lines harboring PIK3CA mutations that were treated with 10nM everolimus over the course of 48 hours demonstrated an increase in AR protein expression and gene expression (Figure 1). Additionally, everolimus resulted in increased protein expression of phospho-HER3 in the BT474-HR20 cells (Figure 1A), and both phospho-HER2 and phospho-HER3 in the MDAMB453 cells (Figure 1B). These everolimus-dependent increases were abrogated by enzalutamide. Interestingly, treatment of the PIK3CA-wild type cell line SKBR3 with everolimus did not result in upregulation of AR, HER2, or HER3 (Figure 1C). In all cell lines tested, everolimus treatment caused a decrease in protein expression of phospho-S6, which is a downstream readout of mTOR activity. Interestingly, enzalutamide treatment also caused a decrease in pS6 expression. In the BT474-HR20 and MDAMB453 cells, an increase in AR gene expression occurred within 12 hours of everolimus treatment and was maintained through 48 hours in BT474-HR20 and MDAMB453 cells (Figure 1D, 1F). An AR target gene, PIP (prolactin-induced protein) displayed a similar expression pattern, suggesting that AR transcriptional activity is increased by everolimus (Figure 1E, 1G). (Figure XX).

To confirm AR upregulation by everolimus, a PDX was explanted and cultured ex vivo for 48 hours in the presence of enzalutamide, everolimus, or the combination. There was an increase in AR protein expression as measured by immunohistochemical staining when explants were treated with everolimus compared to vehicle, and a subsequent downregulation when explants were treated with enzalutamide+everolimus (Figure 1H).

A reverse-phase protein array was performed to determine the potential downstream effects of everolimus in addition to AR upregulation….(*results pending)*

To examine the effects of everolimus on target protein expression over a longer time course, cells were treated with low-dose everolimus (1nM) for 3 weeks….(*results pending)*

AR and mTOR antagonists synergistically inhibit breast cancer cell proliferation

Breast cancer cells were treated with a dose matrix of enzalutamide and everolimus at three clinically relevant doses per drug. Enzalutamide and everolimus synergistically inhibited proliferation in the BT474, BT474-HR20, MDAMB453, BT549 and HCC1806 cell lines (Figure 1), but not in SKBR3 or SUM159 cells. In the BT474 cells in particular, there was a synergistic inhibition at all dose combinations measured, whereas in the BT549 cells the synergistic effect was limited to the higher doses of enzalutamide. Interestingly, synergistic inhibition of growth was observed only in cell lines harboring activating PIK3CA mutations (BT474, MDAMB453, BT549). In PIK3CA wild-type cell lines, the effect was additive or antagonistic (Supplemental Figure 1). Interestingly, in the HER2-amplified cell line MDAMB453, the three-drug combination of everolimus, enzalutamide, and the HER2-inhibitor trastuzumab resulted in significantly greater inhibition of proliferation when compared to any two-drug combination or any single agent treatment (Supplementary Figure 2).

We examined potential synergy of everolimus with a second AR antagonist, VT-464 (Seviteronel, Innocrin, Inc). Similar to enzalutamide, synergistic inhibition of growth was observed in multiple cell lines, including MDAMB453, and BT474 (Supplemental Figure 3).

Antitumor activity of AR antagonist enzalutamide combined with mTOR inhibitor everolimus

Trastuzumab-resistant BT474-HR20 cells, which are ER-positive, HER2-amplified, and harbor an activating PIK3CA mutation, were injected orthotopically into NOD/SCID mice to determine if combining enzalutamide with everolimus would inhibit tumor growth more than either single-agent treatment. For analysis of tumor growth as measured by IVIS signal, due to missing and unbalanced data, the repeated measures mixed model approach was used. The data were transformed by taking the square root to meet the assumption of normality. Tumors in all treatment groups increased in size over time ($p<0.0001$), and the treatment groups grew at different rates ($p<0.0001$, Figure 3 A-C). Mice treated with either single-agent enzalutamide or single-agent everolimus had significantly reduced tumor viability when compared to mice treated with vehicle. The enzalutamide+everolimus treated tumors had significantly less viability as measured by IVIS signal than all other treatment groups ($p<0.0001$) and they grew at a slower rate ($p<0.0001$).

Interestingly, examination of protein expression from xenografts revealed changes that were distinct from short term in vitro assays described above. After 26 days of treatment, enzalutamide caused an increase in phospho- and total-HER2 protein expression (Figure 3D). Total AR expression was not affected by enzalutamide. Everolimus caused a decrease in phospho- and total-HER2 and HER3, as well as a decrease in AR.

DISCUSSION

Everolimus targets the mTOR signaling axis, which is highly integrated with multiple pathways previously shown to be critical for breast cancer progression, including estrogen receptor signaling and HER2 signaling. The BOLERO-2 phase III clinical trial was designed in part to address this, with patients receiving everolimus in combination with the aromatase inhibitor exemestane. Indeed, the results of this trial indicated that dual inhibition of mTOR and ER significantly improved progression-free survival for patients[12]. However, two other phase III clinical trials, BOLERO-1[15], and BOLERO-3[13], were designed to dually inhibit HER2 and mTOR in trastuzumab-refractory breast cancer, but yielded far less promising results. Patients in these trials who received everolimus did achieve a statistically significant improvement in PFS when compared to the non-everolimus arm, however this benefit was clinically insignificant, with a survival benefit of only one month in the BOLERO-3 trial. These results suggest that some HER2+ breast cancers may not respond to combined mTOR/HER2 inhibition due to compensatory activation of another pathway. Studies in prostate cancer indicate there is cross-regulation between the mTOR signaling axis and the androgen receptor[16], and a pre-clinical study in TNBC showed that the combination of the anti-androgen bicalutamide with PI3K (phosphoinositide

3-kinase) inhibitors slows tumor growth[17]. Additionally, activating PI3K mutations are associated with increased AR expression[18]. The results presented here demonstrate regulation of AR by mTOR in breast cancer. Interestingly, we find this regulation to only be present in cell lines harboring activating PIK3CA mutations. This may be due to the mutation-induced hyper-activation of the pathway, where mTOR is downstream of PI3K.

We elected to use the trastuzumab-resistant cell line BT474-HR20 for the HER2+ in vivo study, which is ER-positive, HER2-amplified, and harbors an activating PIK3CA mutation, due largely to the recent clinical trials described above, in which patients with HER2-positive, trastuzumab-refractory breast cancer received minimal clinical benefit from everolimus. The in vitro and in vivo findings presented here show that in this disease setting, mTOR inhibition significantly activates AR in the short-term. Analysis of pathway component proteins resulted in disparate results when examining short-term vs. long-term everolimus treatment. The upregulation of HER2, HER3, and AR after 48 hours of everolimus treatment in vitro was not observed after long term treatment in vivo. In fact, the opposite was observed, where HER2, HER3, and AR were all downregulated by everolimus. The acute exposure to a high dose of everolimus (10nM) resulted in these compensatory effects that have also been observed in prostate cancer cells in vitro[16]. However, these short-term assays may not fully replicate what occurs in tumors in vivo over a longer treatment course, with a possiably lower chronic exposure to drug. Overall, the effects on cell proliferation and viability were similar when comparing short-term in vitro assays to long-term in vivo assays, with the combination of everolimus and enzalutamide significantly inhibiting growth compared to either single agent. But it appears that the effect on protein expression of dually inhibiting AR and mTOR is dynamic over time. Long-term treatment with low-dose everolimus…

Figure 1. Everolimus upregulates AR protein expression and transcriptional activity. (A) Trastuzumab-resistant BT474-HR20, (B) MDAMB453, and (C) SKBR3 cells were grown in either charcoal-stripped serum (DCC) or full serum (FBS) for 48 hours. Cells grown in DCC were then treated with DHT, enzalutamide, everolimus, or combinations for 48 hours, as shown. Cells grown in full serum were treated with either enzalutamide, everolimus, or combination for 48 hours. (D,E) BT474-HR20 cells and (F,G) MDAMB453 cells were treated with 10nM everolimus and RNA was harvested at timepoints shown. RT-qPCR was performed for AR and an AR target gene, PIP (prolactin-induced protein). GAPDH was used as a housekeeping gene for qPCR. (H) A triple-negative breast cancer patient-derived xenograft was explanted and grown in culture medium containing vehicle, enzalutamide, everolimus, or the combination, for 48 hours. Explants were harvested and embedded, then stained for AR protein expression by immunohistochemistry (*Still working on this figure).*

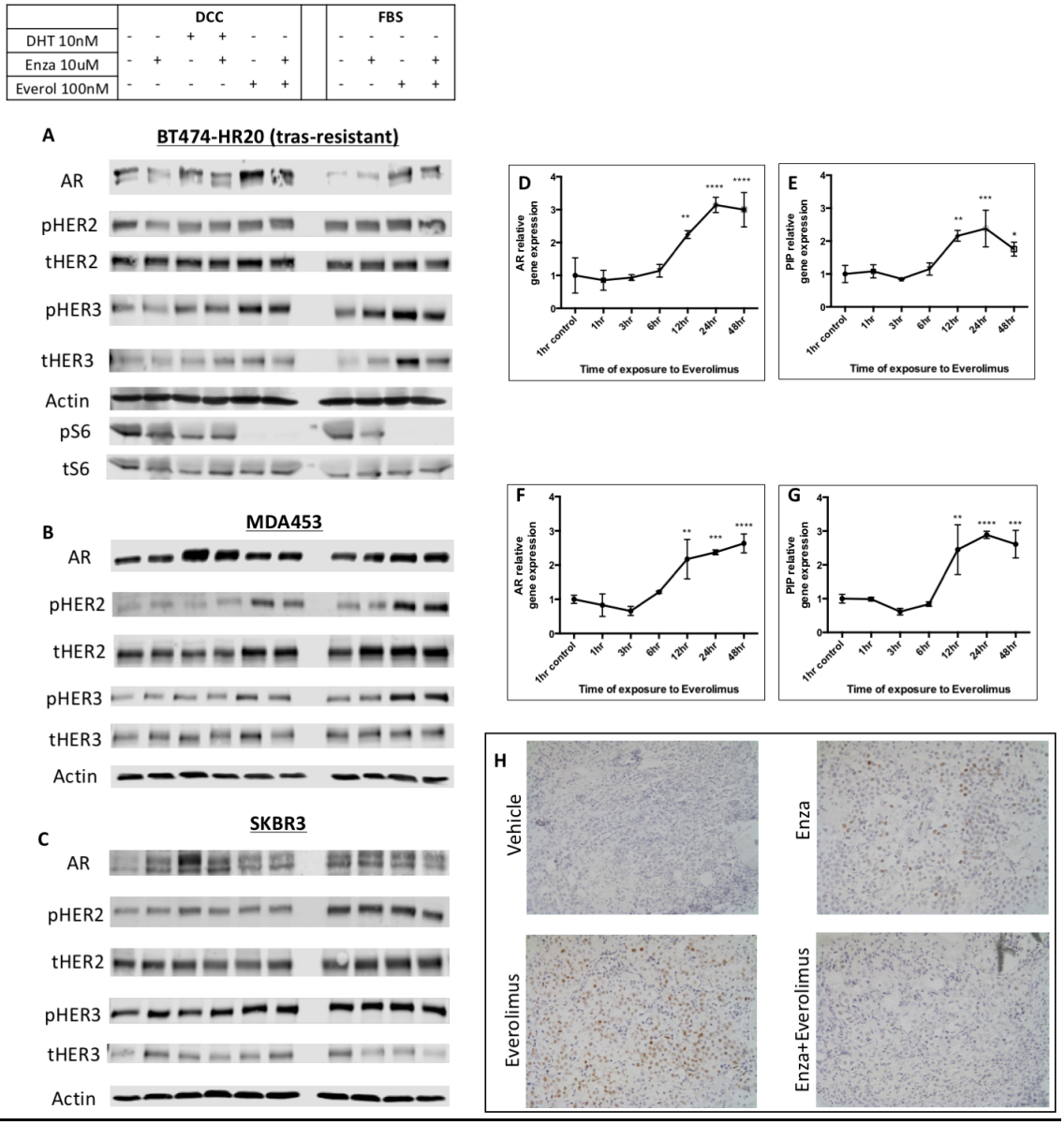

Figure 2. Enzalutamide synergizes with everolimus to inhibit breast cancer proliferation *in vitro.* HER2-amplified BT474 cells and HER2-overexpressing MDAMB453 cells were labeled with nuclear red fluorescent protein, and were treated with enzalutamide and everolimus at doses indicated for six days. Proliferation was measured on an IncuCyte live cell imager using nuclear-RFP to quantify. Percent inhibition of growth was used to calculate synergistic interaction between the two drugs, using CalcuSyn software. A combination index (CI) <0.9 indicates synergy at a given dose, CI 0.9-1.1 indicates additivity, and CI>1.1 indicates antagonism.

A.

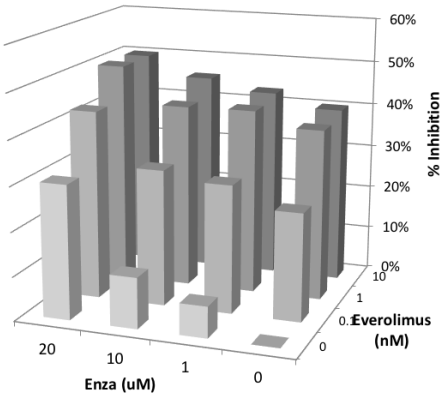

Enza (uM)	Everol (nM)	% Inhibition	Combination Index
1	0.1	29.01%	**0.459**
1	1	42.01%	**0.127**
1	10	43.05%	**0.913**
10	0.1	30.86%	**0.469**
10	1	41.78%	**0.210**
10	10	45.54%	**0.542**
20	0.1	42.72%	**0.166**
20	1	50.06%	**0.101**
20	10	49.97%	**0.244**

B.

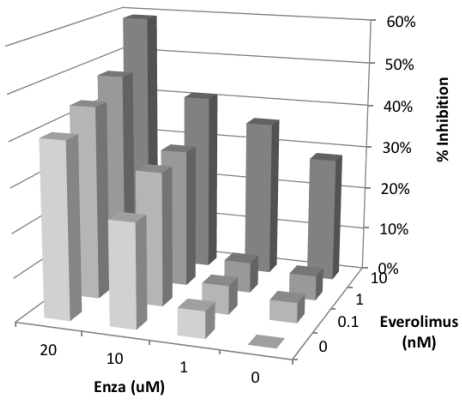

Enza (uM)	Everol (nM)	% Inhibition	Combination Index
1	0.1	6.06%	**1.011**
1	1	7.05%	**2.822**
1	10	35.95%	**0.319**
10	0.1	30.64%	**0.759**
10	1	31.68%	**0.747**
10	10	41.09%	**0.576**
20	0.1	44.05%	**0.701**
20	1	48.05%	**0.574**
20	10	59.13%	**0.345**

Figure 3. Combination treatment with enzalutamide and everolimus inhibits tumor viability significantly more than single agent treatment. *Still working on this figure.* (A) Total flux growth curve of trastuzumab-resistant BT474-HR20 xenografts. Mice were randomized to one of four treatment groups at day -3 and treatment was initiated at day 0. (B) IVIS signal on last day of study. (C) Change in total flux from day of randomization to end of study on day 26. (D) Western blots from 3 representative tumors per treatment group: vehicle, enzalutamide (Enza), everolimus (Everol), and combination (Enza/Everol). *p<0.05, **p<0.01, ***p<0.001, ****p<0.0001.

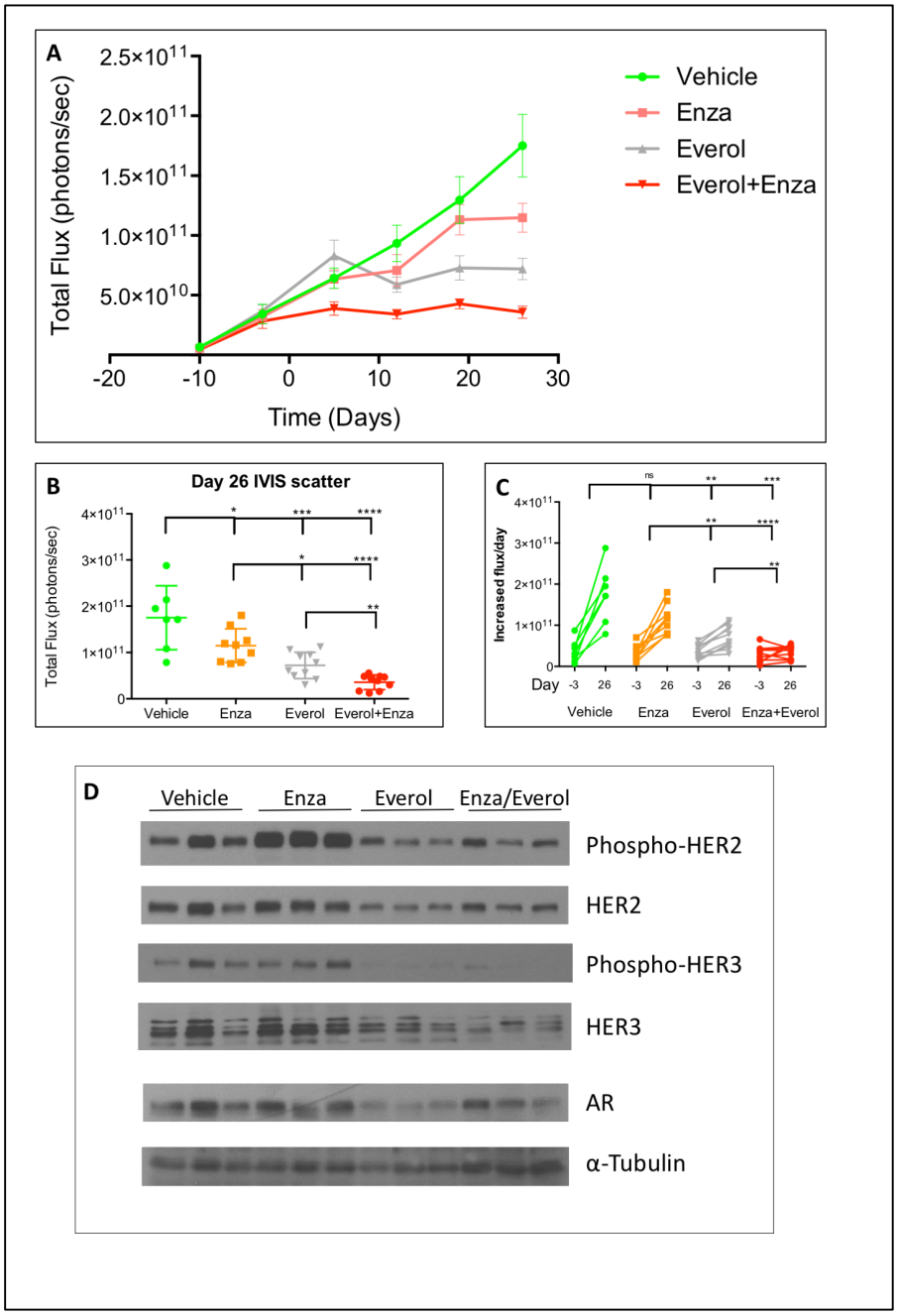

REFERENCES

1 Collins, L. C. *et al.* Androgen receptor expression in breast cancer in relation to molecular phenotype: results from the Nurses' Health Study. *Mod Pathol* **24**, 924-931, doi:10.1038/modpathol.2011.54 (2011).

2 Barton, V. N. *et al.* Multiple molecular subtypes of triple-negative breast cancer critically rely on androgen receptor and respond to enzalutamide in vivo. *Mol Cancer Ther* **14**, 769-778, doi:10.1158/1535-7163.MCT-14-0926 (2015).

3 Lehmann, B. D. *et al.* Identification of human triple-negative breast cancer subtypes and preclinical models for selection of targeted therapies. *J Clin Invest* **121**, 2750-2767, doi:10.1172/JCI45014 (2011).

4 Gucalp, A. *et al.* Phase II trial of bicalutamide in patients with androgen receptor-positive, estrogen receptor-negative metastatic Breast Cancer. *Clin Cancer Res* **19**, 5505-5512, doi:10.1158/1078-0432.CCR-12-3327 (2013).

5 Traina, T. A. M., K.; Yardley, D.A.; et al. Results from a phase 2 study of enzalutamide (ENZA), an androgen receptor (AR) inhibitor, in advanced AR+ triple-negative breast cancer (TNBC). *J Clin Oncol* **33 suppl; abstr 1003** (2015).

6 Adamczyk, A. *et al.* Prognostic value of PIK3CA mutation status, PTEN and androgen receptor expression for metastasis-free survival in HER2-positive breast cancer patients treated with trastuzumab in adjuvant setting. *Pol J Pathol* **66**, 133-141 (2015).

7 Agrawal, A. *et al.* Expression of Androgen Receptor in Estrogen Receptor-positive Breast Cancer. *Appl Immunohistochem Mol Morphol*, doi:10.1097/PAI.0000000000000234 (2015).

8 Elebro, K. *et al.* Combined Androgen and Estrogen Receptor Status in Breast Cancer: Treatment Prediction and Prognosis in a Population-Based Prospective Cohort. *Clin Cancer Res* **21**, 3640-3650, doi:10.1158/1078-0432.CCR-14-2564 (2015).

9 Dunnwald, L. K., Rossing, M. A. & Li, C. I. Hormone receptor status, tumor characteristics, and prognosis: a prospective cohort of breast cancer patients. *Breast Cancer Res* **9**, R6, doi:10.1186/bcr1639 (2007).

10 Wenger, C. R. *et al.* DNA ploidy, S-phase, and steroid receptors in more than 127,000 breast cancer patients. *Breast Cancer Res Treat* **28**, 9-20 (1993).

11 Martin, L. A. *et al.* Effectiveness and molecular interactions of the clinically active mTORC1 inhibitor everolimus in combination with tamoxifen or letrozole in vitro and in vivo. *Breast Cancer Res* **14**, R132, doi:10.1186/bcr3330 (2012).

12 Baselga, J. *et al.* Everolimus in postmenopausal hormone-receptor-positive advanced breast cancer. *N Engl J Med* **366**, 520-529, doi:10.1056/NEJMoa1109653 (2012).

13 Andre, F. *et al.* Everolimus for women with trastuzumab-resistant, HER2-positive, advanced breast cancer (BOLERO-3): a randomised, double-blind, placebo-controlled phase 3 trial. *Lancet Oncol* **15**, 580-591, doi:10.1016/S1470-2045(14)70138-X (2014).

14 von Minckwitz, G. *et al.* Survival after neoadjuvant chemotherapy with or without bevacizumab or everolimus for HER2-negative primary breast cancer (GBG 44-GeparQuinto)dagger. *Ann Oncol* **25**, 2363-2372, doi:10.1093/annonc/mdu455 (2014).

15 Hurvitz, S. A. *et al.* Combination of everolimus with trastuzumab plus paclitaxel as first-line treatment for patients with HER2-positive advanced breast cancer

(BOLERO-1): a phase 3, randomised, double-blind, multicentre trial. *Lancet Oncol* **16**, 816-829, doi:10.1016/S1470-2045(15)00051-0 (2015).
16 Carver, B. S. *et al.* Reciprocal feedback regulation of PI3K and androgen receptor signaling in PTEN-deficient prostate cancer. *Cancer Cell* **19**, 575-586, doi:10.1016/j.ccr.2011.04.008 (2011).
17 Lehmann, B. D. *et al.* PIK3CA mutations in androgen receptor-positive triple negative breast cancer confer sensitivity to the combination of PI3K and androgen receptor inhibitors. *Breast Cancer Res* **16**, 406, doi:10.1186/s13058-014-0406-x (2014).
18 Gonzalez-Angulo, A. M. *et al.* Androgen receptor levels and association with PIK3CA mutations and prognosis in breast cancer. *Clin Cancer Res* **15**, 2472-2478, doi:10.1158/1078-0432.CCR-08-1763 (2009).